GUIDANCE PARAMETERS AND CONSTRAINTS FOR CONTROLLED ATMOSPHERIC ENTRY

ROBERT C. DUNCAN

GUIDANCE PARAMETERS AND CONSTRAINTS FOR CONTROLLED ATMOSPHERIC ENTRY

by

Robert C. Duncan, Lieutenant Commander, U.S. Navy
B.S. United States Naval Academy, 1945
B.S. United States Naval Postgraduate School, 1953
S.M. Massachusetts Institute of Technology, 1954

Volume I of II

Chapters 1 through 7

SUBMITTED IN PARTIAL FULFILLMENT OF THE
REQUIREMENTS FOR THE DEGREE OF
DOCTOR OF SCIENCE
at the
MASSACHUSETTS INSTITUTE OF TECHNOLOGY
1960

GUIDANCE PARAMETERS AND CONSTRAINTS FOR CONTROLLED ATMOSPHERIC ENTRY

by

Robert C. Duncan

Submitted to the Department of Aeronautics and Astronautics, Massachusetts Institute of Technology, on January 11, 1960, in partial fulfillment of the requirements for the degree of Doctor of Science.

ABSTRACT

Entry of astronautical vehicles into planetary atmospheres is examined in this thesis with respect to interactions of the guidance function, vehicle performance, trajectory prediction, and mission objectives.

All entry missions which originate from planetary reconnaissance orbits are classified into two broad categories: the direct entry profile and the degenerate orbital profile. These classifications are distinguished by the fact that some form of thrust generating mechanism is required to effect controlled entry in the direct entry profile, while engines are not required for controlled entry in the degenerate orbital profile.

Approximate analytical solutions of guidance parameters and constraints are derived for both classes of profiles. As used in this thesis, guidance parameters include:

(1) Predicted values of distance flown, range, range-to-go, altitude, velocity, time of flight, and specific force level;
(2) Sensitivity of the foregoing quantities to errors and uncertainties in the specification of aerodynamic characteristics of the vehicle, density characteristics of the atmosphere, magnitude and direction of the engine thrust vector.

Constraints are defined as trajectory limitations resulting from:

(1) Permissible specific force levels of the vehicle and its human occupants;
(2) Heat flow rates to the skin of the vehicle, and stagnation point temperatures;
(3) Radiation hazards.

A major shortcoming of numerical studies performed in the conceptual and early design phases of astronautical entry systems is that an infinite number of possible trajectories and guidance schemes must be explored. In order that the engineer understand the effect of changing various design parameters and in order to compare different guidance schemes, simple analytical results, even though only approximate, can be far more informative than a long series of machine computations. The philosophy advanced in this thesis, therefore, emphasizes the use of dynamical approximations, with specified limitations, to derive simple analytical solutions of important guidance quantities.

It is shown in this thesis that the trajectories of both the direct and degenerate orbital profiles possess three distinct operational regimes, defined as the Keplerian, Intermediate, and Gas-Dynamic Phases. A parameter, called the Conservation Parameter, is defined to specify precisely the boundary conditions between these operational phases. The Conservation Parameter is an index of the influence of the operating environment on vehicular motion and may be used as a switching function for the guidance computer and as an external aid for adaptive control of the vehicle.

Three-dimensional dynamical equations of motion are developed for entry of lifting or non-lifting vehicles in banking or wings-level flight with variable thrust capabilities into the atmosphere of oblate, rotating planets with or without atmospheric winds. The figure of the planet, the gravitational model, and the atmospheric model for important bodies of the solar system are summarized. Special problems associated with first-time entry into the atmospheres of strange planets are discussed.

Thesis Supervisors: Dr. Walter Wrigley

Professor of Instrumentation and Astronautics

Paul E. Sandorff

Associate Professor of Aeronautics and Astronautics

Dr. Winston R. Markey

Assistant Professor of Aeronautics and Astronautics

ACKNOWLEDGMENT

The author wishes to express his appreciation to the many personnel of the Instrumentation Laboratory, Massachusetts Institute of Technology, who assisted in the preparation of this thesis. The author is particularly indebted to the following:

Professor Walter Wrigley, Professor Paul E. Sandorff, and Professor Winston R. Markey, who as thesis supervisors offered guidance, direction, and encouragement throughout the entire investigation.

Professor C. Stark Draper for his example of vision, leadership, and professional stature.

Mr. John Hovorka for his interest and advice.

Professor James L. Stockard, Captain Paul V. Osburn, USAF, Messrs. Richard Rosenbaum, Robert G. Stern, and Myron Kayton, who, as fellow students, provided many stimulating discussions, offered many suggestions, and evaluated critically many of the ideas developed during the course of this work.

Mr. James L. Nevins, Jr. for his interest, encouragement, and for his many helpful suggestions.

Mr. John W. Hursh, Assistant Director of the Instrumentation Laboratory, for providing access to facilities and literature and for his counsel and advice.

Mrs. R.C. Duncan for assuming added responsibilities in the home.

Messrs. Arthur L. Webber, Laurence R. Young, and D. Alexander Koso for their interest and suggestions.

Mr. Lawrence J. Berman for recommending and providing research material.

Miss Lorraine A. Joyce and Miss Betty B. Belknap for their capable assistance in the preparation of the manuscript.

The naval personnel, officer and civilian, who initiated and fostered the postgraduate program of which this thesis is a part.

The graduate work for which this thesis is a partial requirement was performed while the author was assigned to the Massachusetts Institute of Technology for postgraduate instruction sponsored by the U.S. Naval Postgraduate School.

This report was prepared under the auspices of DSR Project 52-154, sponsored by the AMC Aeronautical Systems Center, through USAF Contract AF 33(600)-38967. Work under this contract was under the technical guidance of a WADC Weapons Guidance Laboratory Project Engineering Team.

The publication of this report does not constitute approval by the Navy, the Air Force, or the Instrumentation Laboratory of the findings or the conclusions contained therein. It is published only for the exchange and stimulation of ideas.

OVERALL TABLE OF CONTENTS

Table of Contents: Volume I

Contents, cont.

Contents, cont.

List of Illustrations: Volume I

Illustrations, cont.

List of Tables: Volume I

Chapter 1

INTRODUCTION

1.1 Object

The object of this thesis is to formulate analytical techniques for specifying important parameters and constraints necessary in the preliminary development of guidance concepts for a wide class of entry missions into planetary atmospheres.

To be of maximum efficacy, analytical techniques and solutions formulated must be of sufficient generality as to apply to many vehicles and missions, of sufficient utility to enable a clear understanding of the relation between trajectory and performance, of sufficient simplicity to enable rapid determination of numerical answers from a diversity of initial conditions, and of sufficient accuracy when compared to more exact machine computations that engineering decisions can be deduced with confidence.

1.2 Guidance Parameters and Constraints

As used in this thesis, guidance parameters include:

(1) Predicted values of distance flown, range, range-to-go, altitude, velocity, time of flight, and specific force level.

(2) Sensitivity of the foregoing quantities to errors and uncertainties in the specification of aerodynamic characteristics

of the vehicle, density characteristics of the atmosphere, magnitude and direction of the engine thrust vector.

Guidance constraints are defined as trajectory limitations imposed by:

(1) Permissible specific force levels of the vehicle and its human occupants.

(2) Heat flow rates to the skin of the vehicle, and stagnation point temperatures.

(3) Radiation hazards.

1.3 The Family of Astronautical Vehicles

Astronautical vehicles existing today may be classified into various types according to the specific function for which each is designed. Examples of these classes are sounding rockets, ballistic missiles, Earth satellite research vehicles to accumulate data concerning the Earth and its environment, meteorlogical satellites, manned research vehicles (such as the X-15), lunar and solar probes.

Vehicles under development for use in the immediate future extend the above list to manned orbital vehicles (such as Projects Mercury and Dyna-Soar), unmanned planetary probes, navigation satellites, reconnaissance satellites, communication-relay satellites, and special purpose satellites to map more extensively the recently discovered radiation patterns in space, to verify Einstein's relativity theories, etc. A host of other astronautical vehicles have been suggested, most of which depend on successful completion of projects already in progress. Among these are international inspection satellites, manned orbital space stations, manned lunar and planetary reconnaissance vehicles, hypersonic

gliders for transportation and other logistic functions, astronautical vehicles designed to perform specific military functions such as to destroy missiles and satellites, to perform military reconnaissance functions, to jam communication facilities, to serve as bombing platforms, to exercise supply and logistic functions.

The above enumeration of astronautical vehicles frequently referenced in the unclassified literature is by no means a complete tabulation; yet, it is a dramatic demonstration of the rapid growth of the space family in the few years since the birth of the V-2 rocket, which must surely be classified as the father of this modern family. The spectacular growth of this family suggests a truly fertile expansion in the future.

This thesis is devoted to an investigation of a special portion of the trajectory of some of these vehicles, namely that portion in or near the atmosphere of a planet or a natural planetary satellite. The investigation is sufficiently general as to apply to manned and unmanned vehicles, to a diversity of mission concepts, and to a wide class of vehicles both lifting and non-lifting. The study is oriented toward determination of optimal guidance requirements for directing the vehicle to a particular landing site selected prior to entry. Emphasis is placed on the manned vehicle and the guidance constraints resulting from its human occupants. General constraints imposed by the operational environment are considered, with special emphasis on atmospheric constraints.

It is intended in this introductory chapter to show how the work of this thesis fits into the framework of the entry mission concept and into the large body of previous work recorded in the literature.

Specific conclusions and recommendations for further study are advanced in Chapter 2. Where appropriate in relating the work of this thesis to the broad problem of guidance and control systems design, general conclusions are proffered in this introductory chapter.

1.4 Manned Planetary Missions

Taylor and Blockley[1]* have stated eloquently man's motivation for space exploration:

> "The feat of putting man into orbit and the final triumph of interplanetary and even interstellar exploration are supreme human goals, transcending the purely pragmatic question of which performs more efficiently, man or machine."

A competent team of trained and motivated men cannot be surpassed by machine to perform exploratory functions, as contrasted to reasonably well-established routine functions (such as data collection and computation). The machine can do only those functions for which it is designed; it cannot seek new functions beyond the scope of its sensory transducers. The design of the machine may be elaborate in order to encompass limited decision-making capabilities, the ability to adapt its performance to a changing environment, the faculty for rapid determination, computation, cataloging, and storing of data. A machine or group of machines that can perform an almost unlimited diversity of tasks such as the following, however, will probably never be built in a package weighing less than 200 pounds:

(1) Correlate many non-related observations.

- - - - - - - - - - - - - - - -

* Superscript numerals refer to similarly numbered references in the Bibliography.

(2) Readily perform multifarious physical tasks, in any order, such as moving from place to place, replacing or repairing a faulty engine and electronic component, controlling a flying vehicle, collecting minerals and plant life, comparing observations with data previously accumulated, etc.

(3) Make rapid decisions based on seemingly independent events.

(4) Has intuition*.

Man has a unique facility for exercising judgment; he can reason inductively and has the ability to draw inferences from isolated elements of one situation and apply them to another. The trained human being has the capacity to analyze problems never before encountered and to make decisions on the basis of general rather than specific experience. He is a valuable technical trouble shooter and can better assure reliable operation of all equipment on the astronautical vehicle by continuous checking, repairing, and replacing of faulty equipment. It has been demonstrated over a half-century of flight that he is a versatile flight controller; there is much expert opinion to substantiate the belief that he can exercise this function to a useful extent even at escape velocities.

The planning of an astronautical mission and the design of the vehicle and its guidance and control system is a problem of optimum system design to effect a successful mission with maximum flexibility

- - - - - - - - - - - - - - - - -

* "Immediate apprehension or cognition; the power of knowing or the knowledge obtained without recourse to inference or reasoning; insight; familiarity, a quick or ready apprehension." (Webster's Collegiate Dictionary).

and reliability, minimum initial weight, and the most efficient power utilization. A realistic approach to analyzing the mission problem is to assign to humans those functions performed best by them and to relegate to machines the functions that they can perform more efficiently. Taylor and Blockley state man's role:

> "Man will perform primarily as a strategist, as a correlator of data at many probability levels, a maker of insightful interpretations from these data, and a formulator of effective plans of action. Although it is possible to conceive of a machine that could perform some or all of these functions, it would be very large, complicated, and expensive.
>
> Man is needed as a scientific observer of space phenomena. He can act to control the instrumentation toward the most significant and reliable readings, to make the unexpected observation, and to gain basic insights into the pattern of results. Although machines could conceivably do this job, man will <u>want</u> to do the job personnaly, whether required or not."

Before any attempt is made to explore the surface of a strange planet, sufficient data regarding the planet must be accumulated in advance to demonstrate that the potential benefits of such an exploration are great enough to justify not only the tremendous cost but also the attendant risk to human life. Preceding the manned mission will be a certain number of unmanned exploratory probes in order to collect data on radiation hazards, gravity, magnetic field, atmospheric properties such as temperature, density and wind characteristics, terrain mapping, etc. Manned exploration of the vicinity of the planet, which may or may not culminate in immediate atmospheric penetration to a landing, <u>should follow relatively few unmanned probes</u>, in the opinion of the author.

It is interesting to compare some of the debits and credits which enter the engineering ledger as a result of designing a mission system

to include the human crew. The man excels over the machine in:

(1) Detecting minimal changes in visual or auditory stimuli;

(2) Perceiving, in the presence of noise, meaningful patterns and information;

(3) Choosing new courses of action with great flexibility and adaptability when circumstances change unexpectedly;

(4) Storing tremendous quantities of data for long periods of time and recalling the required relevant information rapidly.*

Engineering liabilities incurred by incorporating man in the system include the following:

(1) Much engineering effort is required to make the astronautical vehicle habitable and safe due to the inherent vulnerability of man to the space environment.

(2) Engineering provision must be made for living, rest, and recreation that go beyond a utilitarian minimum because more is required of the man than mere survival. He must perform at top efficiency, a requirement closely coupled with morale and physiological considerations.

(3) Equipment required** to make man effective in his duties are costly in weight, size, complexity, and dollars.

The net cost of each unmanned planetary probe, in terms of man

- - - - - - - - - - - - - - - -

* It was estimated in reference (1) that the brain's storage capacity is of the order of 2 to 100 times 10^6 bits. This compares to storage of the order of 10^5 bits in a typical modern high-speed computer.

** Such as human-operator stations, data-processing and storage facilities, sensory displays, etc.

hours and natural resources expended versus data collected, is sufficiently great that emphasis should be placed on the manned mission as early as possible. The potential wealth of knowledge that may be obtained versus expenditure of resources and money is greater, by orders of magnitude, in manned exploration as contrasted to unmanned probes, even though each manned vehicle must itself be more elaborate and costly. Therefore, there is strong justification for manned exploration to follow relatively few unmanned probes; the latter should be undertaken in such numbers only to establish that the risk factor* to man is within acceptable bounds.

In the investigation described subsequently in this thesis, a specific guidance system is not considered in detail, hence the advantages and disadvantages of using man in contrast to machine to perform specific guidance functions are not debated. Major emphasis is placed, however, on an important consideration in systems design of the manned entry vehicle; viz., constraints on the trajectory resulting from allowable human acceleration loads.

1.5 Dynamics of Entry

The analysis of the flight of the entry vehicle is a particular application of the general theory of the dynamics of rigid bodies in three dimensions. It is usual in such theory to separate the motion of the center of mass from the motion of the body around the center of mass. The theory of flight performance embodies the former, the theory of stability and control the latter.

- - - - - - - - - - - - - - - - -

* Such as from radiation and meteor hazards, launch and recovery failure, operational reliability, etc.

The analytical work of this thesis is concerned specifically with performance analysis and the relation of guidance to performance. Stability and control functions are recognized where it is considered appropriate to emphasize their coupling with performance*. In this thesis, therefore, the entry vehicle appears as a point particle of varying mass subject to various forces. Research was commenced with investigation of the three-dimensional equations of motion of a variable mass particle in the vicinity of an oblate rotating planet possessing an atmosphere with winds. The particle was generalized to one capable of generating lift, drag, and thrust forces and capable of generating side forces by banking in order to induce trajectory curvature in the horizontal plane.** As a practical matter, the trajectory was intentionally confined to a fixed plane in much of the analytical work of the thesis. Assumptions required and limitations on the resulting solutions as a consequence of using the theory of planar motion are discussed in detail.

One of the difficulties encountered in any practical study of the dynamics of entry results from the uncertain knowledge of many of the important parameters which influence the trajectory. The lift and drag coefficients of the vehicle at high velocities may differ considerably from expected values since wind tunnel data and other experimental data are fragmentary for velocities in excess of Mach 10 to 15. Atmospheric properties, particularly the densities existing at higher altitudes,

- - - - - - - - - - - - - - - - -

* See, for example, Appendix F.

** In order to simplify the difficult task of the reader in keeping track of the many coordinate frames, symbols, and constants used in this thesis, the author has defined and tabulated all such quantities in Appendix A.

are subject to much uncertainty.

The density of the Earth's atmosphere decreases with altitude until it merges with the very thin solar atmosphere. Chapman[2] advances the theory that the sun possesses a tenuous atmosphere which extends through interplanetary space beyond the distance of the Earth's orbit. He suggests that this solar atmosphere consists mainly of ionized hydrogen, protons, and electrons, with a density of about 10^3 particles per cubic centimeter in the vicinity of the Earth. The solar atmosphere has little effect on the entry mission as conceived in this thesis since the planetary atmosphere is of considerably greater significance at the altitudes considered herein. The solar atmosphere, however, may have a significant effect on interplanetary trajectories. All studies of interplanetary trajectories performed to date have neglected any atmosphere in space; the minute drag terms may be important when integrated over many months.

Lift and drag are the primary gas-dynamic forces influencing the trajectory of the entry vehicle. It is usual to express these in terms of a coefficient based on the frontal area S of the vehicle. For example:

$$\text{Drag} = \frac{1}{2} \rho C_D S V^2$$

$$\text{Lift} = \frac{1}{2} \rho C_L S V^2$$

where ρ is the local free-stream atmospheric density and V is the magnitude of the vehicle's velocity vector with respect to the atmosphere. Lift and drag coefficients depend on the configuration of the vehicle, on the angle of attack and angle of yaw, and on the flight Mach number, M_a.

Even if C_L and C_D were independent of velocity, the insertion of

the lift and drag terms in the equations of motion make it impossible to integrate the dynamical equations of motion except under certain specific restrictions. A number of methods for circumventing this difficulty are discussed in this thesis.

Drag perturbations on Vanguard I and Sputnik III which coincided* with solar flares have led to the suggestion that electrical drag of satellites may be important[3]. Electrical drag may be produced by the motion of a charged satellite through clouds of charged particles. The vehicle can pick up a negative charge, for example, by colliding with high energy electrons in a radiation band. The charge on the vehicle repels other electrons, creating a shell of net positive charge around the vehicle. The area of this shell is the effective drag area of the vehicle. The increased drag area leads to increased atmospheric resistance to motion of the vehicle due to collision with other particles. Electrical drag may be important in perturbing the motion of long lifetime satellites and interplanetary vehicles; it is a higher order effect on the entry mission and is not considered in this analysis.

It is shown in this thesis that the altitude at which the planetary atmosphere is important in vehicle guidance depends strongly on flight path angle, lift, drag, and density characteristics of the entry vehicle. The heating and deceleration loads which accompany high velocity entry into the atmosphere are strong functions of initial penetration angle and vehicle design characteristics.

- - - - - - - - - - - - - - - - -

* The drag increased about a day or so after the intense solar activity was observed. This lends credence to the theory that <u>particles</u> emitted from the sun, and not <u>radiation</u>, caused the drag perturbations.

1.6 The Entry Mission

The entry mission, as defined in this thesis, is that portion of an astronautical vehicle's consignment which starts from a reconnaissance orbit in the vicinity of a planet, asteroid, or natural satellite of a planet, and ends with a landing on the surface of the body.

The Reconnaissance Orbit

The reconnaissance orbit may fall into one of two main categories, called in this thesis the stable orbit and the degenerate orbit. These two major classes of reconnaissance orbits are shown in Fig. 1.1. The significant difference between the two types of reconnaissance orbits is that an engine or some other form of external thrust generating mechanism is required in order to initiate controlled entry from the stable orbit, while entry may be effected without an external thrust generating system in the degenerate orbit.

It is difficult to draw a clear line of demarkation between the two classes of reconnaissance orbits, except in terms of total satellite lifetimes. A vehicle in a stable orbit experiences little or no atmospheric perturbations, hence it has a long lifetime (months or years). A vehicle in a degenerate orbit encounters significant perturbations in the vicinity of perigee*; therefore, its apogeal altitude decays rapidly until the orbit is near circular. This phase of orbital flight is frequently called the "circularization" process; i.e., the ellipse decays to a circle. The lifetime of the vehicle in a degenerate orbit is short (hours or days). Gravitational perturbations, which lead to

---

* Definition of terms frequently used to describe elliptical orbital motion is given in Appendix A.

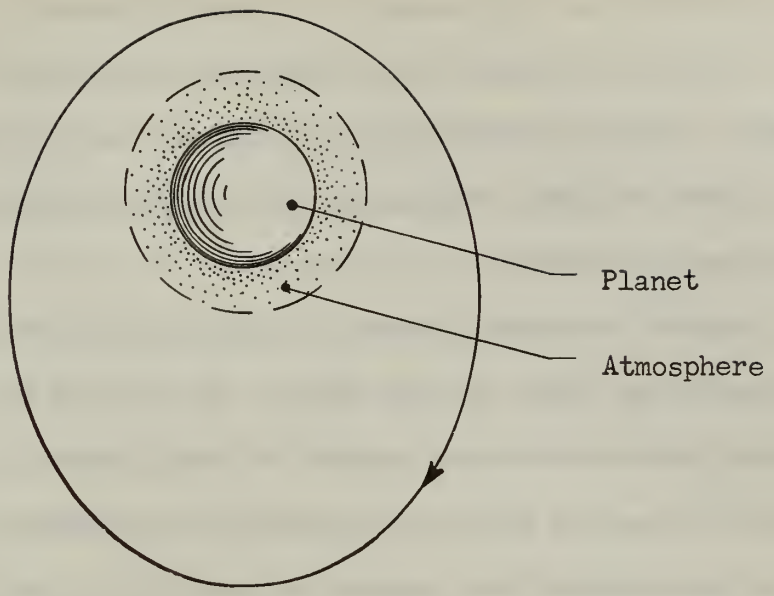

(a) A stable reconnaissance orbit.

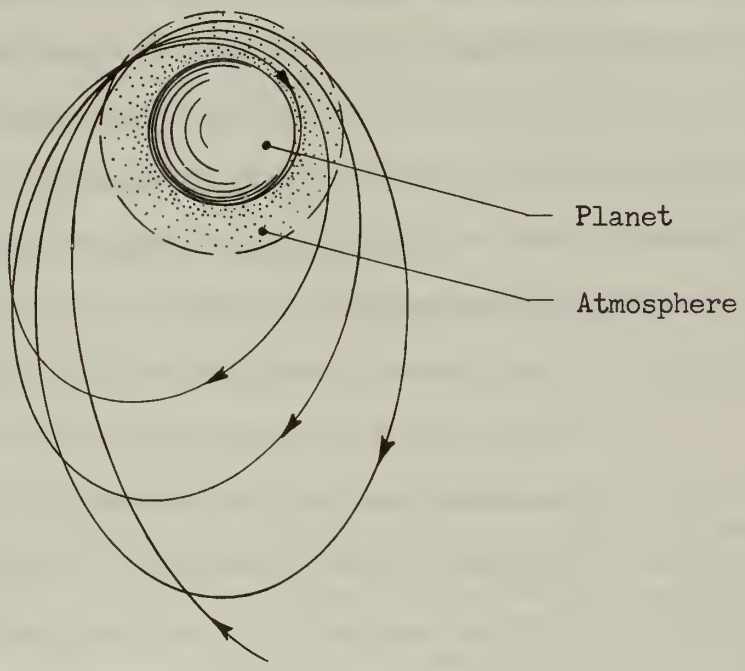

(b) A degenerate reconnaissance orbit.

Fig. 1.1: Two Major Classes of Reconnaissance Orbits.

phenomena such as regression of the line of nodes and movement of the line of apsides (advance of perigee), are considered briefly in this thesis. The major perturbation of interest in this work, however, is due to the planetary atmosphere; all other perturbations are generally higher order effects.

Methods by which the vehicle establishes the reconnaissance orbit are beyond the scope of this thesis. It is noted that both classes of reconnaissance orbits are planned for manned Earth orbital missions. Eggers[4] suggests using the degenerate reconnaissance orbit as a transition phase between the transfer ellipse and the entry trajectory in interplanetary missions. The interplanetary transfer ellipse terminates in a series of braking passes through the atmosphere of the planet; each pass reduces the total energy of the vehicle by transfer of energy to the planetary atmosphere. In this way, the need for using engines to reduce total vehicle energy is avoided; higher payloads are possible because very little vehicle mass must be invested in propellent fuel.

There are serious disadvantages to Egger's mission concept:

(1) Extreme guidance accuracy is required in order to graze the planetary atmosphere at just the right altitude for proper energy transfer and, concurrently, not incur excessive deceleration and heating loads. The perigeal altitude of the first pass, the total energy transferred, vehicle heating rates, and deceleration loads are extremely sensitive to small aiming errors in the interplanetary transfer ellipse. Trajectory corrections of this transfer ellipse near the destination planet are almost mandatory.

(2) The apogee of the first few orbital ellipses may be sufficiently high above the planet to encounter severe radiation hazards from the Van Allen belts.* Though Van Allen belts around planets other than Earth have not been detected, it is reasonable to assume that they may exist around any planet possessing a magnetic field. Drake[5] has advanced the theory that the radio waves from Jupiter originate from the Jovian version of the Van Allen belts. He estimates radiation intensities to be 100 times as strong in the Jovian belts as in the Earth belts.

Hazards from planetary radiation belts conceivably could make multiple atmospheric braking passes an unpleasant experience. It may be more profitable to accept the weight penalty of rocket braking in the interest of radiation safety.

The stable reconnaissance orbit can be established either by using rocket braking directly, or by suitable application of rocket thrust after energy is reduced in one braking pass. The second method has the advantage of reducing the total propellant mass required, the disadvantage of

- - - - - - - - - - - - - - - -

* The radiation belts named after Dr. James A. Van Allen, who first disclosed their discovery, were detected by the Army's Pioneer III lunar probe launched in December 1958. There are two main belts containing energetic particles trapped in the Earth's magnetic field. Pioneer III showed the inner belt to be centered approximately 2400 miles above the Earth and the outer belt centered at 10,000 miles. Maximum radiation rate was estimated to be 5-10 Roentgens per hour. A comparatively free area exists between the two belts; for example, the measured radiation rate at 6000 miles was 0.3 Roentgens per hour. Pioneer IV (March 1959) reported particle densities in the outer belt to be many times greater than those measured by Pioneer III. It is believed that the particles in these belts are of solar origin.

requiring extreme guidance accuracy in setting up the braking pass.

A distinct advantage of establishing a stable orbit is that the time and location for initiating final entry by retro-thrust may be freely chosen. Extensive reconnaissance of the surface of the planet is possible and a wise selection made of a site for eventual landing. If a landing appears unwise for any reason, the stable reconnaissance orbit is a relatively easy staging point for starting the return mission. An attractive feature in establishing a stable reconnaissance orbit, particularly for first time entry into strange planets, is that a navigational satellite can be left in this orbit as a source of external tracking information in the absence of ground based tracking stations.*

A single-pass landing has also been suggested for planetary entry(6). The reconnaissance trajectory is omitted in this concept of the interplanetary mission. The vehicle is braked by the atmosphere to a landing in its initial encounter with the atmosphere. The vehicle must be guided down a narrow corridor if gas-dynamic drag is to reduce the velocity sufficiently for landing without producing accelerations beyond human tolerances. The Earth's landing corridor for a non-lifting vehicle is less than seven miles wide, for a lifting vehicle the corridor may be broadened to 60 miles. The corridor for Venus is about like that of the Earth, for Mars the corridor is broader, and for Jupiter the corridor is much more narrow.

The guidance problem of traversing such a corridor during the first pass from an interplanetary journey is obviously severe and the ability to land at a predetermined location is subject to many

---

* See Appendix D.

uncertainties. The single-pass entry mission is a special case of the direct entry profile.* It is special in the sense that:

(1) The initial velocity for the entry mission is greater than orbital velocity;

(2) It is the only method for generating the direct entry profile without using engines.

If a reconnaissance orbit is part of the planetary mission, it is considered herein as prescribing the initial conditions of the entry phase of the mission. Analytical techniques are developed for approximate determination of guidance parameters and constraints for entry from both elliptical and circular, stable and degenerate, reconnaissance orbits.

1.7 Entry Profiles

In general, entry systems may be classified into two broad types: lifting and non-lifting. Precision landing point control is obtainable with either system, providing the non-lifting vehicle has variable drag capabilities. No comparison is made in this thesis with respect to the relative merits of one system versus the other; an analytical framework is presented which will enable analysis of either type.

Two dissimilar entry profiles are analyzed in this thesis:

(1) The direct entry profile is generated in either of the following two ways:

(a) Large scale perturbations of the stable reconnaissance orbit by means of retro-rocket thrust forces;

- - - - - - - - - - - - - - - -

* See section 1.7 for definitions of the classes of entry profiles.

(b) First pass termination of an interplanetary transfer ellipse.

(2) The degenerate orbital profile consists of a series of braking passes through the outer reaches of the atmosphere in order to reduce the energy level preparatory to final direct entry. The degenerate orbital profile is the consequence of entering from (a) the degenerate reconnaissance orbit, or (b) minor retro-rocket perturbations of the stable reconnaissance orbit.

The entry trajectory may be viewed as made up of a number of separate functional phases. Fig. 1.2 shows the functional phases for both classes of entry profiles.

The functional phases of the direct entry profile are:

(1) Orbital phase: The vehicle is in a stable reconnaissance orbit; this is at all times beyond altitudes where the planetary atmosphere has a significant effect on the trajectory. This phase is omitted if entry is made during the first atmospheric perturbation of an interplanetary transfer ellipse; viz., the "first pass" entry mission concept.

(2) Departure Phase: Entry is initiated at the trajectory modification point by application of retro-rocket thrust forces. The departure phase terminates when engines have flamed out. This phase may be omitted if entry is made during the first pass of an interplanetary mission.

(3) Free-fall phase: Consists of that portion of the trajectory from the point where departure thrust is "turned off" to the point where significant gas-dynamic forces (e.g., lift, drag) are generated.

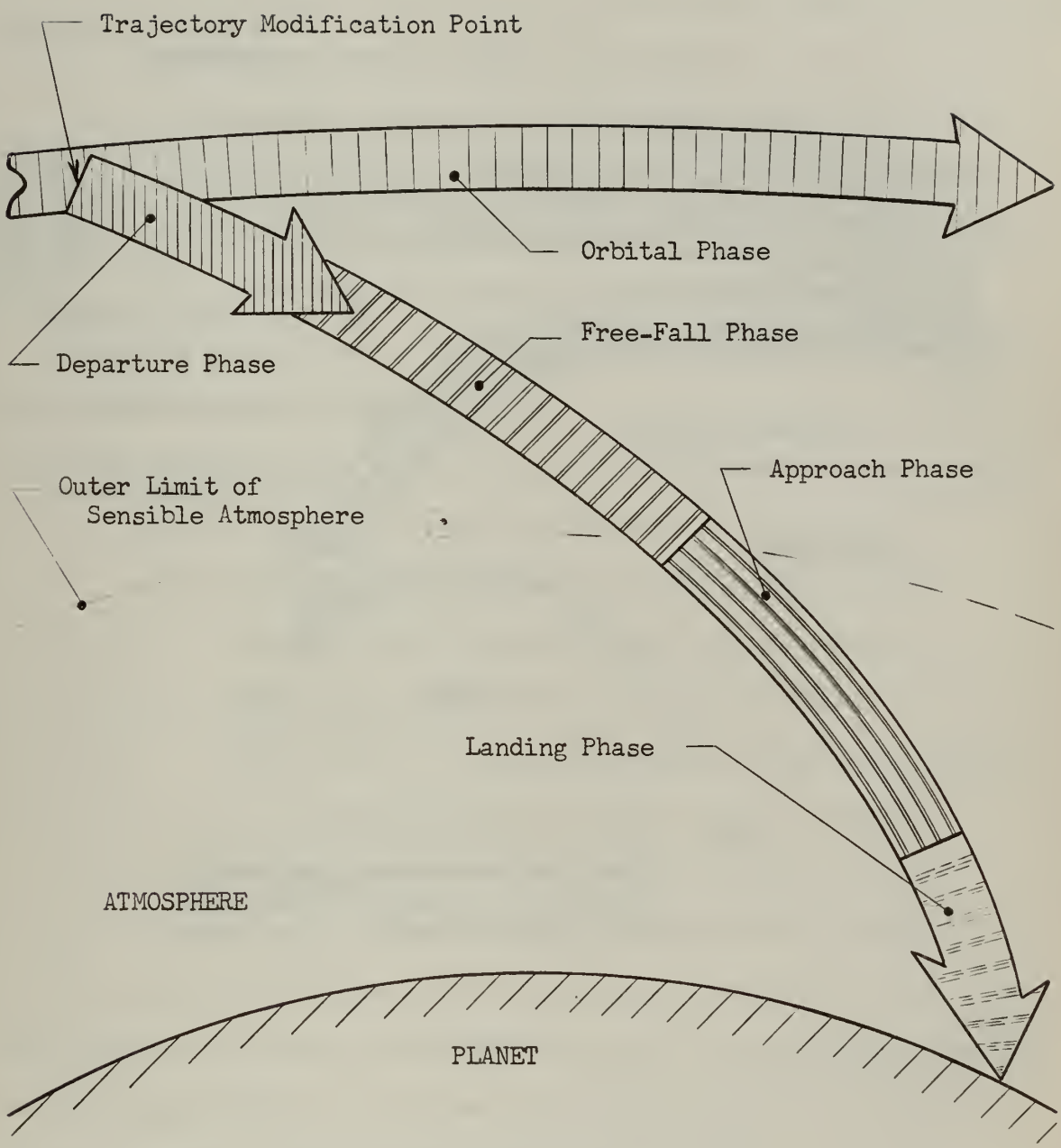

(a) The Direct Entry Profile

Fig. 1.2: Functional Phases of Entry

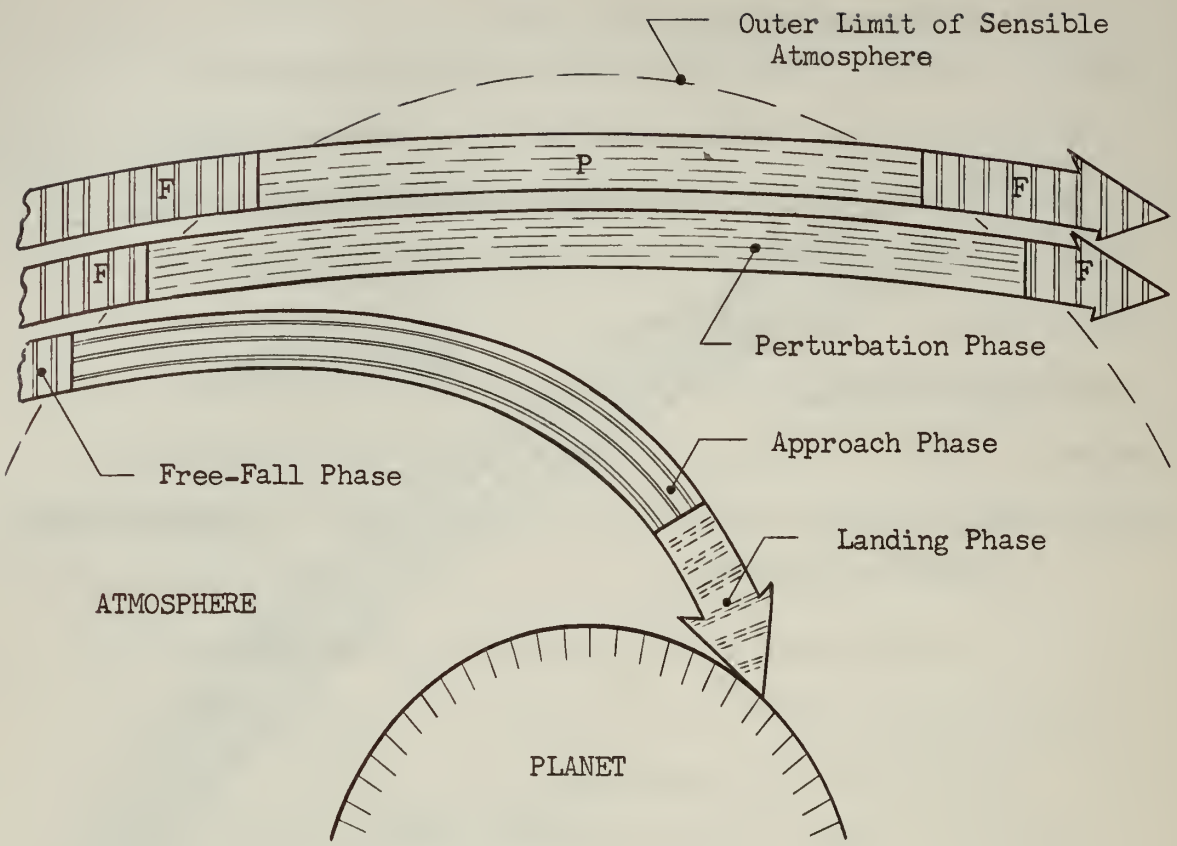

Note: Only two perturbation passes are shown for convenience; perigeal separation is grossly exaggerated for pictorial clarity.

(b) The Degenerate Orbital Entry Profile

Fig. 1.2 (continued) Functional Phases of Entry

(4) Approach phase: The atmospheric portion of the trajectory traversed from the point where gas-dynamic forces are measurable to the point where landing is initiated.

(5) Landing phase: That portion of the trajectory, near the intended destination and characterized by low altitudes and velocities, which terminates in either impact with the surface or a glide landing to rest.

The functional phases of the degenerate orbital profile are shown in Fig. 1.2 (b). These are:

(1) Orbital phase: The vehicle is in a degenerate reconnaissance orbit consisting of two sub-phases:

(a) Free-fall phase: Consists of that portion of the elliptical orbit beyond the sensible atmosphere.

(b) Perturbation phase: Consists of that portion of the elliptical orbit near perigee where significant energy is transferred from the vehicle to the atmosphere.

(2) Approach phase: Same as for the direct entry profile.

(3) Landing phase: Same as for the direct entry profile.

In this thesis, it is shown that a more convenient division of the trajectory for guidance analysis is in terms of the operational regimes or operational phases. The three operational phases were defined as follows:

(1) Keplerian Phase: That segment of the trajectory, at high altitudes, where gas-dynamic forces are insignificant. ($\rho \cong 0$)

(2) Intermediate Phase: That segment of the trajectory where accelerations due to gas-dynamic forces are of comparable

magnitude with other terms in the dynamical equations of motion.

(3) Gas-Dynamic Phase: That segment of the trajectory where gas-dynamic accelerations are the predominant terms affecting the shape of the trajectory.

In order to specify precisely the boundary conditions between phases, an auxiliary quantity was defined. It was shown in Chapters 8 and 9 that this auxiliary quantity, called the Conservation Parameter*, has a sharp behavior at certain critical points in the entry mission and is a valuable index of the influence of the atmosphere on the vehicle and its trajectory. The Conservation Parameter was defined as follows:

$$\text{Conservation Parameter} = \left| \frac{-\left[\begin{array}{l}(\text{Percentage change in vehicle's horizontal component of inertial velocity}) \\ +\ (\text{Percentage change in radial distance from the planet center})\end{array}\right]}{(\text{Percentage change in radial distance from the planet center})} \right|$$

This is equivalent to the following definition:

$$\text{Conservation Parameter} = \left| \frac{1 - \xi}{\xi} \right|$$

where $$\xi \equiv \frac{-\dot{R}/R}{\dot{V}_{I\phi}/V_{I\phi}}$$

R is the distance of the entry vehicle from the planet center and $V_{I\phi}$

- - - - - - - - - - - - - - - - -

* The name Conservation Parameter was selected because of its close relation to conservation of energy and angular momentum:

Time rate of transfer of angular momentum: $p' = -(\text{Cons. Parameter})h'v_{I\phi}$

Time rate of transfer of energy: $\frac{E'(\text{kin})}{E'(\text{pot})} \cong -\left[(\text{Cons. Parameter})v_{I\phi}^2 r + 1\right.$

is the horizontal component of velocity with respect to inertial coordinates.

It is shown in this thesis that the Conservation Parameter may be computed from navigational data. It has potential application as an environmental index for adaptive control systems and as a switching function for the guidance computer.

In terms of the Conservation Parameter, the operational phases of the entry trajectory were defined as follows:

(1) Keplerian Phase:

A true Keplerian trajectory exists only when the Conservation Parameter is zero. The trajectory is near-Keplerian when the magnitude of the Conservation Parameter is less than 0.1.

(2) Intermediate Phase:

The magnitude of the Conservation Parameter is greater than 0.1 and less than 10.

(3) Gas-Dynamic Phase:

The magnitude of the Conservation Parameter is greater than 10.

The phase boundary between the Keplerian and Intermediate phases is at the point where the magnitude of the Conservation Parameter is 0.1. The phase boundary between the Intermediate and Gas-Dynamic Phases is at the point where the magnitude of the Conservation Parameter is 10. Fig. 1.3 shows the operational phases for the two classes of entry profiles.

1.8 Guidance

The guidance process consists of measurements of vehicle position

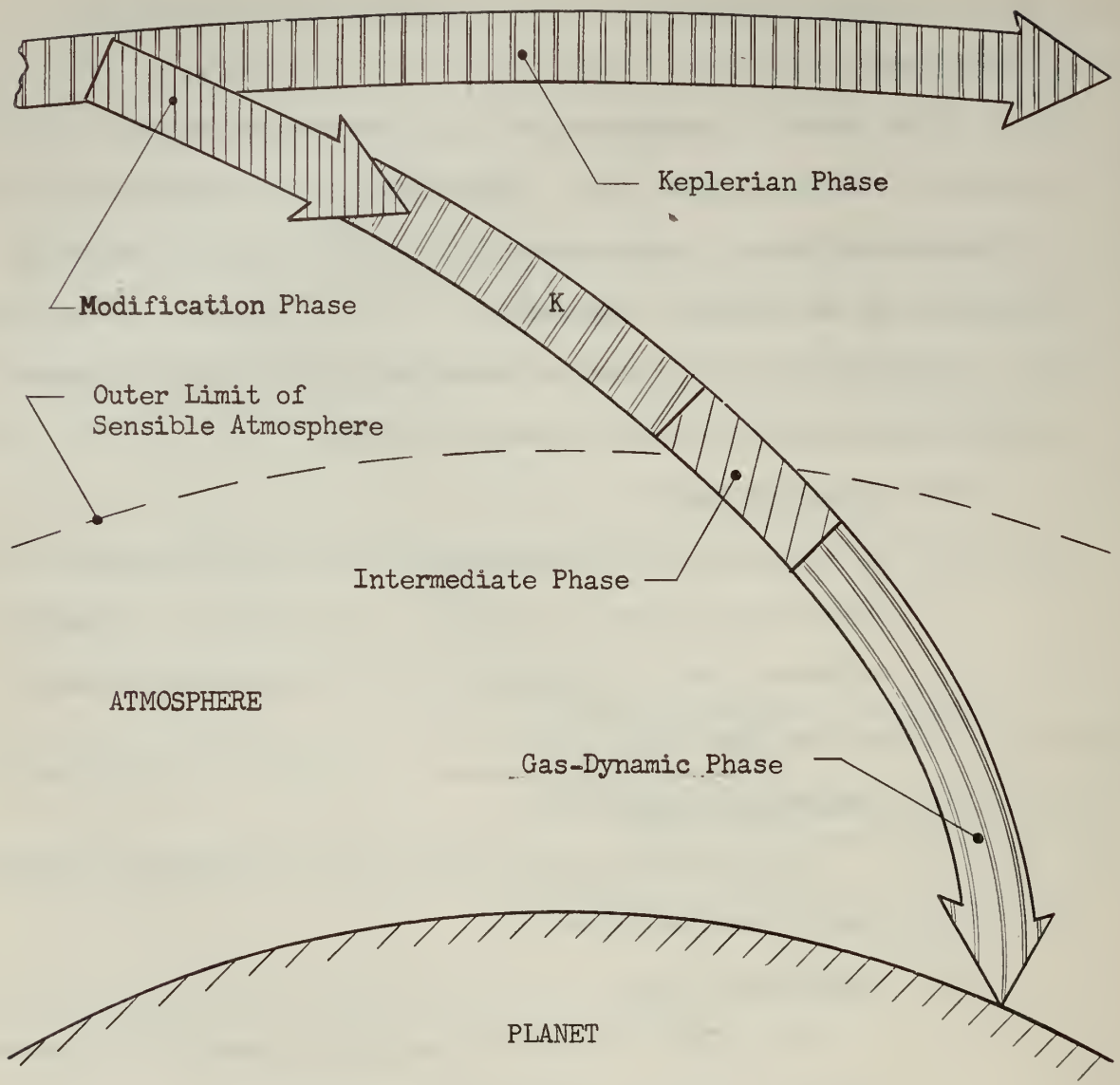

Boundary Conditions between Keplerian and Intermediate Phases:
Conservation Parameter = 0.1

Boundary Conditions between Intermediate and Gas-Dynamic Phases:
Conservation Parameter = 10

(a) The Direct Entry Profile

Fig. 1.3 Operational Phases of Entry

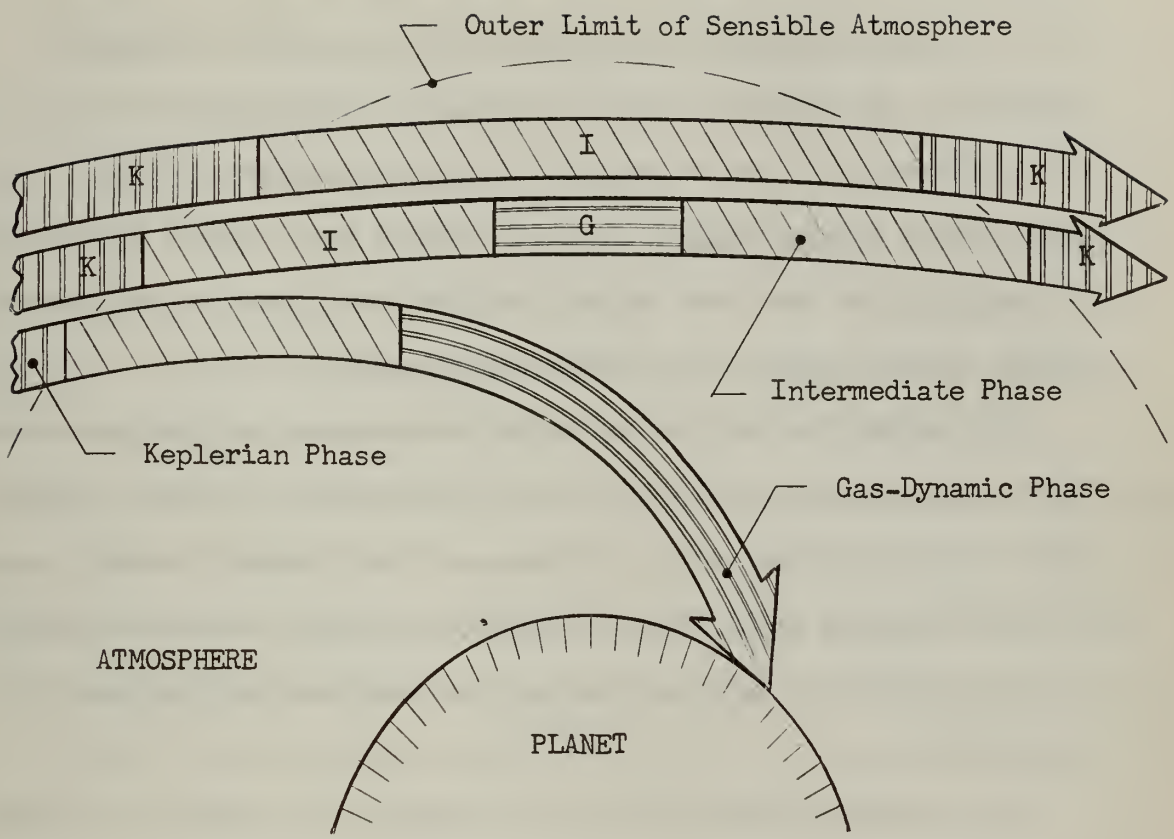

Boundary Condition between Keplerian and Intermediate Phases:
Conservation Parameter = 0.1

Boundary Condition between Intermediate and Gas-Dynamic Phases:
Conservation Parameter = 10

Note: Only two perturbation passes are shown for convenience; perigeal separation is greatly exaggerated for pictorial clarity.

(b) The Degenerate Orbital Entry Profile

Fig. 1.3 (continued) Operational Phases of Entry

and velocity, computation of control actions necessary to properly adjust position and velocity, and delivery of suitable adjustment commands to the vehicle's control system.(7) The guidance system, of which a human pilot may or may not be an integral part, operates as a force vector control system; i.e., the system must control the direction and magnitude of the force vector* in such a way that the vehicle eventually arrives safely at the desired destination.

Any method for guiding the entry vehicle to a selected geographic point on the surface of the planet must necessarily involve a perturbation of its original orbit. Because of the tremendous energy possessed by the vehicle in orbit, it is difficult to perturb the orbit greatly without investing a large portion of the total mass of the vehicle in rocket fuel.

The trajectory that follows the initiation of entry from a satellite orbit beyond the sensible atmosphere is a part of the general problem of transfer between orbits that has received considerable attention in the literature. The special nature of the entry problem, however, requires solutions that are not available in general treatises on the subject of transfers between orbits.

Various methods are available for perturbing the satellite orbit to bring about controlled entry:

(1) Impulsive application of forces at the trajectory modification point by means of chemical rockets or other high thrust propulsive systems.

- - - - - - - - - - - - - - - - -

* The controllable force vector is the vector sum of all external forces (lift, drag, thrust) that are capable of being adjusted by the guidance system.

(2) Continuous application of low thrust (e.g., ion rockets);

(3) Multiple impulses at intermediate* thrust levels;

(4) Drag modulation, if portions of the orbit pass through the planetary atmosphere.

Fig. 1.4(a) shows a generalized functional diagram of the guidance and control system for the entry mission. It is to be emphasized that this is a functional diagram and not an operational component diagram; for example, the digital computer, a key component of the system, performs computations for all four functional elements shown in Fig. 1.4(a).

The generalized entry trajectory is shown in Fig. 1.4(b). This trajectory may be controlled by use of continuous, piecewise continuous, or impulsive thrust forces as commanded, and, in the atmospheric portion of flight, by suitable adjustment of lift and drag forces. Attitude may be controlled by gas-dynamic moments and/or reaction control**. In the Keplerian phase of the mission, thrust is the only means by which substantial trajectory alterations can be made. If the trajectory modification point shown on Fig. 1.4(b) is at sufficiently high altitudes for lift and drag forces to be negligible, then thrust is the only means by which entry can be initiated.

A logical step in the direction of simplifying the generalized guidance and control system of Fig. 1.4 is to assume that high thrust impulses are utilized early in the entry mission to initiate and adjust

- - - - - - - - - - - - - - - -

* Thrust levels between those obtainable with chemical rockets and with continuous ion propulsion.

** Reaction control, in the form of expulsion of gases from strategically located nozzles, is a useful method of generating forces to supplement weak aerodynamic forces in the maintenance of vehicular attitude. It is necessary to use reaction control at high altitudes, or in the maintaining of certain extremes in attitude.

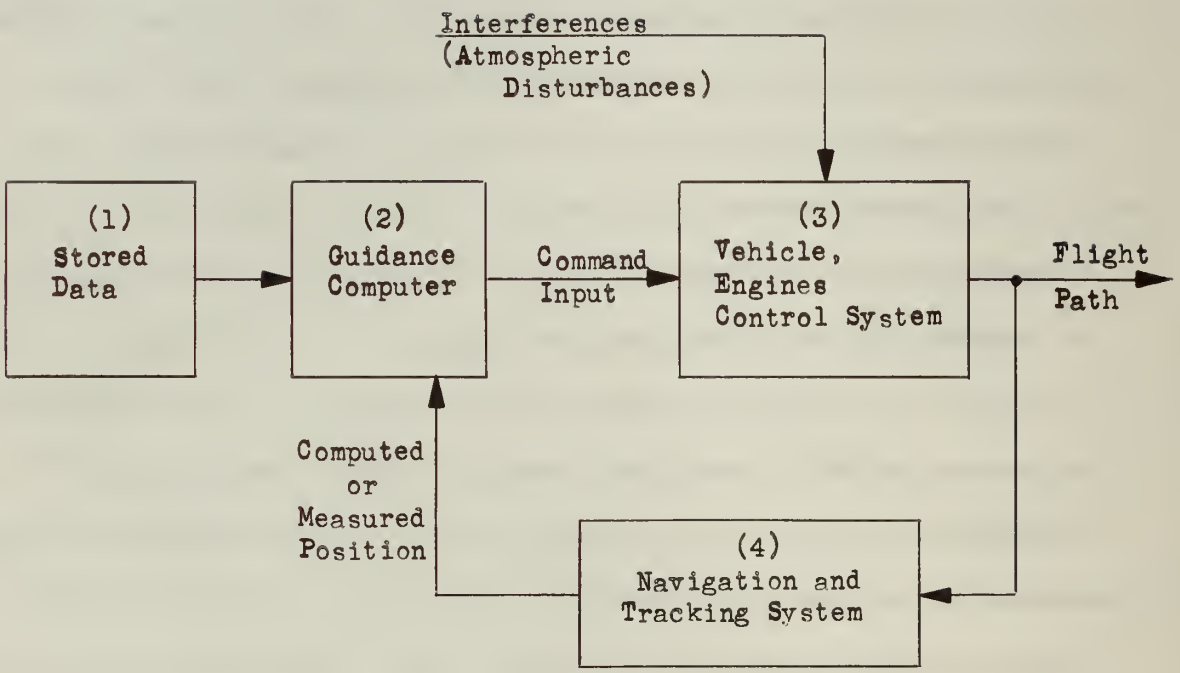

(a) Guidance System.

Fig. 1.4: Functional Diagram of Generalized Guidance and Control System for the Entry Mission

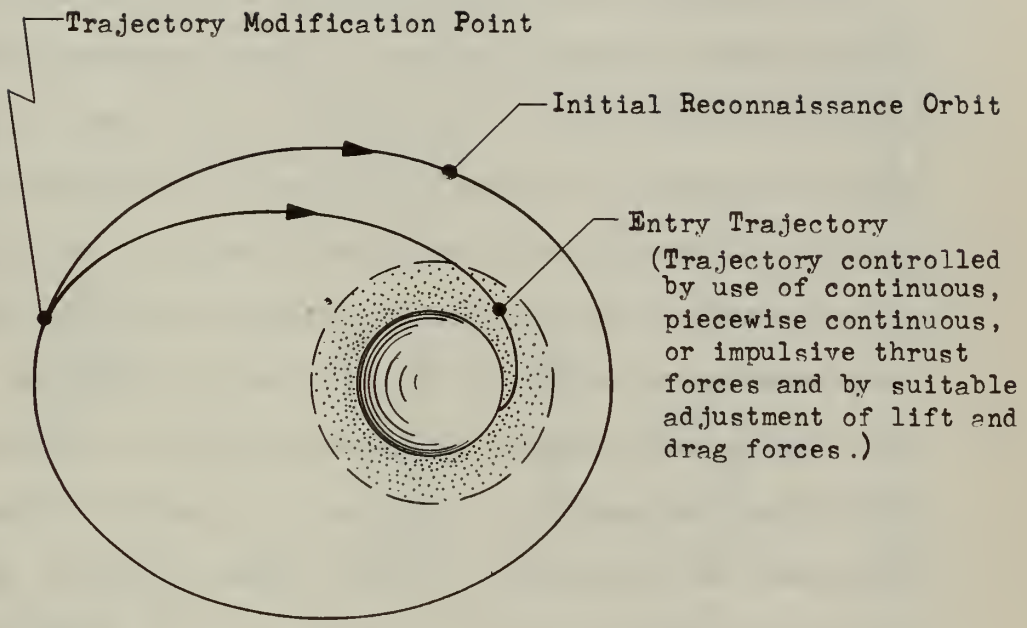

(b) Generalized Entry Trajectory.

Fig 1.4 (cont.): Functional Diagram of Generalized Guidance and Control System for the Entry Mission.

the recovery trajectory, after which the engines are cut off. Gas-dynamic forces are utilized for all subsequent trajectory modifications. This scheme permits separation of the computation functions for engine control and the computation functions for control of the vehicle's aerodynamic surfaces.

Fig. 1.5 shows a function diagram of a guidance and control system for which engine commands and control of the aerodynamic surfaces are uncoupled. Guidance and control systems of this type are generally adopted for almost all classes of astronautical missions. Ballistic missiles, for example, omit the guidance computer, box (2), except for attitude stability and control; the ballistic missile's trajectory is not adjusted after engine cut-off. The basic differences in guidance system design among the various classes of ballistic missiles are in the stored data, the computations performed to determine engine command inputs, and the navigation or tracking scheme employed. Some systems rely on precomputation of many coefficients which do not vary radically with time and storing this information, thus reducing significantly the computational load required of the computer. The navigation and tracking system generally falls into one of three major categories: inertial, radio, or a combination of the two.

Satellite launching systems also utilize the guidance system of Fig. 1.5. For trajectories which require extreme precision, such as lunar probes, some of the computations are performed on the ground and command signals are transmitted by radio to the vehicle for mid-course vernier corrections.

The entry mission differs from the examples cited previously in one major respect; i.e., the most important period of the flight is in

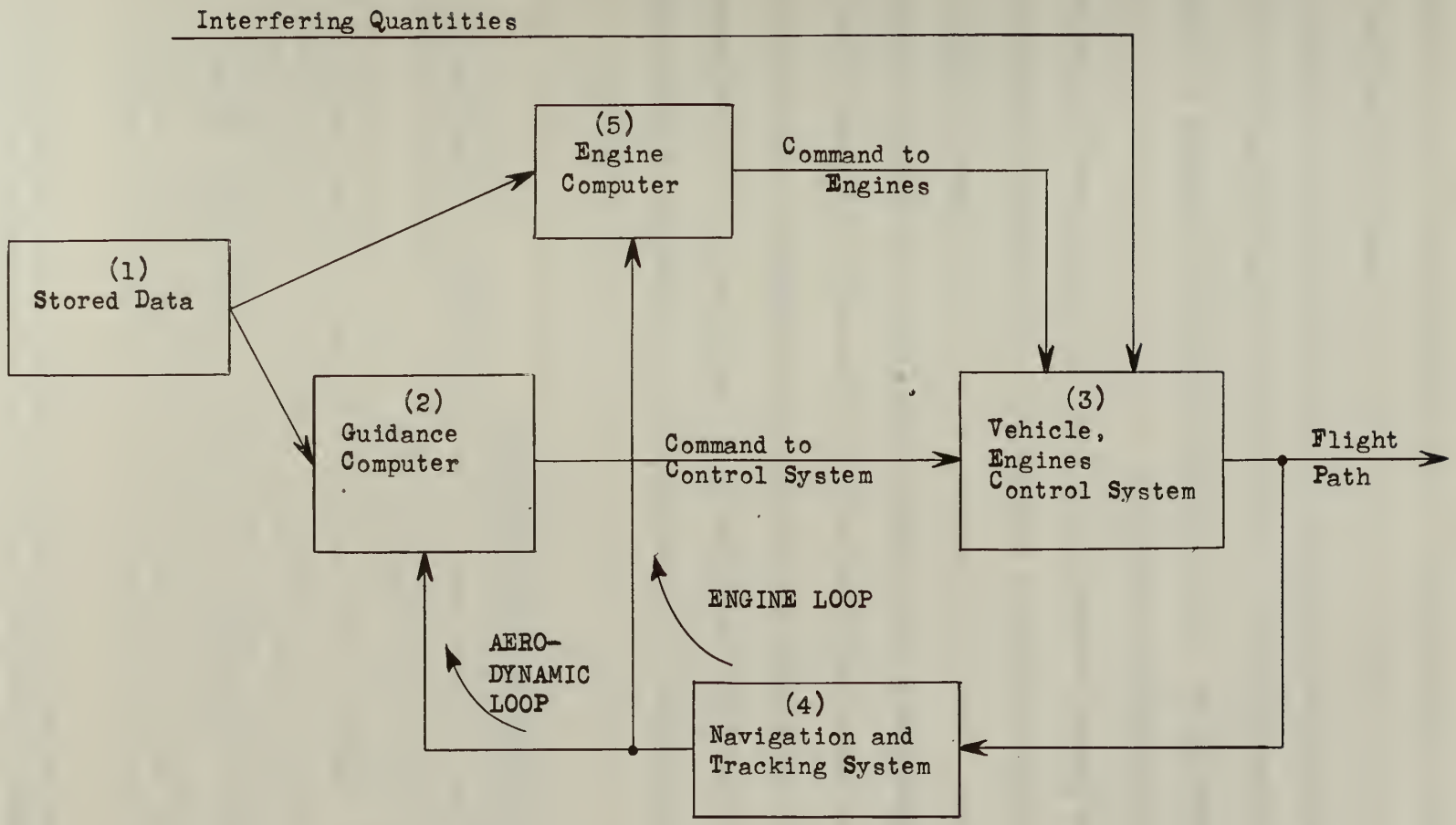

Fig 1.5: Functional Diagram of Guidance and Control System in Which Engine Commands and Control of Aerodynamic Surfaces are Uncoupled.

the atmosphere of the planet where gas-dynamic forces are extremely influential. The atmosphere, like fire and water, can be of invaluable aid if properly harnessed and can lead to disaster if permitted to reign unchecked; witness the parachute on one hand versus the flaming meteor on the other. The relative importance of boxes (2) and (5) in Fig. 1.5 is reversed in the case of the entry mission as compared to launching a satellite or ballistic missile.

Most papers on entry vehicle guidance are devoted to an investigation of the aerodynamic loop in Fig. 1.5, neglecting entirely the engine loop. One of the purposes of this thesis was to consider the entire system as a unity. Major consideration is given to optimal determination of inputs to box (3). For example, Chapter 9 presents graphical and analytical methods for determining optimum engine gimbal angle* for entry by impulsive thrust application at the trajectory modification point from both circular and elliptical reconnaissance orbits.

1.9 Some Suggested Guidance Systems

Various guidance schemes have been proposed for entry missions. Among the more interesting ones are:

(1) Eggleston and Cheatham[8] suggest entry in a variable-lift vehicle flying at near 90° angle of attack in order that large drag forces may be experienced, thus ensuring rapid entry. By use of small amounts of lift, the decelerations may be maintained at moderate levels**

---

* Optimum engine gimbal angle is defined as that angle for which errors in gimbal orientation result in minimum range error.

** See Chapter 9 of this thesis for a quantitative discussion of the effect of lift in reducing accelerations.

and, at the same time, navigational errors may be corrected. By keeping the total drag high, prolonged periods of time and heating in the atmosphere are avoided.

Two trajectory control schemes were proposed by these authors, one involving acceleration control and the other range control. Figs. 1.6 and 1.7 show functionally these two concepts. Analytical solutions derived in this thesis are readily adapted for preliminary investigation of either of these guidance schemes. Range expressions as a function of time derived in Chapter 9, for example, provide a simple method for determining range-to-go.

(2) Detra, Riddle, and Rose[9] envision a guidance scheme for the non-lifting vehicle which is identical in functional form to that shown in Fig. 1.7. The computation requirements are considerably different, however, since range control is effected through varying the drag parameter $(\frac{M}{C_D S})$. Changes of drag parameter by 20 to 1 are possible with a variable high-drag umbrella. The input $\Delta\alpha$ to the control system in Fig. 1.7 is replaced by $\Delta(\frac{M}{C_D S})$ in this particular system.

(3) Webber[10] suggests the use of ballistic perturbation theory to simplify the complexity of the guidance computer during the atmospheric gliding portion of the entry trajectory. The object of the perturbation theory is to calculate the behavior of the entry vehicle near a nominal trajectory.* If the actual flight conditions differ from those for the nominal trajectory, the trajectory of the vehicle will not lie along the nominal path. If the disturbing influences are small,

- - - - - - - - - - - - - - - -

* The nominal trajectory is a certain trajectory with specified initial conditions, atmospheric conditions, and programmed lift and drag.

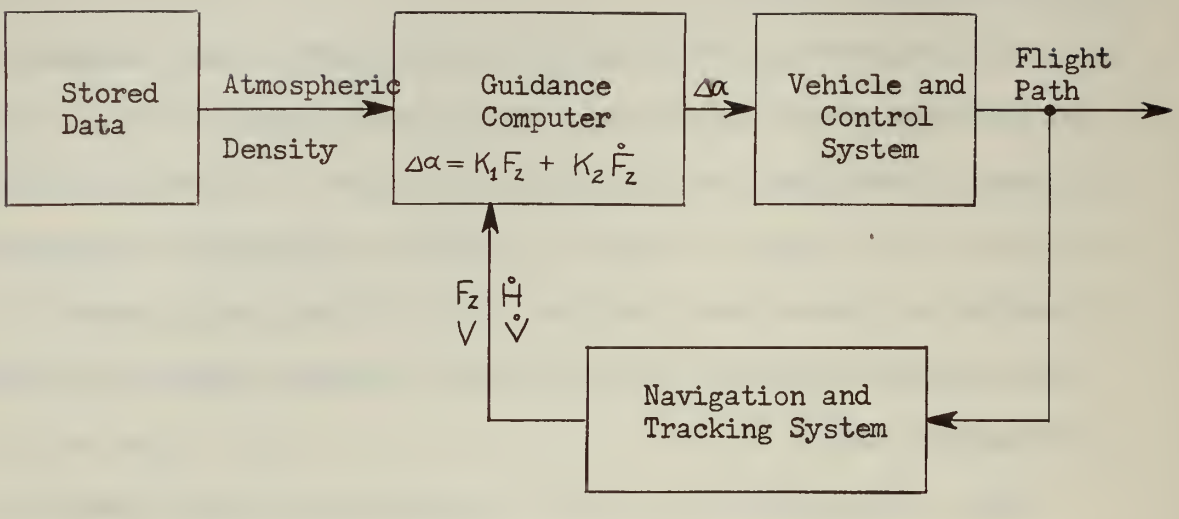

$\Delta\alpha$ = change in angle of attack from trim condition.

F_z = normal accelerations, external specific force measured along z-axis

$\dot{F}_z$ = computed rate of change of normal accelerations, computed from measured values of F_z, V, $\dot{V}$, $\dot{H}$, and stored data on atmospheric properties as a function of altitude.

K_1, K_2 = constants

V, $\dot{V}$ = velocity and time rate of change of velocity

$\dot{H}$ = time rate of change of altitude.

Fig. 1.6 Guidance System which Commands Angle of Attack from Normal Specific Force Measurements

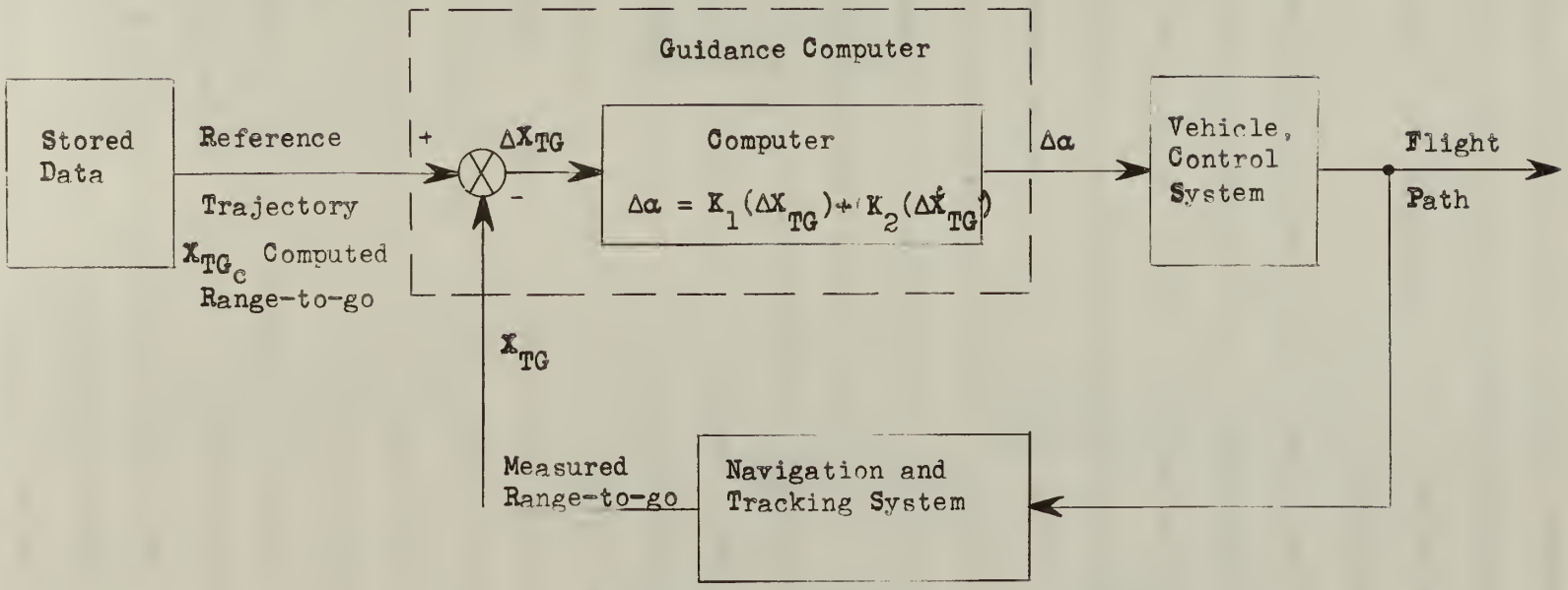

Fig. 1.7: Guidance System which Commands Angle of Attack from Error in Range-to-go from Reference Trajectory

the perturbed trajectory will be in the vicinity of the nominal trajectory. The nearness to a calculated, known trajectory is the basis of linearization of the equations of motion for the perturbed trajectory; the perturbed system is then represented as a linear system with time-varying coefficients.

Fig. 1.8 is a functional representation of Webber's guidance scheme. For convenience, the stored data and the guidance computer boxes are shown in two parts. Dashed lines represent information flow early in the flight; solid lines represent information flow during the major portion of the mission. This guidance system is conceived as one for which the nominal trajectory is specified in terms of acceleration components in the lift and drag directions. Because inaccuracies in specification of vehicle aerodynamic characteristics and in specification of atmospheric properties are anticipated, an exact nominal trajectory is not prescribed in advance of the mission. Instead, it is initially stored as a mathematical model which requires determination of eight parameters before the nominal trajectory is specified.

Early in-flight measurements of vehicle temperatures and accelerations are used to compute the parameters needed to specify the nominal trajectory. This concept is attractive for entry into atmospheres in which the density characteristics are subject to considerable uncertainties. In essence, the nominal trajectory is determined in the early phase of the mission where the ability to alter the trajectory is limited due to small gas-dynamic forces, but where forces and temperatures are of sufficient magnitudes to be measurable. These measurements are used to determine atmospheric properties actually being encountered.

Once the nominal trajectory is computed, this information is used

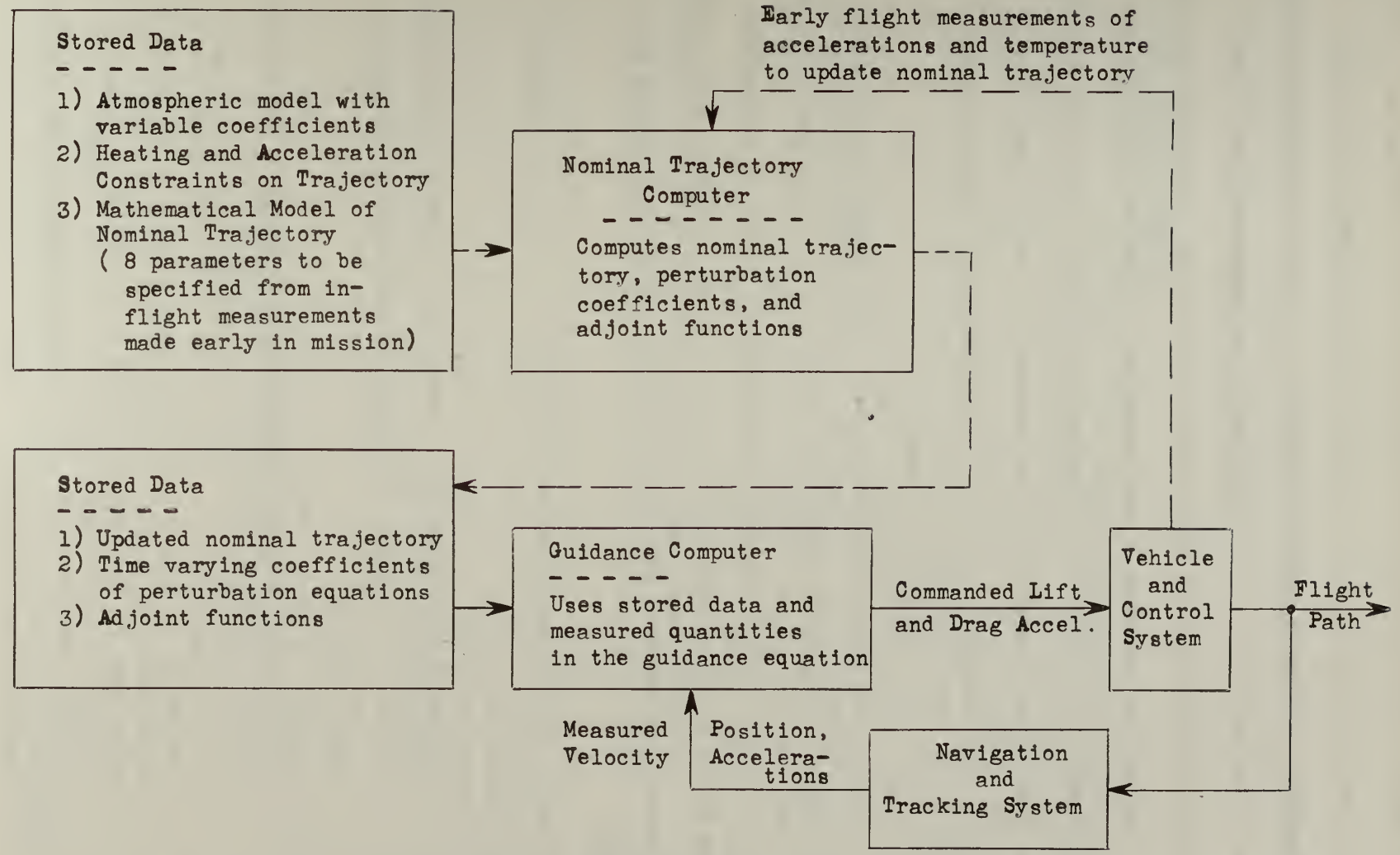

Fig. 1.8: Guidance System Which Utilizes Ballistic Perturbation Theory

to determine the time-varying coefficients of the perturbation equations. The guidance problem cannot be solved, however, without additional information. By using adjoint functions, a guidance equation is derived which is amenable to solution. A fundamental end condition of the guidance equation is that range error vanish at the vehicle's destination.

The nominal trajectory, the perturbation equation coefficients, and the adjoint functions are computed and stored early in the mission. These quantities, together with measurements of vehicle position, velocity, and accelerations from the navigation and tracking system enable solution of the guidance equation.

A particular guidance system is not investigated or proposed in this thesis. Approximate analytical techniques are developed which may be applied to any proposed system, particularly early in the design stages where an understanding of the physical relationships are required and where approximate answers (with a known degree of accuracy) are needed.

Design of instrumentation of any physical problem is composed of three fundamental phases:

(1) Statement of the problem - investigation and analysis of the problem to determine the physical quantities and relationships involved.

(2) Determination of instrumentation requirements - translation and interpretation of physical relations into requirements for design of free and flexible components. These requirements must be determined subject to constraints imposed by the physical problem and by any fixed components in the system.

(3) Design of instrumentation - design and testing of specific

components and equipment to realize the previously determined requirements.

In this thesis, items 1 and 2 above are considered for the general entry mission into the atmosphere of a planet.

1.10 Control System

Detailed examination of the control system and vehicle, lumped together in box (3) of Figs. 1.4 and 1.5, is not a subject of this thesis. The design of these elements is a strong function of the interaction of their stability and control characteristics. It should be noted, however, that guidance and control system design cannot proceed efficiently without unified consideration of all elements of the system because of the complex inter-relationships existing among them.

The control system and vehicle present a severe design problem because of the operational extremes experienced during the course of a typical entry mission. Prior to atmospheric penetration, vehicle skin temperatures are low, gas-dynamic forces and moments are negligible, and the vehicle is in a free-fall condition (zero accelerations). Reaction jets, or their equivalent, offer an effective means for attitude stability and control in this, the Keplerian portion of the trajectory. In the Intermediate Phase of the trajectory, vehicle accelerations due to gas-dynamic forces are large enough to be detectable, yet small enough that only minor trajectory alterations are possible without thrust augmentation. A combination of reaction and gas-dynamic moments for orientation control is feasible in this operational regime. In the Gas-Dynamic Phase, vehicle temperatures rise sharply to a maximum value as the vehicle velocity decelerates to

about 0.8 of circular satellite velocity. Gas-dynamic accelerations increase to maximum values at velocities substantially lower* than that for maximum temperatures and heat flow rates.

The operational extremes experienced during entry suggest a control system that must adapt itself to the changing environment. The Conservation Parameter, defined in section 1.7, is a measurable function that has sharp behavior near the operational phase boundaries. The Conservation Parameter may be useful either as a switching function or a variable sensitivity factor to improve control system operation.

Fig. 1.9 is a partial functional diagram of one channel of a control system which uses the Conservation Parameter as an input to a logic system. The environmental logic system selects the most efficient method to implement the command input; i.e., it selects either aerodynamic controls, reaction controls, or a combination of both, and adjusts loop gains for near-optimum performance. The operation of this particular system is explained in Appendix F.

The system of Fig. 1.9 is not a "self-adaptive" control system; i.e., it does not monitor its own performance and automatically adjust itself for optimum performance in a changing environment. The system is "adaptive", however, in the sense that it uses environmental data from the guidance computer to adjust its performance characteristics. Augmenting the adaptive features of a system like that of Fig. 1.9 with

---

* For example, it is shown in Chapter 9 that a vehicle with lift-drag ratio of 1.0 experiences a maximum of 0.9 g's at about 0.2 circular satellite velocity for gliding entry into the Earth's atmosphere. A non-lifting vehicle, on the other hand, experiences more than 8 g's at about 0.5 circular satellite velocity (zero initial entry angle). If the nonlifting vehicle's entry angle is increased to 6°, maximum accelerations rise to more than 18 g's.

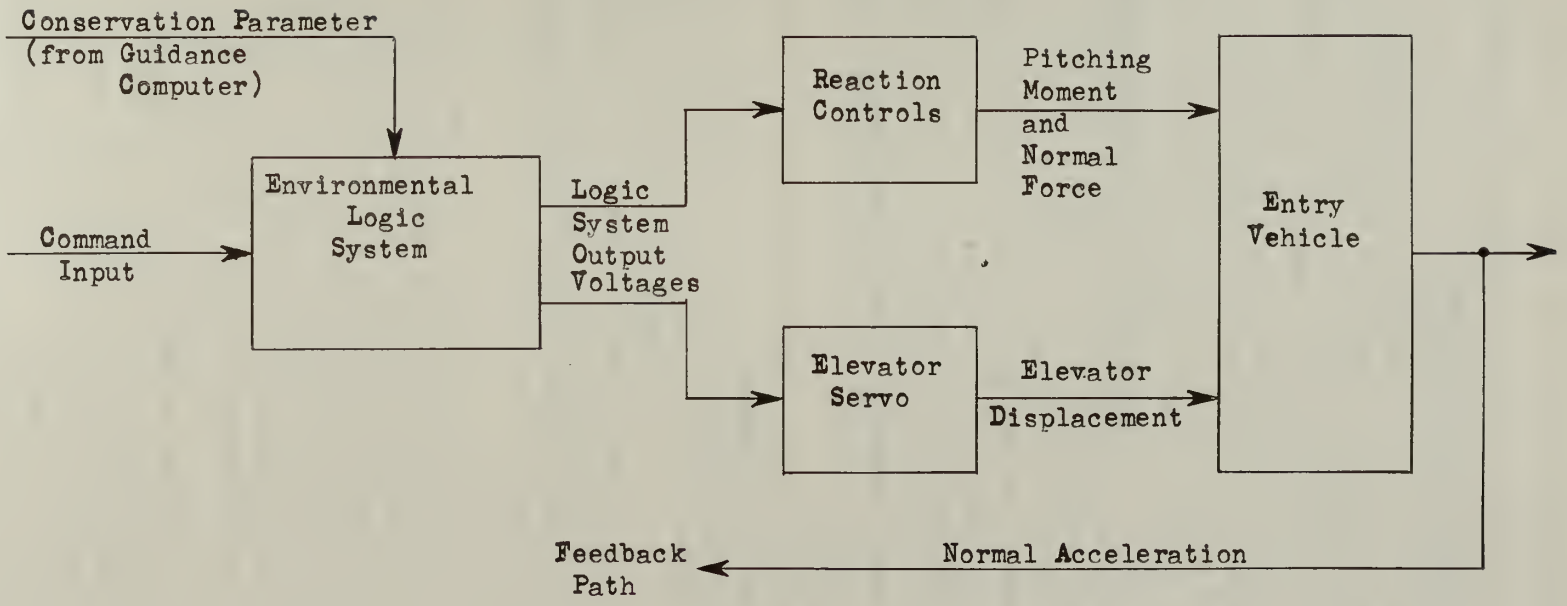

Fig. 1.9: Partial Functional Diagram of Normal Acceleration Control System which Adapts to the Operating Environment

self-adaptive inner loops to optimize control system operation may be worthy of further study.

1.11 Navigation and Tracking System

The guidance of vehicles involves the functions of indication and control[11]. The indication aspect of guidance is navigation. The correct course of action required at any given time is a function of the instantaneous position and velocity vectors; determination of these vectors is the task of the navigation and tracking system. The control aspect of guidance requires that a comparison be made of navigational data with programmed (stored) data, selection of the most appropriate action (decision-making), and executing the action prescribed.

There are three fundamental techniques commonly used for navigating astronautical vehicles:

(1) Inertial Systems;

(2) Systems relying entirely on external radiation data; viz., optical, radio, radar, and infra-red systems;

(3) Externally aided inertial systems (combination of (1) and (2)).

Methods (1) and (2) are pure systems, method (3) results in a hybrid system. The advantages of using any one of these systems in preference to any other is not debated in this thesis. It is well to consider, however, some of the characteristics of these systems.

An inertial navigation system consists basically of three specific force measuring subsystems (accelerometers) mounted on a gyro-stabilized platform and some form of computer. The stabilized platform may be either a physical platform or a mathematical (phantom) platform. One

of the difficulties encountered in using an inertial system in the free-fall phase of flight is that in the "weightless" environment of free space, the accelerometers indicate nothing, regardless of the trajectory. Disturbances due to imperfections of the gyros and accelerometers ("drift") are primary sources of error in inertial systems.

The major difference between the characteristics of an inertial system used in a low-velocity vehicle (aircraft, ships, submarines) and one used in a vehicle which operates at orbital or near-orbital velocities is that the familiar instability in the vertical (altitude) channel of low-velocity systems disappears in orbital vehicles and is replaced by instability in the horizontal (range) channel. Initial condition errors such as in altitude or velocity, concomitant with error in orbital energy, induce diverging errors in range. Constant accelerometer errors produce unbounded range errors. Young[12] shows that the order of range divergence is less for an inertially oriented accelerometer than for a range-oriented accelerometer.

Major advantages of using an inertial system are:

(1) Navigational information is based entirely on measurements made from within the vehicle; no contact with the outside world is required. Communication difficulties resulting from ionized atmospheric layers, weather, etc., have no deleterious influence on the operation of the pure inertial system.

(2) Streamlined guidance and control system design is feasible since certain measurements required in the navigation function may be used for other guidance and control functions.

The inertial navigation system may be the most desirable of the three types of navigation systems for the direct entry profile since flight times are generally short (15 min. - 2 hr.) and the major portion of the trajectory is in the Gas-Dynamic operational regime where external specific forces are measurable.

External radiation systems for navigating or tracking the vehicle use electromagnetic energy as the information medium. These methods suffer from line-of-sight limitations and propagation disturbances (such as ionized layers in the atmosphere and weather). Radio-radar systems are susceptible to man-made jamming.

In a radio-radar tracking system, the target must radiate an appropriate signal either by carrying a radio transmitter or, in the case of a radar system, by reradiating a part of the incident energy as a reflected signal. The basic measurements that can be made with a single radio or radar guidance station are range, radial velocity, and direction of the target relative to the receiving station. The entry vehicle may be either the target or the control point, depending on whether tracking is performed from within the vehicle or at some remote station.

Radio navigational systems may be of two types:

(1) Passive: A coded pulse emanating from the transmitter in the control station is received at the target, which in turn generates a signal (after a known time delay) that is returned to the control station. The target's radio beacon, in this case, is called a transponder; i.e., it transmits a signal in response to an input signal of the proper type. The time delay between the

transmission and reception at the control point serves as a measure of the target's distance from the control point. The direction of the target can be deduced from the incoming signal or by optical means. Observation of the Doppler effect on the target's signal gives the relative velocity of the target with respect to the control point along the line of sight.

(2) Active: The target generates a radio signal either continuously or intermittently. The direction to the target can be determined from this signal; the relative velocity of the target with respect to the control point along the line of sight can be determined from the Doppler shift if the transmitting frequency is known precisely. The distance to the target cannot be determined from a single control point.

Radar, too, may be of two major types: pulse radar for position determination and continuous-wave radar (Doppler) for velocity determination.

The antenna system measures the direction of arrival of the signal. Antennas can be divided into two classes, those using a single mirror to focus the energy into a small region and those using spaced antennas for interferometer measurements. The long distances traveled by the signals makes it necessary for the energy-collecting area of the antenna to be as large as possible. In general, the beam-width decreases and angular accuracy improves as the antenna area is increased.

First-time entry into the atmospheres of strange planets presents special problems in specifying position when compared to navigating

over a well-mapped planet such as the Earth. The choice of a suitable landing site must necessarily be based on reconnaissance of the planetary surface while in orbit around the planet. The orbital altitude for the reconnaissance phase must be high enough such that a prolonged orbit may persist, yet low enough that fairly accurate mapping of the terrain is feasible.

Ground-based tracking stations are of great utility for navigating vehicles over Earth. The crew of the Explorer* vehicle may find it greatly to their advantage prior to initiating entry to launch a network of radio and/or radar beacon missiles suitably dispersed over the planetary surface. Much valuable data on the atmospheric density characteristics and winds can be accumulated by tracking the missiles during their descent. The observed location on the planetary surface where these missiles ultimately land will be valuable landmarks for entry navigation. Another valuable aid to entry navigation will be from a navigation satellite left in the reconnaissance orbit prior to initiating entry. This navigation satellite may be simply a radio beacon, transponder, radar beacon, or balloon; or it may be an elaborate tracking and control center such as an orbital space platform which is the parent or carrier of the entry vehicle. The concept of a navigational satellite for external tracking data is discussed further in Appendix D of this thesis.

- - - - - - - - - - - - - - - - -

* The term "Explorer" vehicle is used in this thesis to denote a vehicle executing first-time entry into strange planets. "Strange planets" signifies natural bodies of the solar system (planets, asteroids, moons) on which a vehicle with human occupants has not previously landed. Therefore, ground-based tracking information is not available during Explorer missions.

Radio and radar tracking systems have the advantage of not being penalized by long periods of operation. This feature suggests the externally-aided inertial system as a hybrid technique for selecting the best features of each of the pure navigating and tracking systems.

1.12 System Optimization

The determination of guidance requirements for the entry mission involves a rather complicated analysis of trajectories, range sensitivity to changes in controllable parameters, uncertainties in specification of parameters such as atmospheric properties and vehicle's aerodynamic characteristics, guidance system capabilities, propulsion system, payload requirements, and system cost. It is of paramount importance in every consideration of the guidance problem that constraints, primarily those due to gas-dynamic heating and deceleration, be recognized in order not to exceed the operational limitations of the vehicle or to endanger its occupants.

One of the most important questions that must be answered is simply: "What trajectory should the entry vehicle follow; i.e., how should it be steered?" A careful formulation of this leads to problems of optimization.[13] What choice of trajectory will maximize or minimize some criterion of performance, where this criterion might be range, payload, flight time, landing point accuracy, cost, etc.? The selection of feasible systems, optimized with respect to guidance accuracy, propulsion requirements, payload, and mission cost requires a comprehensive analysis of the interaction of these parameters. These relationships might be presented as trade-off curves, showing some advantage to be gained in one parameter by varying another.

It is of fundamental importance to recognize that there is no single optimum entry trajectory that holds for all entry missions. The optimum trajectory is a strong function of the purpose of the mission and the initial conditions of the problem. If maximum payload weight is of over-riding importance, then one family of trajectories is superior to all others. If landing point accuracy is of fundamental importance, then a vastly different trajectory is dictated. If both factors are of equal importance, certain compromises are obviously required. In particular entry missions the selection of feasible systems, optimized with respect to guidance accuracy, payload capabilities, and mission cost, requires a detailed analysis of the interaction of these parameters. In this thesis the generalized guidance problem alone is considered; other mission factors are recognized when they have an important modifying effect on the requirements of the guidance system.

In many engineering problems optimization procedures are of small importance, the performance not being particularly sensitive to the choice of operating parameters.(13) This is not the case for the entry mission because system performance is extremely sensitive to small changes in design*, the system is complex with strong interactions among the different subsystems, and the number of variables influencing any single quantity is generally large enough to make intuitive decisions difficult.

Many optimization problems involve straight-forward application of

---

* For example, Chapter 9 demonstrates that large reductions in deceleration loads encountered during entry result from employing small amounts of lift.

the calculus of variations. In this thesis, one-sided constraint** expressions for stagnation point temperature and vehicle accelerations are developed for application of the techniques of the calculus of variations to the determination of extremals of arbitrary guidance functions. It should be noted, however, that many important results can be deduced without invoking the full power of the calculus of variations.

The prediction of the entry trajectory is difficult at best due to the inherent non-linearities in the statement of the problem. Analytical techniques are developed in this thesis for predicting parameters that are important in selecting the optimum trajectory and for preliminary specification of the guidance system, parameters such as the predicted time history of distance flown, range-to-go, time of flight, altitude, velocity, specific force level, atmospheric density variation, heating rates, and stagnation point temperatures under a diversity of initial conditions. Results are presented in non-dimensional form for generalized application. Accuracies and limitations of the solutions derived were determined by comparing them to more exact numerical solutions.

One of the primary purposes of this study was to provide analytical solutions of known accuracy to the engineer who is faced with the difficult task of designing an entry system. It is possible, of course, for the designer to write down complete equations of motion for complicated vehicle models, including gas-dynamic forces and moments, rigid body rotations, feedback loops in the control system, stochastic

- - - - - - - - - - - - - - - - -

** Minimum allowable acceleration loads and temperature levels are <u>not</u> constrained; maximum levels alone are constrained.

interferences, etc.; and digital computers such as the IBM 704 can provide solutions in a short time. A straight numerical approach, however, has many shortcomings in the conceptual and early design phases where an infinite number of possible trajectories and guidance schemes must be explored. One of the major difficulties is that a numerical "run" is required for each set of initial conditions. Machine calculations not only provide more detail than is generally required at this stage, but also fail to indicate straightforwardly the effect of changing various design parameters. In order to compare different guidance concepts and in order to determine the effect of various parameters on system performance, a numerical approach is time consuming, expensive, and unwieldy.

In order that the engineer understand the effect of changing various design parameters and in order to compare different guidance schemes, simple analytical results can be far more informative than a long series of machine computations. The philosophy advanced in this thesis, therefore, emphasizes the use of dynamical approximations, with specified limitations, to derive simple analytical solutions of important guidance quantities. In this way, the requirement for numerical studies may be delayed until later stages in the design process of many entry systems.

1.13: Guidance Trajectories

Related to the concept of guidance is the requirement for specifying a standard, reference, or nominal trajectory. This trajectory is the path described by a standard or nominal vehicle under standard atmospheric conditions. If the atmospheric model of the planet is

accurate, a particular entry vehicle should trace out a spatial path which is close to the nominal trajectory. Inaccurate specification of the atmospheric model and uncertain knowledge of atmospheric winds, particularly in the case of entry into the atmosphere of strange planets, are likely to be the most significant factors leading to departures from the nominal trajectory during a particular entry mission. The nominal trajectory should be specified as one for which errors and uncertainties in the atmospheric model contribute to minimum total range error. This trajectory must be chosen to optimize other requirements besides guidance accuracy, however; among these additional requirements are:

(1) Payload weight;

(2) Computational complexity required of the computer, and its effect on weight, power consumption, and reliability;

(3) Vehicle range;

(4) Flexibility in changing trajectories;

(5) Gas-dynamic heating and specific force levels encountered.

These are often conflicting requirements; hence compromises in guidance system design are generally necessary. It was emphasized in Section 1.8 that guidance is a closed loop process which includes the vehicle and its control system as part of the loop. This loop must have high enough gains such that dynamic lags are not excessive, and must have acceptable stability characteristics. The design of the guidance and control system for atmospheric entry is an excellent example of a systems problem for which the specific mission, physical constraints, available components, and detailed characteristics of the vehicle must be considered.

A number of interesting papers have been published concerning a suitable choice of entry trajectory consistent with reducing the severe heating and deceleration loads encountered in the atmosphere. Eggers[4], Gazley[14], and Chapman[15] have suggested entry by means of grazing* trajectories with vehicles of moderate lift-drag ratios. It is shown in this thesis that such trajectories may result in large errors in the location of landing for either small errors in the flight path angle or for perturbations in atmospheric density due to incomplete knowledge of the properties of the upper atmosphere.

Lees[16] suggests improvement of guidance accuracy by penetrating the atmosphere at flight path angles greater than 4°. The vehicle is then permitted to partially skip until a design maximum g-load is incurred, at which time lift is either "cut-off" or programmed such that maximum allowable acceleration loads are subsequently not exceeded. Lees' trajectory is attractive for interplanetary missions because it greatly broadens the allowable corridor for the "first-pass" entry mission**. For direct entry from stable reconnaissance orbits, Lees' trajectory has certain guidance advantages: it shifts the location of the Intermediate Phase to lower altitudes and the steep penetration angle reduces considerably the range errors which may accumulate. It is unattractive for direct entry from reconnaissance orbits because a

- - - - - - - - - - - - - - - - -

* Grazing trajectories are these trajectories for which the flight path angle, γ , is approximately zero. In the atmospheric portions of grazing trajectories, it is assumed in most analytical studies that the drag force predominates over the component of gravity forces in the flight direction.

** That is, final direct entry is achieved during the first atmospheric perturbation of the interplanetary transfer ellipse.

large amount of the initial mass of the vehicle must be invested in propellant fuel in order to achieve a substantial flight path angle in the region of initial atmospheric penetration; i.e., a large scale perturbation of the reconnaissance trajectory is required. For both first-pass entry and entry from a stable reconnaissance orbit, Lees' trajectory has the disadvantage that the lift program required in order to obtain accurate landing point control may be difficult to achieve in practice.

Kepler[17] suggests an entry trajectory which embodies many of the advantages of Lees' trajectory, plus some additional guidance advantages in the case of direct entry from the stable reconnaissance orbit. This trajectory, shown in Fig. 1.10, is similar to Lee's trajectory through Phase 2 (except lift is cut-off in horizontal flight in the Kepler trajectory rather than at a certain g-level as suggested by Lees). Kepler's phase 3 has guidance advantages over the trajectory envisaged by Lees since a lift program to hold constant altitude flight is achieved more easily than a lift program to ensure peak accelerations remain below a certain value.*

Sufficient range control may be achieved in the Kepler trajectory with vehicles of moderate lift by adjusting the phase boundary between phase 3 and 4 to correct for range errors which accumulate over the first three phases, even if atmospheric density differs substantially from predicted values. For example, Kepler shows that in entering the Earth's atmosphere from a 200 nautical mile circular reconnaissance

- - - - - - - - - - - - - - - -

* Prediction of expected future g-levels is required of the guidance system in this instance since the acceleration loads encountered in the future are a function of present trajectory adjustments.

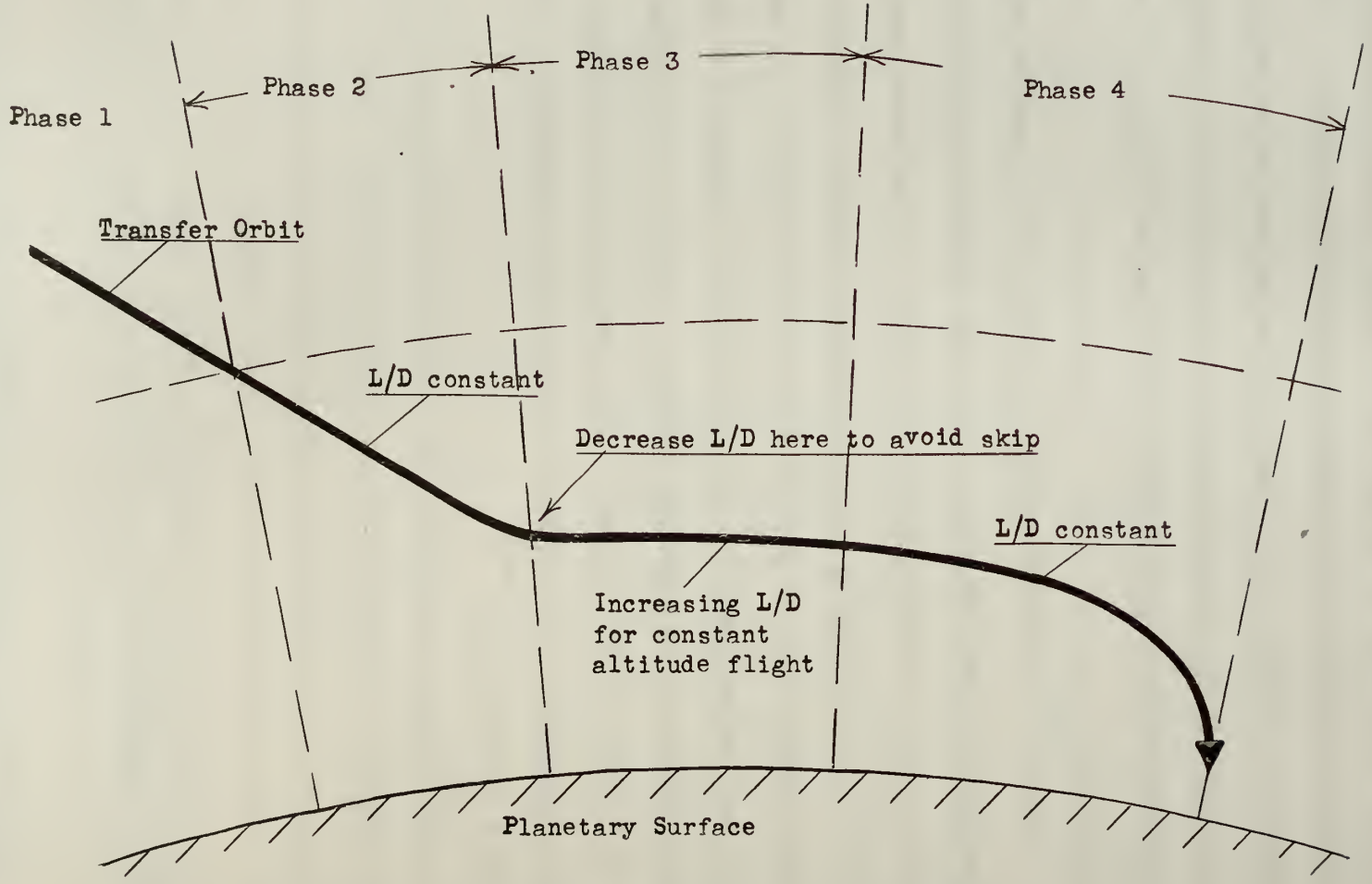

Fig. 1.10: Kepler's[17] Model Trajectory for Lifting Entry.

orbit, a 2% velocity impulse error, a 5 degree error in alignment of the engine gimbals*, and a 10% error in Phase 2 lift-drag ratio results in a total RMS error of 153 nautical miles at the boundary between phases 2 and 3. He shows that these accumulated errors are easy to erase over phases 3 and 4 without incurring excessive accelerations and heating loads.

1.14 Synopsis

Chapter 1 discusses some general concepts of guidance and control for various types of entry missions and correlates the work of this thesis with the entry mission and previous investigations in this area.

Chapter 2 advances certain specific conclusions and recommendations for further study.

Chapter 3 describes the three-dimensional kinematics of entry in two separate sets of position reference frames, the "latitude-longitude" triad, and the "instantaneous great circle" triad.

Chapter 4 discusses the three-dimensional kinematics of entry in elliptical parameters and the possible advantages of performing in-flight position and velocity computations for Explorer vehicles in these parameters.

Chapter 5 formulates a mathematical description of all forces acting on the entry vehicle which affect the three-dimensional characteristics of its trajectory. These forces are described in component form suitable for specifying the dynamical equations of motion in either of the reference frames of Chapter 3 or the elliptical parameters

- - - - - - - - - - - - - - - -

* Kepler uses a 600 ft/sec velocity impulse directed anti-parallel to the velocity vector in orbit. From Fig. 9.5 of this thesis, it is seen that rotating the engines a few degrees toward the orbital center would be more appropriate.

of Chapter 4. It should be noted that the three-dimensional dynamical equations of motion of Chapters 3 through 5 are sufficiently general to permit computer analysis of the trajectory of a lifting or non-lifting vehicle in banking or wings-level flight with variable thrust capabilities entering the atmosphere of an oblate, rotating planet with or without atmospheric winds. The figure of the planet, the gravitational model*, and the atmospheric model for important bodies of the solar system are discussed in Appendix B through E.

Solutions in closed form of the three-dimensional equations of motion for atmospheric entry cannot be obtained by any analytical techniques known at this time. As a practical matter, the trajectory was intentionally confined to a fixed plane in Chapters 6 through 10. The procedure of this thesis departs from that generally followed in dynamical studies; the usual practice is to apply the theory of planar motion before considering the additional complexity of the third dimension. The reverse procedure, as carried out here, has the advantage of clearly delineating those conditions under which planar motion is an accurate approximation.

Derivation of the two-dimensional equations of motion in a number of useful forms, including both differential and integral forms with energy and angular momentum as dependent variables, is described in Chapter 6.

Chapter 7 discusses trajectory constraints imposed by vehicle

- - - - - - - - - - - - - - - - -

* Quantitative description of gravitational harmonics of the pear-shaped model of the Earth are contained in reference (18).

heating rates, stagnation point temperatures, and human acceleration tolerances. These one-sided constraints are represented in both analytical form and graphical form (in the velocity-altitude plane) for entry into atmospheres of terrestrial planets. Altitudes at which specific force level exceeds minimum detectable levels are also discussed in Chapter 7 for various vehicle, accelerometer, and planet combinations.

The generalized entry trajectory is examined in Chapter 8 from a standpoint not presented previously in dynamical studies of atmospheric entry. A "Conservation Parameter"* was selected on the basis of its sharp and predictable behavior as an index of the influence of the atmosphere on the trajectory. This parameter is used to separate the trajectory into three separate operational regimes - the Keplerian, Intermediate, and Gas-Dynamic phases - and to define boundary conditions between phases. All known analytical studies conducted to date omit the Intermediate Phase.** Methods for computing the Conservation Parameter are suggested, and uses for this parameter as a switching function for guidance computations and as an environmental index for adaptive control systems are advanced.

Chapter 9 is devoted to a comprehensive investigation of each of the three separate phases of flight. Closed form analytical solutions of guidance parameters and constraints are obtained for the Keplerian

- - - - - - - - - - - - - - - -

* This parameter is defined in section 1.7 and is used frequently in Chapter 8 and subsequent chapters.

** It is shown in Chapter 8 that the Intermediate Phase spans an altitude band approximately 20 miles wide (for Earth) at an initial altitude which is a sensitive function of flight path angle. Specific force levels encountered in traversing the Intermediate Phase increase approximately 100 times from an initial value of 10^{-4} to 10^{-2} g's (depending on flight path angle).

Phase (for vehicles launched from both circular and elliptical reconnaissance orbits) and for the Gas-Dynamic Phase under initial conditions which induce skipping, gliding, and ballistic flight. Closed form solutions cannot generally be derived in the Intermediate Phase; special solutions in this phase for particular flight programs are discussed.

Chapter 10 describes a method original with this thesis for obtaining a continuous solution of guidance parameters for lifting and non-lifting vehicles initially in circular and degenerate elliptical reconnaissance orbits. Some features of entry trajectories not generally recognized are disclosed in this analysis, which leads to solutions in terms of modified Bessel functions of the first kind.

Chapter 2

Conclusions and Recommendations for Further Study

2.1 Conclusions

The investigation described in subsequent chapters of this thesis analyzes atmospheric entry from both a general and specific point of view. The investigation is general in the sense that a particular entry vehicle, guidance system, or entry trajectory is not examined or proposed. General analytical techniques are developed which may be useful in preliminary analysis of guidance requirements for any particular system. The investigation is specific in the sense that elements which are common to all atmospheric entry systems are examined in detail. All entry missions are characterized, for example, by the fact that the vehicle traverses the three separate operational regimes defined in Section 1.7, the Keplerian, Intermediate and Gas-Dynamic Phases. The time spent in each of these flight regimes is very much a function of the initial conditions of the problem, the trajectory that is to be flown, and the characteristics of both the vehicle and the planetary atmosphere.

The Intermediate Phase of flight has not previously been examined in the literature. This flight regime is defined in this thesis and its importance for a general understanding of the dynamics of entry is

discussed in considerable detail. It is shown that, from the guidance standpoint, the Intermediate Phase cannot be ignored in the direct entry profile and is the most important single phase in the degenerate orbital profile.

All entry missions may be viewed as falling into one of two general categories:

(1) The direct entry profile:

This atmospheric entry trajectory is characterized by sequential transition from Keplerian flight through the Intermediate Phase into Gas-Dynamic flight.

(2) The degenerate orbital profile:

This atmospheric entry trajectory consists of a series of braking passes through the outer reaches of the atmosphere in order to reduce the energy level preparatory to final direct entry.

The direct entry profile is the result of either:

(1) Large scale perturbations of a stable reconnaissance orbit by means of retro-rocket thrust.

(2) Controlled first-pass entry at the termination of the interplanetary transfer ellipse.

The degenerate orbital profile results if the vehicle at perigee possesses an energy excess over the energy level corresponding to circular orbital flight. This situation may occur under a variety of mission concepts:

(1) If the vehicle is launched from the surface of the planet for the purpose of making a number of orbits around the planet and re-entering, the degenerate

orbital profile results when the energy at engine cut-off in the launch phase exceeds circular orbital energy.

(2) In the case of interplanetary operations in which the high energy level of the vehicle in the interplanetary transfer ellipse is to be reduced by atmospheric braking, the degenerate orbital profile follows first perigeal passage through the planetary atmosphere if the energy transfer is sufficient during this passage for the planet to capture the vehicle.

Flight times in the direct entry profile are short, generally ranging from 15 minutes to two hours, while in the degenerate orbital profile the time of flight may run from two hours to a number of days.

Guidance parameters and constraints for the direct entry profile were developed in Chapter 9 of this thesis by examining separately each of the three operational phases. The Conservation Parameter* was used for purposes of matching boundary conditions between phases. It was shown in Chapter 9 that the Intermediate Phases is the most difficult phase from the guidance standpoint because none of the simplifications in the equations of motion permitted in the Keplerian and Gas-Dynamic Phases of the trajectory are warranted.

Chapter 9 shows that the trajectory in the Gas-Dynamic Phase is a strong function of the initial flight conditions at the onset of this phase and of the lift-drag characteristics of the vehicle. Three basic trajectory patterns are possible:

- - - - - - - - - - - - - - - - -

* The Conservation Parameter was defined in Section 1.7 and is discussed in detail in Chapter 8.

(1) Ballistic trajectory: Non-lifting vehicle with large initial flight path angle.

(2) Glide trajectory: Lifting vehicle with zero initial flight path angle.

(3) Skip trajectory: Lifting vehicle with finite initial flight path angle.

Approximate analytical solutions were developed in this thesis for each of these classes of trajectories. Fig. 9.7 shows the conditions under which these approximate analytical soltuions are an accurate representation of the trajectory when compared to numerical solutions.

It is interesting to note that the range, stagnation temperatures, and vehicle decelerations are independent of the exponential decay parameter, K, of the planetary atmosphere in the special case of the gliding trajectory.

Chapter 10 examines the trajectory of a vehicle in the degenerate orbital profile. Results were presented in dimensionless form suitable for analysis of entry into the atmosphere of any planet. Two separate trajectory phases were examined:

(1) The circularization phase for the degenerate elliptical orbit.

(2) The entry phase which follows the circularization process.

In the special case where the vehicle is initially at circular orbital velocity, the first of these two phases obviously does not exist.

The solution for altitude during the circularization process was derived as equation (10-79). This solution was written in terms of a number of constants which depend on the initial conditions of the problem and on the characteristics of the vehicle. Some of the

important constants in this equation were written in terms of Bessel functions. Since these functions are tabulated, numerical answers to the resulting equations are easily obtained. The time variation of perigeal and apogeal altitudes were given in equations (10-81) and (10-83) and the rate of decay for most practical problems is described by equations (10-84) and (10-85). Analytical representation of other quantities which are important in the conceptual and preliminary design stages of guidance systems are summarized in equations (10-86) through (10-94).

It was shown in the analysis of the circularization phase that the drag characteristics of the vehicle are important in specifying the resulting trajectory and that the lift characteristics of the vehicle are relatively unimportant. It was shown that, within the approximations made in the analysis, lift does not enter in the specification of the decay rates of apogee and perigee. Perigeal altitude, to a first order, remains essentially constant. The major difference between the decay rate of apogee and perigee is that the perigeal decay rate is proportional to the <u>difference</u> of two near-equal large numbers* while apogeal decay rate is proportional to the <u>sum</u> of these same numbers.

The solution for altitude in circular orbital entry was given by equation (10-41). This solution was written in simplified form suited to almost all practical problems as equation (10-47) and (10-48). It was shown in this thesis that a true circular orbit or a linear decaying

- - - - - - - - - - - - - - - - -

* Perigeal decay is proportional to $(I_o - I_1)$, where I_o and I_1 are the first two modified Bessel functions of the first kind with an argument that is generally greater than 10.

circular orbit cannot exist even under idealized conditions of injecting a vehicle exactly at circular orbital velocity above a spherical planet. The influence of the atmosphere on the dynamics of energy transfer result in undamped oscillatory motion in altitude and flight path angle.

The analytical solutions derived in Chapter 10 were compared to machine-computed numerical solutions under a variety of initial conditions. It was shown that the analytical solutions give an accurate history of the resulting motion except after relatively long periods of time. The analytical solutions depart from more accurate computer solutions only after there is a significant increase in atmospheric density from the assumed initial value as a result of altitude loss during entry. This limitation on the solution may be largely overcome by periodically starting the problem over again under a new set of initial conditions in accordance with the procedure outlined in Chapter 10.

One of the troublesome factors arising in the design of guidance systems for missions of the degenerate orbital type is the undamped oscillations in altitude and flight path angle due to the dynamics of energy transfer between vehicle and atmosphere. Quantities such as total energy, orbital eccentricity, and angular momentum, which have monotonic behavior (generally as a series of steps in the vicinity of perigee), are more suited for minimal guidance system design than are quantities which characteristically behave in an oscillatory manner. Management of the energy history, for example, is feasible by command changes in the aerodynamic configuration of the vehicle; i.e., the lift and drag characteristics are varied by changing the vehicle geometry or angle of attack.

Chapters 4 and 5 examine the three-dimensional dynamics of entry in terms of parameters of a time-varying ellipse which instantaneously matches the position and velocity vectors of the vehicle. This technique is not new[20][21]. The particular elliptical parameters chosen in this thesis, however, are original and are shown to have the distinct advantage of considerable simplification in the resulting equations of motions and at the same time are free of singularities in the special case of circular orbits (eccentricity equal to zero). The parameters selected were as follows:

(a) Orientation of the instantaneous ellipse:

(1) Inclination of the orbital plane with respect to the equatorial plane.

(2) Longitude of the ascending line of nodes.

(b) Specification of the instantaneous ellipse:

(3) Angular momentum.

(4) $\varepsilon_1 = \varepsilon \cos\theta$

(5) $\varepsilon_2 = \varepsilon \sin\theta$

where ε is eccentricity of the instantaneous ellipse and θ is true anomaly.

(c) Position of vehicle in the instantaneous ellipse:

(6) Angle in the plane of the ellipse from the line of nodes to vehicular position.

It is shown in Chapter 6 that the entry trajectory is confined to a single plane in space only if lift, drag, and thrust are programmed such as to maintain $\dot{\psi}$ and $\dot{\lambda}_{IT}$ equal to zero. In the special case of

an equatorial trajectory ($\psi = 0$), planar motion follows if:

(1) Components of atmospheric winds normal to the trajectory plane are zero.

(2) The angle of bank of the vehicle is zero.

(3) There are no components of thrust normal to the trajectory plane.

It was concluded in this thesis that the optimum engine thrust program for entry is a strong function of mission objectives. There is no single optimum thrust program that is applicable to all entry missions.

If the vehicle is in a stable reconnaissance orbit, and if maximum payload weight is an overriding requirement for the mission, then the minimum energy trajectory is desired; i.e., it is desired that entry be effected with minimum expenditure of propellant mass. In the stable reconnaissance orbit, minimum propellant mass is expended by generating retro-thrust tangentially at apogee. As a result of this reduction in velocity at apogee, the perigee next following will be at a lower altitude. By generating enough thrust for the perigee to drop within the sensible atmosphere, the degenerate reconnaissance orbit is established. Controlled entry is possible from the degenerate reconnaissance orbit by varying the drag parameter.

If payload requirements are not as critical as the requirement for a relatively short time of flight, or if the vehicle has only modest capabilities for changing its aerodynamic characteristics, then the minimum energy profile is not necessarily the most efficient method for satisfying mission objectives. Under these conditions, a second retro-thrust application at perigee, in addition to the initial thrust

perturbation at apogee, is a more suitable mission concept than the minimum energy profile. This scheme for the entry mission indudes the direct entry profile.

If payload capabilities of the entry vehicle are secondary to stringent requirements on landing point accuracy, the initial retro-thrust application at apogee in the reconnaissance orbit may be increased a sufficient amount to cause the following perigee to fall beneath the surface of the planet. For example, if the propellant mass expended at apogee is approximately twice that required to cause the perigee to fall within the atmosphere, then the entry transfer ellipse will intersect the atmosphere after the vehicle travels approximately one-fourth of the distance around the planet rather than one-half. The flight path angle at atmospheric penetration is considerably greater under these conditions than when lesser amounts of fuel are expended, hence variations in atmospheric density from standard will result in much lower range errors. This mission concept has advantages from the guidance standpoint, but these advantages are paid for in terms of payload capabilities.

Chapter 9 discusses analytical and graphical methods for determination of range sensitivity to errors in magnitude and direction of the thrust vector generated by the retro-rocket system for entry from both circular and elliptical reconnaissance orbits. Figs. 9.5 and 9.6 show the vacuum ground range for the particular case of entry from a circular reconnaissance orbit from a dimensionless altitude of approximately 0.0758 (corresponds to 300 mi. altitude in the case of entry to the surface of Earth). These figures show that a given range may be obtained with a particular velocity impulse at two distinct engine

deflection angles. Minimum errors in range accrue, however, if the engine is aligned in such a direction as to obtain minimum range; engine deflection angle is unique and single-valued for minimum flight range and is a two-valued function for all ranges in excess of this minimum. These figures also show that the capability to reduce total range is less effective as the impulsive velocity level is increased. At high impulsive velocity levels, however, range is less sensitive to errors in engine alignment.

It is shown in this thesis that, from the guidance standpoint, the altitude of the sensible planetary atmosphere depends strongly on flight path angle, lift, drag, and density characteristics of the vehicle. The heating and deceleration loads which accompany high velocity entry into the atmosphere are strong functions of the initial penetration angle and the design characteristics of the vehicle.

The build-up of appreciable heating and deceleration loads are two of the most important effects encountered during entry of a vehicle into the planetary atmosphere. These manifestations of energy transfer from the vehicle to the planetary atmosphere are examined in this thesis from the standpoint of the restrictions they impose on the allowable guidance trajectories. Both the deceleration loads and the heating rates are most severe when there is a combination of high atmospheric density and high vehicular velocity. It is therefore necessary that the guidance system operate in such a way as to prohibit high velocities from persisting down to low altitudes. This undesirable condition most likely will occur if the flight path angle is large and the approach velocity is very great.

The velocity of the vehicle at atmospheric penetration depends on

the type of entry mission. If atmospheric penetration follows interplanetary transfer, then the velocity at penetration is of the order of escape velocity. If entry is initiated from a planetary reconnaissance orbit, then the velocity at atmospheric penetration is of the order of orbital velocity. The velocity at initial atmospheric penetration can be changed a significant amount only by large scale thrust perturbations; this leads to severe penalties in terms of payload capabilities.

The flight path angle, on the other hand, may generally be selected at a smaller weight penalty, provided thrust perturbations are generated at the proper time and in the proper direction. For example, a small thrust perturbation during the interplanetary transfer ellipse (when the vehicle is far from its destination planet) can change the flight path angle at initial atmospheric penetration a very large amount. It must be emphasized, however, that small errors in thrust perturbations at this point can lead to gross errors in penetration angle; guidance accuracy requirements are more stringent when the system is highly sensitive to small control actions.

Selection of the best entry profile for a given mission requires analysis of the coupling of payload requirements, aerodynamic characteristics, range sensitivity to control actions, vehicular heating rates, deceleration loads, and effects of errors and uncertainties in the knowledge of the physical characteristics of the planet and the vehicle.

A shallow flight path angle (tangential approach) tends to limit the region of high velocities to high altitudes. Consequently, choosing a shallow trajectory tends to minimize heating rates and deceleration loads encountered. Inaccurate knowledge of the density characteristics

of the planetary atmosphere, however, may lead to considerably greater range errors for entry at shallow flight path angles than for steep flight path angles. It is shown in this thesis that the flight path angle at atmospheric penetration must be selected as a compromise between two conflicting mission requirements:

(1) Heating rates and deceleration loads are appreciably reduced at shallow flight path angles.

(2) Range accuracy is generally greater for steep flight path angles.

It is shown in this thesis that both heating and acceleration constraints must be examined in arriving at a suitable entry profile. Specific force level generally is more restrictive on the allowable operating region at lower altitudes while heating considerations are more restrictive at higher altitudes. The lower the maximum allowable heating rates, skin temperatures, and g-tolerances, the more severe are the limitations of these constraints on permissible guidance trajectories.

Measured temperatures at the surface of the vehicle may be useful as inputs to the guidance system. The temperature history for a particular entry profile may be predicted. Guidance information, particularly with respect to atmospheric properties, may be obtained by comparing measured and predicted values. Temperature readings may be more useful than accelerometer outputs in early determination of atmospheric conditions actually being encountered in flight. It is shown in this thesis that temperatures generally attain maximum values much earlier in the mission than the maximum specific force level. In most situations, the temperature level is a maximum before the specific force level exceeds a small fraction of one g.

Among the special problems associated with first time entry into the atmospheres of strange planets are requirements for:

(1) Terrain mapping and selection of a suitable landing site.

(2) Accumulation of data on the atmosphere of the planet, wind and climatic characteristics, the figure of the planet, and its gravitational properties.

(3) Provision for augmentation of guidance measurements made from within the vehicle with data derived via external radiations.

It was concluded in this thesis that the above requirements suggest an entry system that embodies the following features:

(1) Setting the entry vehicle up in a stable reconnaissance orbit in order to:

  (a) Map the surface of the planet as thoroughly as required prior to initiating entry.

  (b) Provide considerable freedom in the selection of the time and location of the point for initiating controlled entry.

(2) Launching a navigation satellite from the entry vehicle while it is still in the reconnaissance orbit; this satellite may be tracked during the course of entry in order to provide position data on the entry craft.

(3) Launching radar and/or radio beacon missiles from the reconnaissance orbit to the planetary surface before initiating entry in order to:

  (a) Provide data on atmospheric density and wind characteristics by tracking the missiles as they

descend to the surface of the planet.

(b) Establish a network of navigational landmarks on the planetary surface.

It was concluded in this thesis that there is no single optimum entry profile which applies to all entry missions. The optimum trajectory is a strong function of the purpose of the mission and the initial conditions of the problem.

2.2 Recommendations for Further Work

The investigations of this thesis provide an analytical explanation for many of the important consequences of entry of an astronautical vehicle into a planetary atmosphere under a variety of initial conditions. Emphasis was placed on features which are common to all entry missions. Many additional problems associated with atmospheric entry are worthy of extensive study. Some of these problem areas are suggested below.

(1) Constraints on Entry Imposed by Van Allen Radiation Belts

The discovery in December 1958 of belts of energetic particles trapped in the Earth's magnetic field has suggested re-evaluation of certain entry mission concepts. The radiation belts may be viewed in the context of this thesis as restricting the initial conditions of the entry mission. The direction of approach to the planet prescribes the initial orientation of the trajectory plane. If a reconnaissance orbit is part of the mission concept, the radiation belts restrict the initial values of parameters of the reconnaissance ellipse to certain maximums.

Quantitative constraints on the entry trajectory resulting from

radiation belts cannot be accurately determined until more data on these belts is published. The presence of planetary radiation belts may require that severe restrictions be established on allowable eccentricities of the first few braking passes. Because of Van Allen radiation hazards, the direct first-pass entry profile is worthy of serious consideration, even though it presents a more serious guidance problem with respect to heating and acceleration problems.

(2) Gaseous Radiation Contribution to Total Vehicular Thermal Input

In the analysis performed in this thesis, thermal inputs to the surface of the vehicle as a result of gaseous radiation were ignored in the specification of heating constraints on allowable guidance trajectories (Chapter 7); convective heating alone was considered in this thesis. In the case of small vehicles, gaseous radiation contributes very little to total thermal input[37]. For large vehicles, particularly winged vehicles at angles of attack near 90°, gaseous radiation may contribute as much as 10% of the total thermal input. Gaseous radiation heating rate was represented as equation (7-2); solution of this equation requires knowledge of the stagnation temperature of the gas and the radiation emissivity of the gas per unit path length. Simplified methods for computing thermal contributions due to gaseous radiation are not available at present. Development of analytical methods for incorporating gaseous radiation in the specification of thermal constraints on entry guidance is recommended for further study.

(3) Effects of Solar Atmosphere on Interplanetary Trajectories

Chapman[2] advances the theory that the Sun possesses a tenuous

atmosphere which extends through interplanetary space beyond the distance of the Earth's orbit. This atmosphere is believed to consist mainly of ionized hydrogen, protons, and electrons with a density of 10^3 particles per cubic centimeter in the vicinity of the Earth, considerably greater density in the vicinity of Venus, and much less density near Mars. All known studies of interplanetary trajectories performed to date have neglected any atmosphere in space; the minute drag terms may be important, however, when integrated over flight times of many months.

(4) Externally Aided Adaptive Control

The operational extremes experienced by a vehicle during entry into a planetary atmosphere suggest a control system that must adapt itself to the changing environment. Self-adaptive control of the entry vehicle was not investigated in this thesis; it was suggested, however, that data which is measured or computed by the guidance system may conceivably be utilized by the control system to augment self-adaptive features of this system. The Conservation Parameter, defined in Section 1.7, was shown in Chapter 8 to be a measurable function which has sharp and predictable behavior during the course of entry. It was suggested that this parameter may be useful as a switching function and as a variable sensitivity factor to improve control system operation by augmenting self-adaptive features of the system. A logical extension of the present work is that of examining motions about the center of mass in order to specify stability and control requirements during the course of atmospheric entry.

Chapter 3

THREE-DIMENSIONAL KINEMATICS OF ENTRY

3.1 Statement of the Entry Problem

The general problem of guidance of astronautical vehicles entering planetary atmospheres can be stated as follows:

> How can a vehicle be guided from an initial state (position, velocity) in or near a planetary atmosphere to a final state on or near the surface of the planet without compromising the structural integrity of the vehicle or endangering its human occupants (if any)?

This statement at once implies that the initial and final conditions of the problem are fundamental elements of the problem statement. Physical constraints are also fundamental to the statement of the problem and must be considered on all solutions to the problem.

3.2 A General Theory of Controlled Atmospheric Entry

The basic problem of entry appears in various forms in the literature: it may involve lifting or non-lifting vehicles, manned or unmanned missions, entry from stable or degenerate reconnaissance orbits, direct entry from an interplanetary transfer ellipse*; it may

- - - - - - - - - - - - - - - - -

* Called "first-pass entry" in Section 1.6.

involve various trajectory schemes such as glide decay or a trajectory separated into various phases each with a specific guidance program**. The diversity of approaches taken in studying the entry problem has resulted in the growth of philosophies with many elements in common and other elements at odds. In general, the written matter describing a general or specific technique has dealt with one or a few entry mission concepts. It is sometimes very difficult to compare these approaches on any common ground because of the differing approaches taken toward solving the same basic problem.

All of these concepts of the entry mission are simply variations of the same single basic situation: the guiding of a manned or unmanned vehicle from some initial point at which the decision is made to initiate controlled entry into the planetary atmosphere to the point at which its dynamical state is suitable for either impact or landing on the planetary surface. Underlying this situation is a certain element of prediction; control actions instituted at one time have a distinct influence on the dynamical state of the vehicle at some later time.

It was shown in Chapter 1 that all entry profiles may be considered as falling into one of two major classes:

(1) The direct entry profile;

(2) The degenerate orbital profile.

This thesis advances a generalized treatment of controlled entry into planetary atmospheres in the following manner:

(1) The entry guidance problem is stated. This problem is the same regardless of the mission concept or the instrumentation

- - - - - - - - - - - - - - - - -

** See Fig. 1.10, for example.

system chosen for the purpose of solving the problem.

(2) The fundamental physical parameters that are available to solve the problem are discussed. The many different mission concepts and instrumentations systems are distinguished one from another by the:

(a) Initial conditions chosen in setting up the problem;

(b) Methods by which these fundamental physical parameters are utilized in arriving at a solution.

(3) Physical constraints on the problem of atmospheric entry are discussed. These are truly part of the statement of the problem since they must be recognized at all times in its solution; discussion of physical constraints are enough of a subject in themselves, however, to warrant a separate chapter in this thesis.

(4) Dynamical elements which are common to all entry missions are examined. The investigations performed in this thesis led to the separation of all trajectories into three operational regimes and to the definition of an environmental index, the Conservation Parameter, to define precisely the boundary conditions between phases.

(5) Approximate methods for predicting quantities which are important in the conceptual and early design phases of guidance systems are discussed for both of the major classes of entry profiles.

Item (1) above is discussed in chapters 3 and 4, item (2) in chapter 5, item (3) in chapter 7, item (4) in chapter 8, and item (5) in chapters 9 and 10.

3.3 Kinematics of Entry

The atmospheric entry problem is expressed in terms of its dynamics (forces) and kinematics (velocities). The dynamics of various mission concepts are different; this subject is considered in subsequent chapters of this thesis. The forces may be measured and controlled in many different ways. The major portion of the current unclassified literature which is concerned with the problem of atmospheric entry is devoted to advancing schemes for controlling these forces. A particular lift or drag program, for example, may induce a trajectory which has some desirable qualities under a certain set of initial conditions. Instrumentation methods for

(1) Measuring these forces,

(2) Controlling the forces,

(3) Establishing stabilized reference frames,

(4) Selecting the most convenient reference frame for computation purposes

are dealt with much less frequently in the unclassified literature. Comprehensive systems studies are generally concerned with a specific mission concept and/or vehicle; as a result, military security classifications are usually assigned to such studies.

Kinematics is the study of motion of particles and rigid bodies without consideration of the forces required to produce these motions. The kinematical statement of the entry problem is common to all mission concepts; it is basically a description of the geometry of the problem. The three-dimensional kinematics of the entry vehicle, considered as a point mass, is described in two separate guidance grids in this chapter.

3.4 Coordinate Systems

Inherent with any investigation of vehicle guidance is the requirement that a suitable set of coordinate frames* and trajectory parameters be chosen to describe the motion.

Fig. 3.1 shows three separate planet centered coordinate systems:

(1) Planet Centered Inertial Frame (subscript I):

Newton's laws are valid in an inertial frame. The use of a planet centered inertial frame is justified because gravitation and acceleration effects are indistinguishable.

(2) Planet Reference Frame (subscript 0):

Establishes the orientation of the planet with respect to the inertial frame.

(3) Instantaneous Trajectory Plane Frame (subscript T):

Establishes the orientation of the instantaneous plane of the trajectory with respect to the inertial frame. The orientation of the trajectory plane changes with time; the plane is normal to the vector cross product of the position and velocity vectors of the vehicle ($\bar{R}$ and $\bar{V}_I$, respectively**).

In order to analyze the trajectory of the entry vehicle, it is convenient to describe the motion in spherical polar coordinates. Reference frames for this purpose are usually selected with one axis along the radius vector from the center of the planet to the point at

- - - - - - - - - - - - - - - - -

* In this thesis, "frame", "reference space", "frame of reference", etc., are used synonymously.

** V_I denotes velocity measured with respect to inertially fixed coordinates.

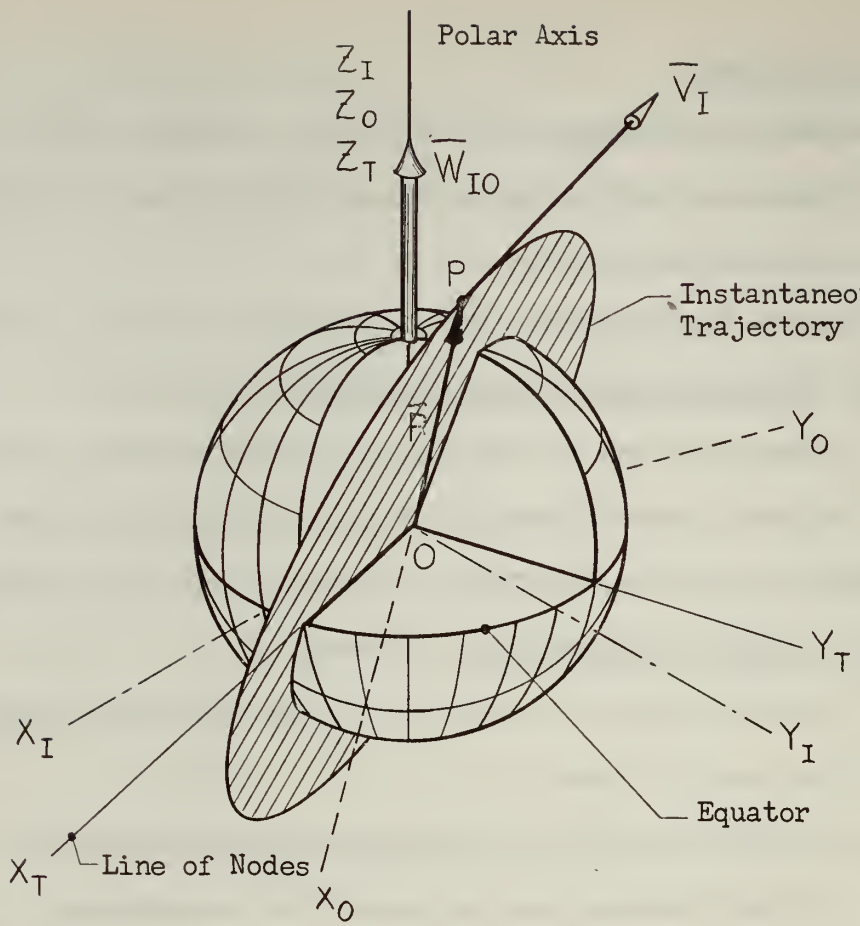

Planet Centered Inertial Frame: Centered at the center of the planet and sidereally nonrotating relative to the "fixed stars". X_I and Y_I are in the equatorial plane and Z_I is directed along the polar axis (North).

Planet Reference Frame: Centered at the center of the planet and nonrotating with respect to the planet. This frame rotates about the planet's polar axis relative to the inertial frame at the planet's daily sidereal rate. X_O and Y_O are in the equatorial plane and fixed with respect to the planet. Z_O is directed along the polar axis.

Instantaneous Trajectory Plane Frame: Centered at the center of the planet. X_T is the line of intersection of equatorial plane with the instantaneous plane of the trajectory; Y_T is in equatorial plane perpendicular to X_T ; Z_T is directed along the polar axis.

Fig. 3.1: Definition of the Inertial, Planet, and Instantaneous Trajectory Plane Coordinate Systems.

which the guidance is taking place, $\bar{1}_r$. This radius vector, for the planet, Earth, is the geocentric radius. In this thesis, the term "geocentric" is used in a more general sense (i.e., "planetocentric") to identify quantities associated with the spherical polar coordinates of any planet*.

Two separate sets of guidance grids are shown in Fig. 3.2, the Geocentric Latitude-Longitude Triad ($\bar{1}_r$, $\bar{1}_\lambda$, $\bar{1}_\Lambda$) and the Instantaneous Great-Circle Triad ($\bar{1}_r$, $\bar{1}_\phi$, $\bar{1}_\psi$). The following angles are defined in Fig. 3.2:

ψ : inclination of the instantaneous trajectory plane with the equatorial plane (measured from equator to trajectory plane).

λ_{IT} : "inertial" geocentric longitude of the ascending line of nodes; i.e., angle measured in equatorial plane from X_I to X_T.

λ_{IP} : "inertial" geocentric longitude of the vehicle; i.e., angle measured in equatorial plane from X_I to entry vehicle at P.

Λ : geocentric latitude of the vehicle.

ϕ : angle measured in the plane of the trajectory (in the direction of vehicle motion) from the ascending line of nodes to the vehicle.

β : bearing angle of entry vehicle as seen by an inertially fixed observer in the vehicle; angle between North ($\bar{1}_\Lambda$) and the horizontal component of velocity (directed along $\bar{1}_\phi$).

The geocentric latitude of the vehicle, λ, is not shown in Fig. 3.2. This is defined as the angle measured in the equatorial plane from X_0 to the vehicle.

Angular relations that are useful for converting quantities from one guidance grid to the other are summarized in Table 3.1:

- - - - - - - - - - - - - - - - -

* The interpretation of "geocentric" in this thesis may be considered to be a shortening of "geometric-centric" rather than the more precise "geoid-centric".

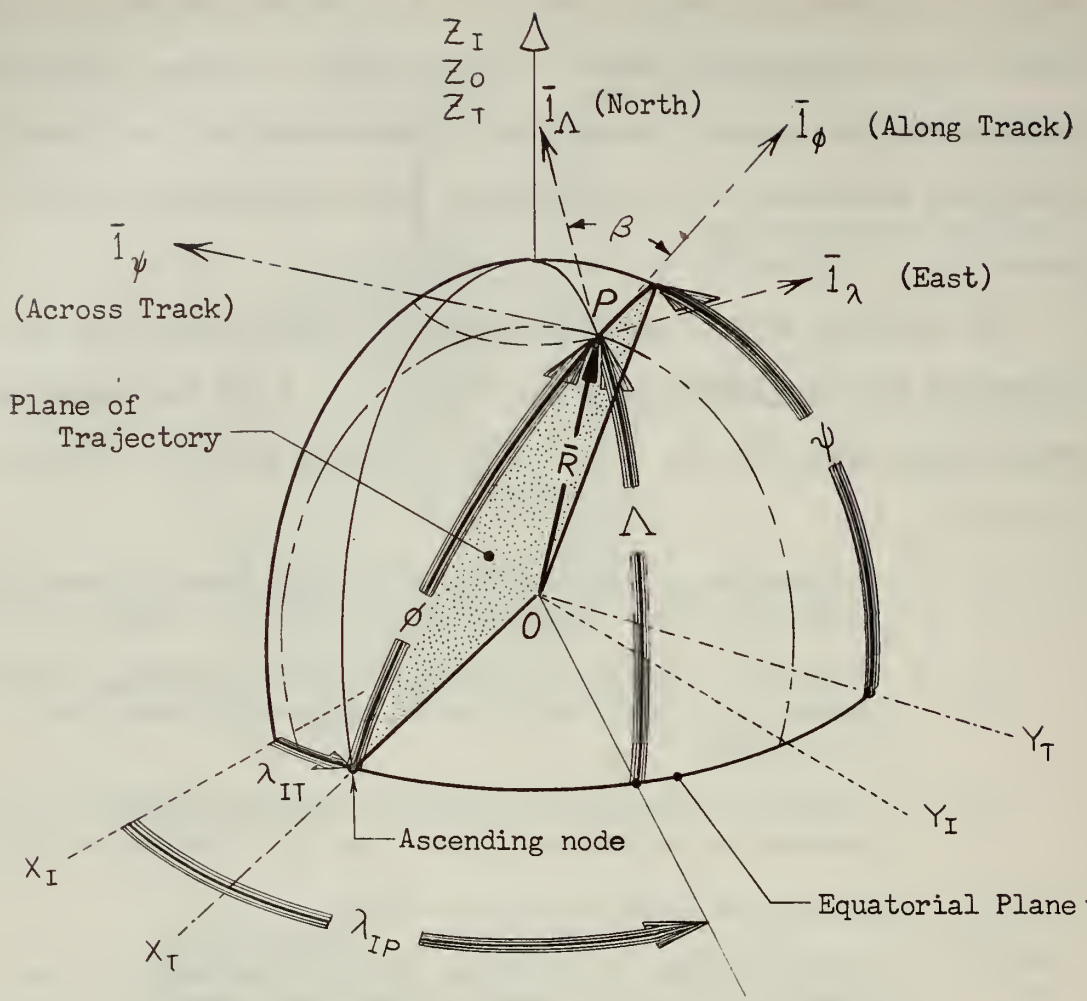

$\bar{i}_r, \bar{i}_\lambda, \bar{i}_\Lambda$ Geocentric Latitude-Longitude Triad: Orthogonal set of unit vectors centered at the entry vehicle center of mass and directed in radial, longitude, and latitude directions respectively.

$\bar{i}_r, \bar{i}_\phi, \bar{i}_\psi$ Instantaneous Great Circle Triad: Orthogonal set of unit vectors centered at the vehicle center of mass and directed in radial, along-track, and across-track directions respectively.

Fig. 3.2: Definition of Latitude-Longitude and Great Circle Guidance Grids.

Table 3.1: Angular relations among guidance grids shown in Fig. 3.2.

$$\sin\Lambda = \sin\phi \sin\psi \qquad (3.1.1)$$

$$\sin(\lambda_{IP}-\lambda_{IT}) = \frac{\sin\phi\cos\psi}{\sin\Lambda} \qquad (3.1.2)$$

$$\cos(\lambda_{IP}-\lambda_{IT}) = \frac{\cos\phi}{\cos\Lambda} \qquad (3.1.3)$$

$$\sin\psi\cos\phi = \cos\Lambda\cos\beta \qquad (3.1.4)$$

$$\cos\psi = \cos\Lambda\sin\beta \qquad (3.1.5)$$

$$\tan\psi = \frac{\tan\Lambda}{\sin(\lambda_{IP}-\lambda_{IT})} \qquad (3.1.6)$$

Direction cosines between $\bar{l}_r$, $\bar{l}_\phi$, $\bar{l}_\psi$ system and $\bar{l}_r$, $\bar{l}_\lambda$, $\bar{l}_\Lambda$ system:

	$\bar{l}_r$	$\bar{l}_\phi$	$\bar{l}_\psi$
$\bar{l}_r$	1	0	0
$\bar{l}_\lambda$	0	$\sin\beta$	$-\cos\beta$
$\bar{l}_\Lambda$	0	$\cos\beta$	$\sin\beta$

(3.1.7)

Direction cosines between $\bar{l}_{XT}$, $\bar{l}_{YT}$, $\bar{l}_{ZT}$ system and $\bar{l}_r$, $\bar{l}_\phi$, $\bar{l}_\psi$ system:

	$\bar{l}_r$	$\bar{l}_\phi$	$\bar{l}_\psi$
$\bar{l}_{XT}$	$\cos\phi$	$-\sin\phi$	0
$\bar{l}_{YT}$	$\sin\phi\cos\psi$	$\cos\phi\cos\psi$	$-\sin\psi$
$\bar{l}_{ZT}$	$\sin\phi\sin\psi$	$\cos\phi\sin\psi$	$\cos\psi$

(3.1.8)

Navigational parameters are often measured in coordinates that are not spherical polar coordinates; examples are latitude and longitude measured with respect to astronomic and geographic* reference frames. Appendix D discusses these and other navigational reference frames, which are related to the figure of the planet. Mathematical methods for relating geographic and geocentric angles for the planets of the solar system are also derived in Appendix D. It will be noted that a numerical value of the eccentricity of the planet is required in order to convert angles from geocentric to geographic angles and vice-versa. The eccentricity of the planet is readily determined from the physical data of major bodies of the solar system summarized in Appendix B.

3.5 Kinematics of Entry in Geocentric Latitude-Longitude Coordinates

It is usual in the theory of the dynamics of rigid bodies to separate the motion of the center of mass from the motion about the center of mass. The former constitutes the study of flight performance while the latter embodies the theory of stability and control. The analytical work of this thesis is concerned specifically with performance analysis, hence motion about the center of mass is not considered.

Geocentric latitude longitude coordinates $(R, \lambda_{IP}, \Lambda)$ are a special set of spherical polar coordinates. Position of the vehicle is as follows:

$$\bar{R} = (R \cos\Lambda \cos\lambda_{IP})\,\bar{1}_{XI} + (R \cos\Lambda \sin\lambda_{IP})\bar{1}_{YI} + (R \sin\Lambda)\bar{1}_{ZI} \qquad (3\text{-}1)$$

The vector angular velocity of the center of mass of the vehicle (with

- - - - - - - - - - - - - - - - -

* "Geographic" is used in this thesis as a shortening of "geometric-graphic" rather than the more precise "geoid-graphic."

respect to inertial space) expressed in latitude-longitude coordinates is:

$$\bar{W}_{IP} = (\dot{\lambda}_{IP} \sin\Lambda)\bar{i}_r - \dot{\Lambda}\,\bar{i}_\lambda + (\dot{\lambda}_{IP}\cos\Lambda)\,\bar{i}_\Lambda \qquad (3\text{-}2)$$

The linear velocity (with respect to inertial space) expressed in latitude-longitude coordinates is:

$$\bar{V}_I = \dot{R}\,\bar{i}_r + (R\dot{\lambda}_{IP}\cos\Lambda)\,\bar{i}_\lambda + (R\dot{\Lambda})\,\bar{i}_\Lambda \qquad (3\text{-}3)$$

The Law of Coreolis is used to derive an expression for the acceleration of the vehicle:

$$\bar{A} = \left[\frac{d\bar{V}_I}{dt}\right]_I = \left[\frac{d\bar{V}_I}{dt}\right]_{moving} + \bar{W}_{IP} \times \bar{V}_{IP} \qquad (3\text{-}4)$$

Performing the operations indicated in Eq. (3-4) gives the kinematic equation of the entry vehicle in the latitude-longitude triad:

$$\bar{A} = \left(\ddot{R} - R\dot{\Lambda}^2 - R\dot{\lambda}_{IP}^2\cos^2\Lambda\right)\bar{i}_r + \left[\frac{1}{R\cos\Lambda}\frac{d}{dt}(R^2\dot{\lambda}_{IP}\cos^2\Lambda)\right]\bar{i}_\lambda$$
$$+ \left(R\ddot{\Lambda} + 2\dot{R}\dot{\Lambda} + R\,\dot{\lambda}_{IP}^2\cos\Lambda\sin\Lambda\right)\bar{i}_\Lambda \qquad (3\text{-}5)$$

The inertial geocentric longitude (λ_{IP}) differs from geocentric longitude (λ) by an angle equal to the time integral of the planet's angular velocity about its polar axis, $\bar{W}_{IO}$. Eq. (3-5) may be written in terms of λ by making the following substitution:

$$\dot{\lambda}_{IP} = \dot{\lambda} + W_{IO} \qquad (3\text{-}6)$$

3.6 Kinematics of Entry in Instantaneous Great-Circle Coordinates:

Most of the investigations described subsequently in this thesis

are based on equations of motion written in terms of components in the $\bar{l}_r$, $\bar{l}_\phi$, $\bar{l}_\psi$ triad. In these coordinates, four quantities must be specified in order to position the vehicle: R, ϕ, ψ and λ_{IT}.

The angular velocity of the vehicle is:

$$\bar{W}_{IP} = \dot{\phi}\,\bar{l}_\psi + \dot{\psi}\,\bar{l}_{XT} + \dot{\lambda}_{IT}\,\bar{l}_{ZT} \tag{3-7}$$

Using the angular relations given in table 3-1, this is written:

$$\bar{W}_{IP} = \left[\dot{\lambda}_{IT}\sin\phi\,\sin\psi + \dot{\psi}\cos\phi\right]\bar{l}_r + \left[\dot{\lambda}_{IT}\cos\phi\,\sin\psi - \dot{\psi}\sin\phi\right]\bar{l}_\phi$$

$$+\left[\dot{\phi} + \dot{\lambda}_{IT}\cos\psi\right]\bar{l}_\psi \tag{3-8}$$

The velocity of the vehicle is determined by applying the law of Coreolis to the radius vector:

$$\bar{R} = R\,\bar{l}_r \tag{3-9}$$

Thus:

$$\bar{V}_I = \left(\frac{d\bar{R}}{dt}\right)_I = \left(\frac{d\bar{R}}{dt}\right)_{moving} + \bar{W}_{IP} \times \bar{R} \tag{3-10}$$

Carrying out the operations indicated by equation (3-10) gives:

$$\bar{V}_I = \dot{R}\bar{l}_r + \left[R\,\dot{\phi} + R\dot{\lambda}_{IT}\cos\psi\right]\bar{l}_\phi - \left[R\dot{\lambda}_{IT}\cos\phi\,\sin\psi - R\dot{\psi}\sin\phi\right]\bar{l}_\psi \tag{3-11}$$

The instantaneous plane of the trajectory is defined as a plane normal to $\bar{R} \times \bar{V}_I$; therefore, there is no velocity component normal to this plane. From Fig. 3.2:

$$V_I = \dot{R}\,\bar{l}_r + V_{I\phi}\,\bar{l}_\phi \tag{3-12}$$

Comparing Equation (3-11) and (3-12) gives the following kinematic

relations:

$$\frac{V_{I\phi}}{R} = \dot{\phi} + \dot{\lambda}_{IT}\cos\psi \qquad (3\text{-}13)$$

$$\dot{\lambda}_{IT}\cos\phi\sin\psi = \dot{\psi}\sin\phi \qquad (3\text{-}14)$$

Differentiating equation (3-12) in the manner prescribed by Eq. (3-4) gives:

$$\bar{A} = \left(\ddot{R} - \frac{V_{I\phi}^2}{R}\right)\bar{1}_r + \left(\dot{V}_{I\phi} + \frac{\dot{R}}{R}V_{I\phi}\right)\bar{1}_\phi + \left[V_{I\phi}\left(\dot{\lambda}_{IT}\sin\phi\sin\psi + \dot{\psi}\cos\phi\right)\right]\bar{1}_\psi \qquad (3\text{-}15)$$

Equations (3-13) through (3-15) are a set of five differential equations which, under arbitrary initial conditions, describe the time history of vehicular motion.*

- - - - - - - - - - - - - - - - -

* Noting that the $\bar{1}_\psi$ component of $\bar{A}$ in Eq. (3-15) is $V_{I\phi}\,W_{IP_r}$, where W_{IP_r} is the $\bar{1}_r$ component of $\bar{W}_{IP}$, these five equations may be described more simply as follows:

(a) Eq. (3-14) is replaced by two equations:

$$W_{(IP)_r} = \dot{\lambda}_{IT}\frac{\sin\psi}{\sin\phi} = \frac{\dot{\psi}}{\cos\phi} \qquad (3\text{-}16)$$

(b) Eq. (3-13) is unchanged.

(c) Eq. (3-15) becomes:

$$\bar{A} = \left(\ddot{R} - \frac{V_{I\phi}^2}{R}\right)\bar{1}_r + \left(\dot{V}_{I\phi} + \frac{\dot{R}}{R}V_{I\phi}\right)\bar{1}_\phi + V_{I\phi}\,W_{(IP)_r}\,\bar{1}_\psi \qquad (3\text{-}17)$$

Chapter 4

KINEMATICS OF ENTRY IN ELLIPTICAL PARAMETERS

4.1 The Instantaneous Ellipse

It is common in celestial mechanics to describe the motion of heavenly bodies in terms of parameters of conic sections. There are many definitions of conics; the following definitions are convenient:

(1) Ellipse: The locus of points the sum of whose distances from two fixed points (foci) is constant.

(2) Circle: The locus of points equidistant from a single point (special case of the ellipse).

(3) Hyperbola: The locus of points the difference of whose distances from two fixed points (foci) is constant.

(4) Parabola: The locus of points equally distant from a fixed point (focus) with a fixed straight line (directrix).

When a body is in motion under the action of an attractive central force that varies as the inverse square of the distance, and if no external forces act on the body, the path described will be a conic whose focus is at the center of attraction. A particle moving according to such a force obeys Kepler's laws. Kepler's three laws of planetary motion, published about 1610, were the result of his pioneering analysis of planetary observations, and laid the groundwork for many of the

important contributions of Sir Isaac Newton. Kepler's laws may be summarized as follows:

A particle moving under the action of an attractive central force that varies as the inverse square of the distance

(1) travels in an ellipse or hyperbola (or their special cases, a circle or parabola) with the attracting center at one of the foci;

(2) the radius vector from the center to the particle sweeps out equal areas in equal time*;

(3) for the elliptic orbit, which results in periodic motions, the squares of the periods of rotation are proportional to the cubes of the major axis of the orbits.

The computational complexity involved in solving any physical problem depends to a large extent on the coordinates chosen for describing the problem. It is clear, for example, that a rectilinear problem may be solved more easily in rectilinear coordinates than in spherical polar coordinates or oblate spheroidal coordinates. Much of the trajectory of a vehicle entering the atmosphere of a planet is elliptical in nature, hence the motion is most easily described in terms of elliptical parameters.

Elliptical parameters are useful for analyzing the motion of the entry vehicle during the orbital phases and in the early phases of entry where gas-dynamic forces are negligible in comparison to other terms in

---

* Kepler's second law, the conservation of areal velocity, is a general theorem for central force motion[19] since angular momentum is always conserved. The first and third laws are restricted specifically to the inverse square law of force.

the dynamical equations of motion*. Particular portions of the flight where it is appropriate to describe the trajectory in elliptical parameters are:

(1) In the reconnaissance orbit (whether stable or degenerate);

(2) In the Keplerian portion of the direct entry profile;

(3) During circularization of the degenerate orbital profile.

It may be desirable to perform computations in terms of elliptical parameters during these phases of the trajectory, then to switch to a more conventional computational scheme for the atmospheric portion of flight. The Conservation Parameter discussed in Chapter 8 may be used as a switching function to convert from one guidance mode to another.

Elliptical parameters may be used throughout the trajectory by the "instantaneous ellipse" technique. At each instant an ellipse is constructed which matches the dynamical state of the vehicle; that is, the ellipse is oriented to pass through the present position of the vehicle and the ellipse has the angular momentum, energy, and velocity characteristics of the vehicle. The trajectory is described, therefore, as a time-varying ellipse; both the orientation and shape of the ellipse change with time. Fig. 4.1 shows the instantaneous ellipse and defines certain important parameters used frequently herein.

It should be noted that even during the stable reconnaissance orbit the trajectory is not planar, nor is the orientation of the ellipse fixed in space. By definition, the atmosphere does not perturb the motion in this case. The non-spherical component of gravitation does perturb the motion, however, such that even the stable orbit is

- - - - - - - - - - - - - - - - -

* This segment of the trajectory is called the Keplerian phase in this thesis.

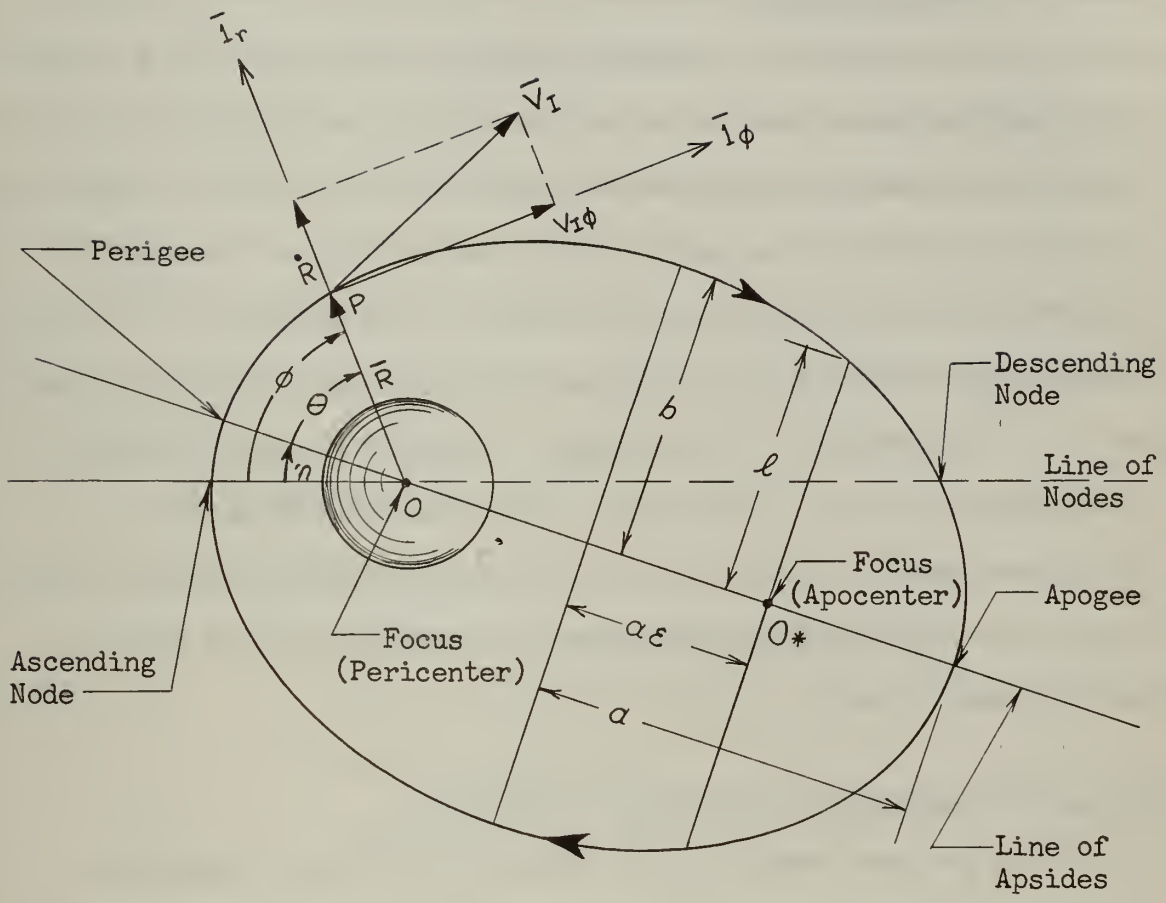

Line of apsides: The major axis of the ellipse, connecting the apsides (apocenter and pericenter).

Major axis = 2a
Minor axis = 2b
Latus rectum = 2l $l = a(1-\varepsilon^2)$

Eccentricity = ε (Always less than 1.0 for ellipse)

$$\varepsilon = \sqrt{1 - (b/a)^2}$$

True anomaly = θ
Area of ellipse = πab

$$n = \phi - \theta$$

Equation of ellipse: $R = \dfrac{a(1-\varepsilon^2)}{1+\varepsilon\cos\theta}$

T = period of orbit: $T = \dfrac{2\pi a^{3/2}}{\sqrt{\gamma_g M_o}}$

Fig. 4.1: The Instantaneous Ellipse.

slowly moving with respect to inertial coordinates. These perturbations result in secular effects* (regression of the line of nodes, $\dot{\lambda}_{IT} \neq 0$; and movement of the line of apsides (advance of perigee), $\dot{\eta} \neq 0$) and in periodic effects (oscillation of the angle of inclination ψ). Atmospheric perturbations of the degenerate orbital profile are generally much more significant than gravitational perturbations. Because of atmospheric and gravitational perturbations, the Keplerian Phase may best be described as a slowly changing instantaneous ellipse and the Intermediate and Gas-Dynamic Phases as a rapidly changing instantaneous ellipse. It is the slowly changing characteristics of the instantaneous ellipse which leads to the conclusion that performing computations in elliptical parameters is the most desirable method in the Keplerian Phase.

4.2 Entry Kinematics in Elliptical Parameters

There are many possible combinations of elliptical parameters which may be used to describe the kinematics of the entry trajectory. The kinematical equations are readily written as six first order equations in terms of elliptical parameters instead of three second order equations as described in Chapter 3. Taratynova[20] selected the latus rectum and eccentricity as two of the primary dependent variables and described the kinematics with either time or θ as independent variables. His solution contains singularities in the special case of circular orbits; no discussion is given with respect to how singularities were handled in obtaining his results. Nielsen, Goodwin, and

- - - - - - - - - - - - - - - - -

* Effects which accumulate with time; i.e., non-periodic components.

Mersman[21] defined two special parameters, p and q, to obtain kinematical equations which were found to be convenient for numerical studies of the trajectories of non-lifting satellites. Singularities were removed by separating q into two additional parameters, v and w.

Many combinations of elliptical parameters were examined during the course of this investigation to determine a particular set which would lead to the most simple kinematical description and still retain much of the geometry of the problem. Of the sets examined, the following was found most convenient:

(1) Independent variable: time, t.

(2) Dependent variables:

(a) Parameters of the instantaneous ellipse:

(1) P = angular momentum = $|\bar{R} \times \bar{V}_I| = RV_{I\phi}$ (4-1)

(2) $\mathcal{E}_1 = \mathcal{E} \cos\theta$ (4-2)

(3) $\mathcal{E}_2 = \mathcal{E} \sin\theta$ (4-3)

In equations (4-2) and (4-3), $\mathcal{E}$ is eccentricity of the instantaneous ellipse and θ is the angle from perigee to vehicular position (see Fig. 4.1).

(b) Orientation of the instantaneous ellipse:

(4) ψ : inclination of orbital plane

(5) λ_{IT} : inertial longitude of ascending line of nodes

(c) Position of vehicle in instantaneous ellipse:

(6) ϕ : angle measured in elliptical plane from line of nodes to vehicle.

The foregoing set does not suffer from singularities in the case of

circular orbits, as will be shown subsequently in this chapter. The six parameters listed are sufficient to describe the state of the entry vehicle and its matching ellipse.

In obtaining the kinematical equations of the above set of quantities, an additional set was derived which may be used for elliptical motion ($\mathcal{E} \neq 0$):

(1) Independent variable: t

(2) Dependent variables:

(a) Parameters of instantaneous ellipse:

(1) P

(2) $\mathcal{E}$

(3) η or θ

(b) Orientation of instantaneous ellipse:

(4) ψ

(5) λ_{IT}

(c) Position of vehicle:

(6) ϕ

In performing machine-aided numerical studies of entry trajectories involving a number of orbits, it is often desirable to examine the motion from the standpoint of the history of various quantities per orbit instead of with time. This is particularly true for deducing periodic and secular trends[21]. If it is desired to examine trends from perigee to perigee, θ is a convenient choice for the independent variable. Similarly, if it is desired to examine trends per orbit, ϕ is a convenient choice. The equations of the foregoing sets may be easily converted to these or any other particular independent variable.

Nielsen[21] shows that the independent variable for computer studies must be chosen with care. In the terminal phase of a non-lifting satellite's trajectory or throughout a ballistic trajectory, for example, the vehicle is traveling in a near-vertical path. Many of the quantities change rapidly for very small changes in ϕ. Time is a much more suitable choice than ϕ as an independent variable in studies of steep trajectories.

The areal velocity of the instantaneous ellipse is constant (by Kepler's second law). The areal velocity is one half the angular momentum. The areal velocity of the ellipse is[22]:

$$\frac{P}{2} = \frac{\pi ab}{T} \qquad (4\text{-}4)$$

where T is the period of the orbit and is equal to[22]:

$$T = \frac{2\pi a^{3/2}}{\sqrt{\gamma_g M_o}} \qquad (4\text{-}5)$$

γ_g is the gravitational constant and M_o is the mass of the planet. From equations (4-4) and (4-5):

$$\frac{P^2}{\gamma_g M_o} = \frac{b^2}{a} \qquad (4\text{-}6)$$

The definition of eccentricity as a function of a and b is given in Fig. 4.1:

$$1 - \varepsilon^2 = (b/a)^2 \qquad (4\text{-}7)$$

Substituting this into the equation of the ellipse:

$$R = \frac{a(1 - \varepsilon^2)}{1 + \varepsilon \cos \theta} \qquad (4\text{-}8)$$

and eliminating a and b with equation (4-6) gives:

$$R = \frac{p^2}{\gamma_g M_o (1 + \epsilon \cos \theta)} \qquad (4\text{-}9)$$

The instantaneous ellipse represents a constant energy trajectory. It is desirable to derive certain energy relations which are useful in obtaining the kinematical description of the ellipse. The total energy per unit mass is:

$$\frac{\mathcal{E}_{tot}}{M} = \frac{\mathcal{E}_{pot} + \mathcal{E}_{kin}}{M} = - \frac{\gamma_g M_o}{R} + \frac{\bar{V}_I \cdot \bar{V}_I}{2} \qquad (4\text{-}10)$$

Since the total energy of the instantaneous ellipse is constant, apogeal or perigeal values may be used for $\bar{V}_I$ and R in equation (4-10). Value of a quantity at perigee is denoted in this thesis by the subscript π and at apogee by the subscript α. The following equations may be written[22]:

$$V_{I\pi} = \sqrt{\frac{R_\alpha}{R_\pi}} \sqrt{\frac{2 \gamma_g M_o}{R_\alpha + R_\pi}} \qquad (4\text{-}11)$$

$$V_{I\alpha} = \sqrt{\frac{R_\pi}{R_\alpha}} \sqrt{\frac{2 \gamma_g M_o}{R_\alpha + R_\pi}} \qquad (4\text{-}12)$$

$$R_\alpha = a (1 + \epsilon) \qquad (4\text{-}13)$$

$$R_\pi = a (1 - \epsilon) \qquad (4\text{-}14)$$

Substituting equations (4-14) and (4-11) into (4-10) gives:

$$\frac{\mathcal{E}_{tot}}{M} = - \frac{\gamma_g M_o}{2a} \qquad (4\text{-}16)$$

Solving equation (4-10) for V_I^2, with equation (4-16) for $\frac{\mathcal{E}_{tot}}{M}$, equation (4-8) for a, and equation (4-9) for R gives:

$$V_I^2 = \frac{\gamma_g M_o}{R\,(1+\epsilon\cos\theta)}(1 + 2\epsilon\cos\theta + \epsilon^2) = (\frac{\gamma_g M_o}{P})^2(1 + 2\epsilon\cos\theta + \epsilon^2)$$

(4-17)

Equation (3-12) showed that:

$$V_I^2 = \dot{R}^2 + V_{I\phi}^2 \qquad (4\text{-}18)$$

Using equation (4-17) and (4-1) in (4-18) gives:

$$\dot{R} = \frac{\gamma_g M_o}{P}\,\epsilon \sin\theta \qquad (4\text{-}19)$$

The foregoing equations provide enough information to determine first order kinematic equations for all of the elliptical parameters. From equation (4-1):

$$\dot{P} = \dot{R}\,V_{I\phi} + R\,\dot{V}_{I\phi} \qquad (4\text{-}20)$$

Comparing this to equation (3-15) shows:

$$\dot{P} = RA_\phi \qquad (4\text{-}21)$$

From equations (3-14) and (3-15):

$$\dot{\psi} = \frac{\cos\phi}{V_{I\phi}} A_\psi = \frac{R}{P}\cos\phi\, A_\psi \qquad (4\text{-}22)$$

$$\dot{\lambda}_{IT} = \frac{\sin\phi}{V_{I\phi}\sin\psi} A_\psi = \frac{R\sin\phi}{P\sin\psi} A_\psi \qquad (4\text{-}23)$$

From equations (3-13) and (4-23):

$$\dot{\phi} = \frac{V_{I\phi}}{R} - \frac{\cot\psi\sin\phi}{V_{I\phi}} A_\psi = \frac{P}{R^2} - \frac{R\cot\psi\sin\phi}{P} A_\psi \qquad (4\text{-}24)$$

The determination of $\dot{\epsilon}$ and either $\dot{\theta}$ or $\dot{\eta}$ to complete the set of

six first order equations is considerably more involved than that required to derive the previous four equations. From equation (4-9):

$$\epsilon = \frac{1}{\cos\theta}\left[\frac{P^2}{\gamma_g M_o R} - 1\right] \tag{4-25}$$

Differentiating this, with equation (4-21) for $\dot{P}$ and (4-19) for $\dot{R}$, gives:

$$\dot{\epsilon} = \epsilon \tan\theta\dot{\theta} + \frac{2PA_\phi}{\gamma_g M_o \cos\theta} - \frac{P\epsilon \sin\theta}{R^2 \cos\theta} \tag{4-26}$$

This equation contains both $\dot{\epsilon}$ and $\dot{\theta}$. It is necessary to determine another independent equation containing $\dot{\epsilon}$ and $\dot{\theta}$, then solve the equations simultaneously. From equation (3-15):

$$\ddot{R} = A_r + \frac{V_{I\phi}^2}{R} \tag{4-27}$$

Differentiating equation (4-19), setting it equal to equation (4-27), and solving explicitly for $\dot{\theta}$ gives:

$$\dot{\theta} = \frac{P}{\epsilon \gamma_g M_o \cos\theta}\left(A_r + \frac{P^2}{R^3}\right) - \tan\theta\frac{\dot{\epsilon}}{\epsilon} + \frac{R\tan\theta}{P}A_\phi \tag{4-28}$$

Substituting equation (4-28) into (4-26) gives:

$$\dot{\epsilon} = \left[\frac{R(1+\epsilon\cos\theta)\sin\theta}{P}\right]Ar + \frac{R}{P}\left[\epsilon + 2\cos\theta + \epsilon\cos^2\theta\right]A_\phi + \frac{P\sin\theta}{R^2} \tag{4-29}$$

Using equation (4-29) in (4-28) gives:

$$\dot{\theta} = \left[\frac{R\cos\theta(1+\epsilon\cos\theta)}{\epsilon P}\right]Ar - \left[\frac{R\sin\theta}{\epsilon P}(2+\epsilon\cos\theta)\right]A_\phi + \frac{P}{\epsilon R^2}(\epsilon + \cos\theta) \tag{4-30}$$

From Fig. 4.1:

$$\eta = \phi - \theta \tag{4-31}$$

Therefore, $\dot{\eta}$ can be written from equations (4-24) and (4-30) as:

$$\dot{\eta} = -\left[\frac{R\cos\theta}{\varepsilon P}(1+\varepsilon\cos\theta)\right] A_r + \left[\frac{R\sin\theta}{\varepsilon P}(2+\varepsilon\cos\theta)\right] A_\phi - \left[\frac{R\cot\psi\sin\phi}{P}\right] A_\psi - \frac{P\cos\theta}{\varepsilon R^2} \tag{4-32}$$

The spherical component of gravitational mass attraction may be written:

$$G_{sp} = \frac{\gamma_g M_o}{R^2} = \frac{P^2}{R^3(1+\varepsilon\cos\theta)} \tag{4-33}$$

Thus equation (4-32) becomes:

$$\dot{\eta} = -\left[\frac{R\cos\theta}{\varepsilon P}(1+\varepsilon\cos\theta)\right]\left[A_r + G_{sp}\right] + \left[\frac{R\sin\theta}{\varepsilon P}(2+\varepsilon\cos\theta)\right] A_\phi - \left[\frac{R\cot\psi\sin\phi}{P}\right] A_\psi \tag{4-34}$$

Equation (4-30) becomes:

$$\dot{\theta} = \left[\frac{R\cos\theta}{\varepsilon P}(1+\varepsilon\cos\theta)\right]\left[A_r + G_{sp}\right] - \left[\frac{R\sin\theta}{\varepsilon P}(2+\varepsilon\cos\theta)\right] A_\phi + \frac{P}{R^2} \tag{4-35}$$

Equation (4-29) is written:

$$\dot{\varepsilon} = \left[\frac{R\sin\theta}{P}(1+\varepsilon\cos\theta)\right]\left[A_r + G_{sp}\right] + \frac{R}{P}\left[\varepsilon + 2\cos\theta + \varepsilon\cos^2\theta\right] A_\phi \tag{4-36}$$

The six kinematical equations are therefore:

(1) $\dot{P}$ Equation (4-21)

(2) $\dot{\varepsilon}$ Equation (4-36)

(3) $\dot{\eta}$ or $\dot{\theta}$ Equations (4-34) or (4-35)

(4) $\dot{\psi}$ Equation (4-22)

(5) $\dot{\lambda}_{IT}$ Equation (4-23)

(6) $\dot{\phi}$ Equation (4-24)

Equation (4-31) is used to relate θ with η and ϕ in these equations. Equation (4-9) gives an expression for R and equation (4-33) an expression for G_{sp}. It will be shown later that G_{sp} in equations (4-34), (4-35) and (4-36) cancels one of the terms in A_r.

If numerical studies are performed in which it is desired to use ϕ or θ as the independent variable instead of time, the above equations are easily converted as follows:

(1) $$\frac{dP}{d\phi} = \frac{dP}{dt}\frac{dt}{d\phi} = \dot{P}/\dot{\phi} \qquad (4\text{-}37)$$

(2) $$\frac{d\varepsilon}{d\phi} = \dot{\varepsilon}/\dot{\phi} \qquad (4\text{-}38)$$

(3) $$\frac{d\eta}{d\phi} = \dot{\eta}/\dot{\theta} \; ; \; \frac{d\theta}{d\phi} = \dot{\theta}/\dot{\phi} \qquad (4\text{-}39)$$

(4) $$\frac{d\psi}{d\phi} = \dot{\psi}/\dot{\phi} \qquad (4\text{-}40)$$

(5) $$\frac{d\lambda_{IT}}{d\phi} = \dot{\lambda}_{IT}/\dot{\phi} \qquad (4\text{-}41)$$

$$(6)\quad \frac{dt}{d\phi} = 1/\dot{\phi} \tag{4-42}$$

A similar procedure may be followed for θ.

Examination of the six kinematic relations shows that singularities exist if:

(1) $P = 0 \quad (V_{I\phi} = 0)$

(2) $\psi = 0$

(3) $R = 0$

(4) $\varepsilon = 0$

The angular momentum can be zero only in vertical flight, a condition that will generally not exist during the entry vehicle's trajectory. $\psi = 0$ causes the $\sin\psi$ term in the denominator of equation (4-23) to vanish; this is not troublesome because, as will be seen in Chapter 5, A_ψ in the numerator also has a $\sin\psi$ term which cancels the sine term in the denominator. R does not go to zero in a realizable trajectory. Therefore, the only troublesome singularity in the above list is that existing in eccentricity (for the special case of a circular orbital trajectory).

Eccentricity is in the denominator in the expressions for $\dot{\eta}$ and $\dot{\theta}$ only; one or the other of these equations is required to complete the set of kinematic equations. This singularity can be removed by replacing θ and ε by two new quantities:

$$\varepsilon_1 = \varepsilon \cos\theta \tag{4-2}$$

$$\varepsilon_2 = \varepsilon \sin\theta \tag{4-3}$$

Effectively, eccentricity is replaced by its components along the major and minor axis respectively. Differentiating:

$$\dot{\epsilon}_1 = \dot{\epsilon} \cos\theta - \epsilon \dot{\theta} \sin\theta \qquad (4\text{-}43)$$

$$\dot{\epsilon}_2 = \dot{\epsilon} \sin\theta + \epsilon \dot{\theta} \cos\theta \qquad (4\text{-}44)$$

Substituting $\dot{\theta}$ and $\dot{\epsilon}$ from equations (4-35) and (4-36) into these two equations gives:

$$\dot{\epsilon}_1 = -\left[P/R^2\right]\epsilon_2 + \frac{2R}{P}(1 + \epsilon_1) A_\phi \qquad (4\text{-}45)$$

$$\dot{\epsilon}_2 = \frac{R}{P}(1 + \epsilon_1)\left[A_r + G_{sp}\right] + \frac{R}{P}\epsilon_2 A_\phi + \frac{P\epsilon_1}{R^2} \qquad (4\text{-}46)$$

It is clear that the troublesome singularity arising in the special case of a circular orbit ($\epsilon = 0$) has been removed. Considerable simplification in the resulting equations has been effected in the process.

The six kinematical equations become:

(1) $\dot{P}$ Equation (4-21)

(2) $\dot{\epsilon}_1$ Equation (4-45)

(3) $\dot{\epsilon}_2$ Equation (4-46)

(4) $\dot{\psi}$ Equation (4-22)

(5) $\dot{\lambda}_{IT}$ Equation (4-23)

(6) $\dot{\phi}$ Equation (4-24)

This set of equations, original with this thesis, is considerably more simple than other sets cited in the literature or examined during the course of this investigation.

Energy as a function of angular momentum and eccentricity is determined by substituting Equation (4-9) and (4-17) into equation (4-10):

$$\frac{\mathcal{E}_{tot}}{M} = \frac{1}{2}\left(\frac{\gamma_g M_o}{P}\right)^2 (\varepsilon_1^2 + \varepsilon_2^2 - 1) = \frac{P^2}{2R^2}\frac{(\varepsilon^2 - 1)}{(1 + \varepsilon_1)^2} \qquad (4\text{-}47)$$

The rate of change of energy transfer is:

$$\frac{d}{dt}\left(\frac{\mathcal{E}_{tot}}{M}\right) = \frac{P\varepsilon_2}{R(1 + \varepsilon_1)}\left[A_r + G_{sp}\right] + (P/R)\, A_\phi \qquad (4\text{-}48)$$

4.3 Computation of Navigation Parameters

The six first order kinematic equations in terms of parameters of the instantaneous ellipse may be easily transformed into latitude-longitude coordinates, or any other desired guidance grid. Fig. 4.2 is a functional diagram of an open loop system which computes altitude, latitude, longitude, velocity, altitude rate, total energy, and time rate of transfer of total energy to the planetary atmosphere. The latter two quantities may be used for predicting total range or lifetime remaining.

It may be seen that the complexity of this three- dimensional system is not great due to the simplicity of the computations for P, ε_1, ε_2, ψ, λ_{IT}, and ϕ. Stored data includes the gravitational model of the planet; the gravitational model is discussed in Appendix C

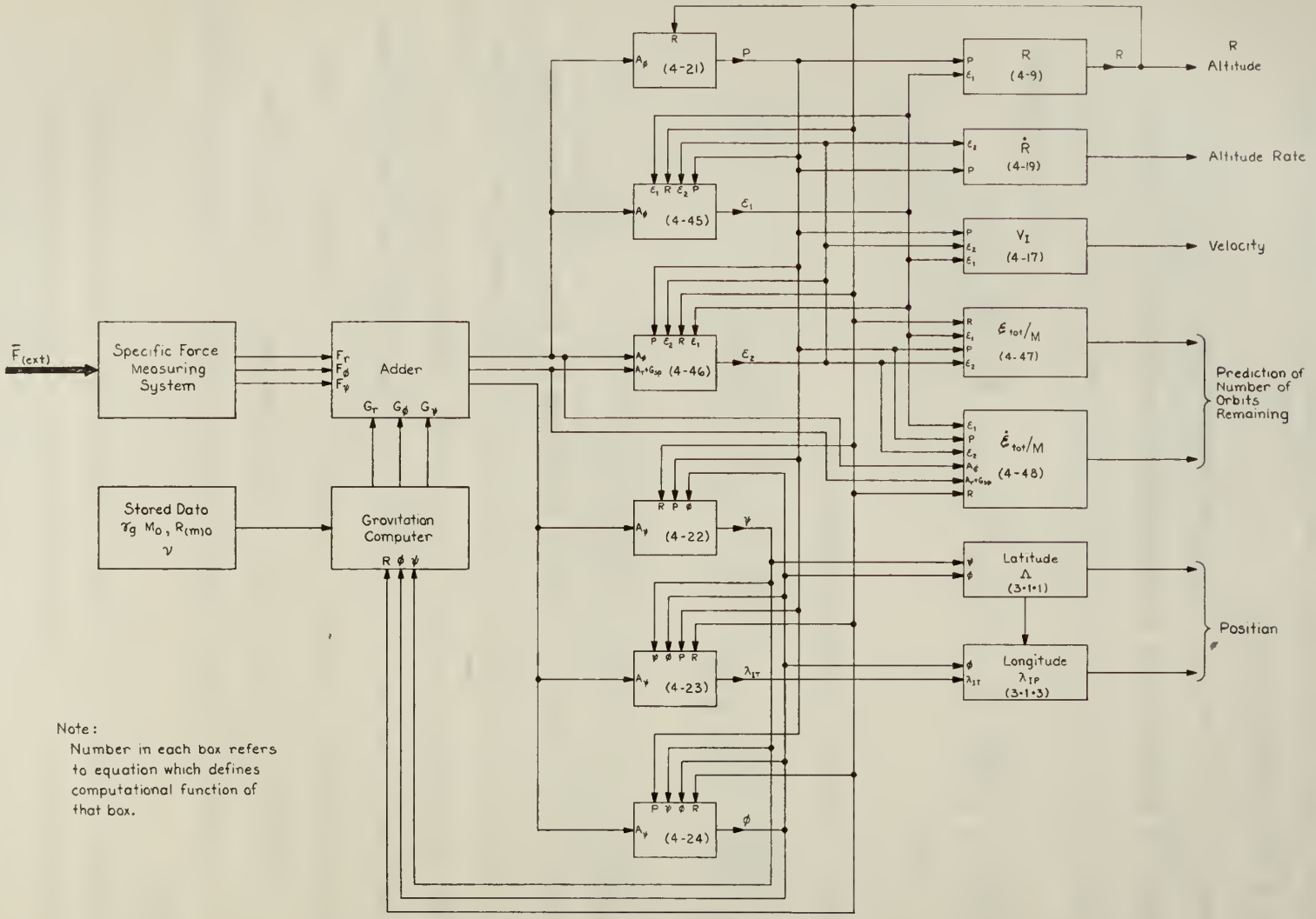

Fig 4.2 Open Loop Navigation System

of this thesis. The input to the system is the external specific force vector, which is the vector sum of lift, drag, and thrust forces. These are discussed in detail in Chapter 5.

The external specific force vector is measured by three orthogonal accelerometers which must be stabilized in some coordinate frame. Outputs of the specific force measuring system are components of external specific force in the $\bar{l}_r$, $\bar{l}_\phi$, and $\bar{l}_\psi$ directions. For numerical trajectory studies, the external specific force may be computed from altitude, velocity, and stored data on the atmospheric model and vehicle characteristics. Appendix E discusses various atmospheric models for the planets.

The acceleration vector $\bar{A}$ represented as outputs of the adder in Fig. 4.2 is the vector sum of gravitational specific force and external specific force. Chapter 5 discusses this further.

4.4 Gravitational and Atmospheric Perturbations

It is possible to deduce much information regarding the general characteristics of the vehicle's motion from the kinematic equations of section 4.2.

For a reconnaissance orbit that is at all times beyond the sensible atmosphere, the A_r , A_ϕ , A_ψ terms in the kinematic equations contain gravitational terms only. It may be seen from these equations that A_r always exists in combination with G_{sp} ; the sum of these two quantities, in this case, is the radial component of non-spherical gravitational effects.

It is shown in Chapter 5 that for an oblate spheroidal planet:

$$G_r \cong - G_{sp} - \frac{6\nu G_{sp} R^2_{(eq)0}}{R^2} \left(1 - 3 \sin^2\phi \sin^2\psi\right) \quad (4\text{-}49)$$

$$G_\phi \cong - \frac{12 \nu G_{sp} R^2_{(eq)0}}{R^2} \sin \phi \cos \phi \sin^2 \psi \qquad (4\text{-}50)$$

$$G_\psi \cong \frac{-12 \nu G_{sp} R^2_{(eq)0}}{R^2} \sin \phi \cos \psi \sin \psi \qquad (4\text{-}51)$$

In these equations:

(1) ν is a constant representing the quadrupole strength of the planet's gravitational field.

(2) $G_{sp} = \frac{\gamma_g M_o}{R^2}$

(3) $R_{(eq)o}$ is the planet's equatorial radius.

For the case of the vacuum trajectory, lift and drag forces are zero. If no thrust is generated by the vehicle's propulsive system:

$$A_r = G_r$$

$$A_\phi = G_\phi \qquad (4\text{-}52)$$

$$A_\psi = G_\psi$$

Inclination of orbital plane for the vacuum trajectory:

Combining equations (4-22) and (4-51) gives:

$$\dot{\psi} = -\frac{3 \nu G_{sp} R^2_{(eq)0}}{PR} \sin 2\phi \cos 2\psi \qquad (4\text{-}53)$$

The inclination of the orbital plane has a very small periodic oscillation due to the non-spherical component of gravitation.

Regression of the line of nodes for the vacuum trajectory:

Combining equations (4-23) and (4-51) gives:

$$\dot{\lambda}_{IT} = - \frac{12\nu G_{sp} R^2_{(eq)o}}{PR} \sin^2\phi \cos\psi \qquad (4\text{-}54)$$

Roberson[23] shows that the regression of the line of nodes per nodal period* can be expressed as:

$$\left[\Delta\lambda_{IT}\right]_{\text{per nodal period}} = - 12\pi\nu \left(\frac{\gamma_g M_o}{P^2}\right)^2 R^2_{(eq)o} \cos\psi \qquad (4\text{-}55)$$

The line of nodes therefore rotates slowly in the equatorial plane opposite in direction (regression) to the projection of the vehicle's motion on the equatorial plane.

Movement of line of apsides (advance of perigee) for the vacuum trajectory:

Combining equation (4-34) with equations (4-49) through (4-51) gives:

$$\dot{\eta} = \frac{6\nu R^2_{(eq)o}}{R^3} \left\{ \frac{P\cos\theta}{\varepsilon R} (1 - 3\sin^2\phi \sin^2\psi) - \frac{2\gamma_g M_o}{P} \left[\frac{(2+\varepsilon_1)\sin\theta \sin^2\psi \sin 2\phi}{2\varepsilon} - \sin^2\phi \cos^2\psi \right] \right\} \qquad (4\text{-}56)$$

Roberson[23] shows that the change of η per nodal period is:

$$\left[\Delta\eta\right]_{\text{per nodal period}} = 6\pi\nu R^2_{(eq)o} \left[\frac{\gamma_g M_o}{P^2}\right]^2 (4 - 5\sin^2\psi) \qquad (4\text{-}57)$$

Comparing (4-51) with (4-55) gives some interesting results. For near

- - - - - - - - - - - - - - - - -

* The nodal period, sometimes called the synodic period, is the time required to go from one ascending node to the next.

equatorial orbits (ψ small), η advances twice as rapidly as λ_{IT} regresses. Thus, the accumulated advance of perigee on the equatorial plane with respect to inertial coordinates is equal to (4-55), or one-half of equation (4-57).*

For a vehicle at an altitude of 300 nautical miles in a circular orbit around the Earth at an orbital inclination of 23° 27' (ecliptic plane), the regression of the line of nodes is less than 9.5 milli-radians per nodal period (less than 32.5 minutes of arc). The rate for Moon is about 1.5° per nodal period. The advance of perigee is about 65 minutes of arc per nodal period (approximately 12.5 milli-radians per hour).

Atmospheric perturbations on angle of inclination

The primary quantity causing the angle of inclination to change is A_ψ . Since drag is in the plane of the trajectory, it has little effect on the angle of inclination. The most significant effect in causing changes in ψ is side forces generated by a lifting vehicle in banking flight.

Atmospheric perturbations on line of nodes:

Nielsen[21] shows that drag forces, being in the plane of the trajectory, have very small influence on the regression of the line of nodes. He shows that equation (4-55) generally applies to zero-lift vehicles to three significant figures. The movement of the line of nodes is a sensitive function of A_ψ , which is significant only for

- - - - - - - - - - - - - - - - -

* The line of nodes cannot be visualized for a true equatorial orbit, hence it is desirable to envision a very small angle of inclination.

lifting vehicles in banking flight.

Atmospheric perturbations on line of apsides

Equation (4-34) shows that η is sensitive to A_r , A_ϕ , and A_ψ . The small motion of the line of apsides due to the non-spherical component of gravity is completely overshadowed when drag forces are significant. Nielsen shows that the introduction of drag terms in the motion of a non-lifting vehicle (initially in a circular, equatorial orbit) causes the line of apsides to move around the orbit with a variable lag at the average speed of the satellite. Lift also influences the motion of the line of apsides, but not as markedly as drag.

4.5 A Navigational Satellite for Position Reference During First-time Entry into the Atmospheres of Strange Planets

First-time entry into the atmospheres of strange planets presents special problems in specifying position when compared to navigating over a well-mapped planet such as Earth. The choice of a suitable landing site must necessarily be based on reconnaissance of the planetary surface while in orbit around the planet. The orbital altitude for the reconnaissance phase must be high enough such that a prolonged orbit may persist, yet low enough that fairly accurate mapping of the terrain is feasible.

The navigation of a vehicle flying from one point to another point on the surface of a planet is generally based on navigational parameters measured with respect to the planet, i.e., latitude, longitude, and altitude. It is less common to use parameters identified with a particular mission, such as angular displacements measured with respect to

the great circle course along-track and across-track.

The entry mission to the surface of a strange planet, on the other hand, does not originate from a point on the planet's surface. The entry mission generally originates from a reconnaissance orbit which, if the perigeal altitude is sufficiently great, is very slowly changing with time. The non-spherical component of the planet's gravitational field causes the line of nodes and the line of apsides to rotate slowly with respect to an inertial framework. Drag forces result in energy transfer from the vehicle to the planetary atmosphere, but for sufficiently high orbits, this transfer causes negligible change in the satellite orbit over periods of time comparable to that required for entry once retro-rocket thrust is generated.

A basic position reference available during the course of entry is the original reconnaissance orbit. If the entry vehicle is launched from a mother satellite, then the mother satellite, which remains in the reconnaissance orbit, may track both the entry vehicle and the preselected landing site and transmit this tracking information to the guidance computer of the entry vehicle. In this way, the parent satellite replaces ground tracking stations which are used as an external source of tracking information for Earth satellites and entry vehicles.

In the event that no parent satellite exists, then a navigational satellite to serve the same purpose may be deposited in the reconnaissance orbit by the entry vehicle prior to initiating the entry phase.

Since a navigational scheme such as outlined briefly above uses the reconnaissance orbit as the basic reference from which to measure positions, it may be found convenient to express position and to carry out the guidance computations in terms of elliptical parameters. The

landing site may be considered to be a target moving in three-dimensional space with respect to the near-stable reconnaissance trajectory represented by the mother or navigational satellite. The entry vehicle is also moving with respect to the initial reconnaissance trajectory. The entry problem is therefore similar to the fire control problem, with the entry vehicle (projectile) fired from the parent satellite (gun) to hit the moving landing site (target). The problem is much more severe than the conventional fire control problem, however, because the projectile must be constrained to paths for which it will not burn up or encounter accelerations beyond tolerable levels.

The nominal or programmed path of the entry vehicle may be computed in advance as one which the vehicle would fly under standard atmospheric conditions starting from the particular initial point and ending at the landing site selected in advance. This trajectory must be consistent with tolerable accelerations and heating rates.

It was shown previously in this chapter that there are six elliptical elements required to specify the position and path of the vehicle. One set of six such elements are:

(1) ψ, λ_{IT}, (to specify the instantaneous orientation of the plane of the trajectory;

(2) P, ϵ_1, ϵ_2 (to specify the ellipse which matches the instantaneous radius and velocity vectors of the vehicle);

(3) ϕ (to specify the position of the vehicle in this ellipse).

P, ψ, and λ_{IT} are constant or very slowly varying with time in the reconnaissance orbit. ϵ_1 and ϵ_2 are sinusoidal with a very slowly changing magnitude of oscillation. ϕ increases monotonically.

The instantaneous dynamical state of the entry vehicle, with respect to the navigational satellite in the reconnaissance orbit, may conveniently be specified in terms of the six elliptical quantities. The orbit of the navigation satellite should be predictable to a fairly high degree of accuracy. The predicted values of six elliptical elements for this orbit are part of the data stored for use during the entry mission.

Chapter 5

FORCES ACTING ON THE ENTRY VEHICLE

5.1 Introduction

The forces acting on the entry vehicle as it moves along its trajectory are of two major types: field forces and non-field forces.

(1) Field forces

The most important field forces which act on the entry vehicle are those arising from the planet's gravitational field and magnetic field. The weight of the vehicle is a field force. If the vehicle should acquire a static charge, a force will act on it as it passes through the magnetic field surrounding the planet; this, too, is a field force.

The planet's gravitational field is the predominant field force acting on the entry vehicle and is the only one considered in this thesis. Gravitational effects of any natural satellites of the planet, the Sun, and other planets in the solar system are considered herein to be negligibly small in the vicinity of the planet in comparison to the gravitational field of the planet itself.

(2) Non-field forces

Non-field forces acting on the entry vehicle are of two

major types: kinetic reaction forces and external forces.

(a) Kinetic reaction forces are apparent forces resulting from accelerations of the reference space which is used in specifying the problem with respect to inertial space (space in which Newton's laws are valid). If the reference space is either fixed or moving at a constant linear velocity relative to a Newtonian frame, then the reference space itself is Newtonian. If the reference space has a translation with constant acceleration $\bar{a}$ relative to a Newtonian frame, then the reference space may be treated as Newtonian if a ficticious force, $-M\bar{a}$, is applied to each particle. If the reference space is rotating with constant angular velocity relative to a Newtonian frame, then the reference frame may be treated as Newtonian, if, to each particle, two kinetic reaction forces are applied: Coreolis force and centrifugal force.

(b) External forces are generated primarily as follows:

(1) Gas-dynamic forces: lift and drag forces which are produced as the vehicle flies through the planetary atmosphere. The magnitude of these forces depends on the characteristics of the atmosphere, the velocity of the vehicle with respect to the atmosphere, and the gas-dynamic characteristics of the vehicle.

(2) Thrust forces: forces produced by the propulsive elements of the vehicle.

Lift and drag forces exist only when the vehicle is flying through

an atmosphere while thrust forces may be generated in a vacuum. In this thesis, lower order external forces are neglected. These may include electric drag, solar radiation pressure, etc.

Application of Newton's laws of motion to the vehicle gives:

$$\bar{A} = \bar{F}_{(li)} + \bar{F}_{(dr)} + \bar{F}_{(th)} + \ldots + \bar{G} + \ldots \qquad (5\text{-}1)$$

where $\bar{A}$ is the acceleration of the vehicle in the Newtonian frame. This term includes all kinetic reaction forces when the reference space is not Newtonian.

$\bar{F}_{(li)}$, $\bar{F}_{(dr)}$, $\bar{F}_{(th)}$ are external specific forces (force per unit mass) resulting from lift, drag, and thrust, respectively. Other external specific force terms are considered to be higher order effects and are neglected in this thesis.

$\bar{G}$ is the field force due to the planet's gravitational field. Other field forces are considered to be higher order effects and are neglected in this thesis.

The derivation of the acceleration vector $\bar{A}$ was discussed in Chapter 3 in two separate guidance grids, the latitude-longitude triad and the instantaneous great-circle triad. It is to be noted that both of these reference frames are rotating with respect to inertial space, hence Coreolis and centrifugal force terms are implicit in $\bar{A}$. Derivation of field and external forces in component form are discussed in subsequent sections of the present chapter to complete the dynamical statement of the entry problem.

It should be emphasized that the right-hand side of equation (5-1) has two distinct roles. In the instrumentation of the guidance system for an entry mission, the vector sum of the external specific force terms

is measured by the specific force measuring subsystem (three orthogonal accelerometer units). In trajectory studies leading to the establishment of a reference or nominal trajectory for the mission, the external specific forces are mathematically derived from the gas-dynamic model of the vehicle, from the atmospheric model of the planet, and from a mathematical model of the engines. Errors in these models when compared to conditions actually encountered during a particular mission lead to departures of the vehicle from its planned path in space and time. It is clear that accurate information is needed on the physical characteristics of both the vehicle and the planet.

The reference trajectory should be selected as one for which errors in the vehicle model and the atmospheric model will not jeopardize the successful completion of the mission; that is, the reference trajectory should be the mean path in a corridor established by upper and lower estimates of errors in these models.* The reference trajectory should also be selected such that errors in the models result in minimum range errors, if landing point accuracy is important to the mission. It is not necessary that the guidance system always return the vehicle to a predetermined reference trajectory when position errors accumulate; a more efficient concept is that of computing during the course of the mission, either continuously or intermittently, new reference trajectories. These trajectories should be based on measured atmospheric data and observed winds and must be at all times consistent with

- - - - - - - - - - - - - - - - -

* The corridor must also be consistent with heating, acceleration, and radiation constraints on the trajectory, discussed in Chapter 7.

mission objectives and physical constraints on the trajectory. For this guidance concept, which is particularly desirable in the case of Explorer missions, the force terms on the right-hand side of equation (5-1) are measured and computed; i.e., the reference trajectory is revised periodically by computations based on measurements accumulated. Other independent measurements, such as vehicle skin temperature, may be used to augment specific force measurements.

5.2 The Gravitational Model of the Oblate Planet

A discussion of gravitational mass attraction and the acceleration of gravity is contained in Appendix C. The gravitational potential of the planet, including the quadrupole contribution of the non-spherical component, is as follows*:

$$\bar{\Phi} = - \frac{\gamma_g M_o}{R} \left[1 - \nu \frac{R^2_{(eq)0}}{R^2} (1 - 3 \cos 2\Lambda) \right] \qquad (C\text{-}7)$$

The gravitational field vector was defined as:

$$\bar{G} = - \nabla \bar{\Phi} \qquad (C\text{-}8)$$

The following equation defines the gradient in spherical polar coordinates[24]:

$$\nabla \bar{\Phi} = \frac{\partial \bar{\Phi}}{\partial R} \bar{1}_r + \frac{1}{R \sin (90 - \Lambda)} \frac{\partial \bar{\Phi}}{\partial \lambda_{IP}} \bar{1}_\lambda + \frac{1}{R} \frac{\partial \bar{\Phi}}{\partial \Lambda} \bar{1}_\Lambda \qquad (5\text{-}2)$$

Carrying out the indicated operations on equation (C-7) gives:

- - - - - - - - - - - - - - - - -

* A quantitative description of the gravitational model for the pear-shaped Earth is contained in reference (18).

$$G_r = -\frac{\partial \bar{\phi}}{\partial R} = -G_{sp} + 3\nu G_{sp}\left(\frac{R_{(eq)o}}{R}\right)^2 (1 - 3\cos 2\Lambda) \qquad (5\text{-}3)$$

$$G_\lambda = -\frac{1}{R \sin(90 - \Lambda)} \frac{\partial \bar{\phi}}{\partial \lambda_{IP}} = 0 \qquad (5\text{-}4)$$

$$G_\Lambda = -\frac{1}{R}\frac{\partial \bar{\phi}}{\partial \Lambda} = -6\nu G_{sp}\left(\frac{R_{(eq)o}}{R}\right)^2 \sin 2\Lambda \qquad (5\text{-}5)$$

In these equations, G_{sp} is the radial component of the gravitational mass attraction for a spherical planet:

$$G_{sp} = \frac{\gamma_g M_o}{R^2} \qquad (5\text{-}6)$$

The gravitational components in the latitude-longitude triad are readily converted to the great-circle triad by using the angular relations given in Table 3.1 together with the following trigonometric identities:

$$\cos 2\Lambda = 1 - 2\sin^2\Lambda \qquad (5\text{-}7)$$

$$\sin 2\Lambda = 2 \sin\Lambda \cos\Lambda$$

The results of this transformation are as follows:

$$G_r = -G_{sp} - 6\nu G_{sp}\left(\frac{R_{(eq)o}}{R}\right)^2 (1 - 3\sin^2\phi \sin^2\psi) \qquad (5\text{-}8)$$

$$G_\phi = -6\nu G_{sp}\left(\frac{R_{(eq)o}}{R}\right)^2 \sin^2\psi \sin 2\phi \qquad (5\text{-}9)$$

$$G_\psi = -6\nu G_{sp}\left(\frac{R_{(eq)o}}{R}\right)^2 \sin\phi \sin 2\psi \qquad (5\text{-}10)$$

5.3 Gas-Dynamic Forces

The interaction of the vehicle and the atmosphere may be both electrical and mechanical in nature. Electrical effects, which may increase the drag over gas-dynamic values, are sensitive to the charge accumulated on the vehicle. Electrical drag has greatest relative influence on the vehicle at high altitudes where gas-dynamic forces are small. The general concensus is that electrical drag contributes less than 10% of the total drag of long-lifetime satellites presently in orbit around Earth[25]; in the atmospheric portion of the entry trajectory, electrical drag should contribute even less of the total drag. Electrical contributions to vehicular drag are therefore not included in the force terms of this thesis.

The entry vehicle passes through a number of flight regimes. Mechanical interaction of the vehicle and atmosphere is a function of the mean free path of the molecules of the planetary atmosphere. Three types of flow regimes are generally traversed by the entry vehicle:

(1) Free molecular flow regime: the mean free path of atoms and molecules which rebound from the entry vehicle is great when compared to vehicle dimensions. In this regime, the atmospheric particles are unaffected by the moving vehicle until they strike its surface.

(2) Slip-flow regime: the mean free path of the atmospheric particles rebounding from the vehicle is not large compared to the dimensions of the vehicle. Outgoing atoms may collide with incoming atoms, thus preventing them from striking the vehicle.

(3) Continuum flow regime: the region where the atmospheric particles are affected before striking the vehicle. In this regime, the mean free path of atmospheric particles is very much less than the dimensions of the vehicle.

For Earth, the mean free path at 300,000 feet is approximately 0.1 ft.; at 500,000 feet, the mean free path is approximately 100 feet. Di Taranto[26] suggests these altitudes as approximate boundaries between the above flow regimes.

The drag coefficient of the entry vehicle decreases as it passes from the free-molecular flow regime to the continuum flow regime.* Fig. 5.1 shows the drag force as a vector having a direction opposite that of the velocity vector of the vehicle with respect to the atmosphere, $\overline{V_{(AM)}}$. The lift force vector acts in a direction normal to $\overline{V_{(AM)}}$ in the plane of symmetry of the vehicle. In this analysis, it is assumed that the atmosphere surrounding the planet rotates with the

- - - - - - - - - - - - - - - -

* Henry[27] estimates the average molecular mass of particles at high altitudes above the Earth to be of the order of 14.5 on the atomic scale, since the air is assumed largely monatomic; he estimates the velocities of the particles to be of the order of 1.5×10^5 cm/sec. This velocity is about 0.2 the velocity of a circular orbital satellite. Henry estimates the temperature of a satellite at high altitudes to be approximately 280-300° Kelvin when exposed to the Sun and about 50° cooler when in the Earth's shadow. Assuming the particles bouncing off the surface of the satellite have a temperature roughly the same as the vehicle, reflected particles should therefore have velocities in the neighborhood of 10^5 cm/sec. Since speeds of atmospheric particles both before and after collision with the satellite are much less than the satellite's velocity, it is reasonable to assume that, in a coordinate frame in which the satellite is at rest, the molecules approach with a relative velocity equal to the satellite's velocity and rebound with zero relative velocity. The change in momentum of all of the free molecules striking the satellite in unit time is $\rho S V_{(AM)}^2$, which is equal to the drag of the vehicle. Hence the drag coefficient in the free molecular flow regime is $C_D = 2$. Spheres in hypersonic (attached shock) continuum flow, on the other hand, have drag coefficients of the order of 0.7.

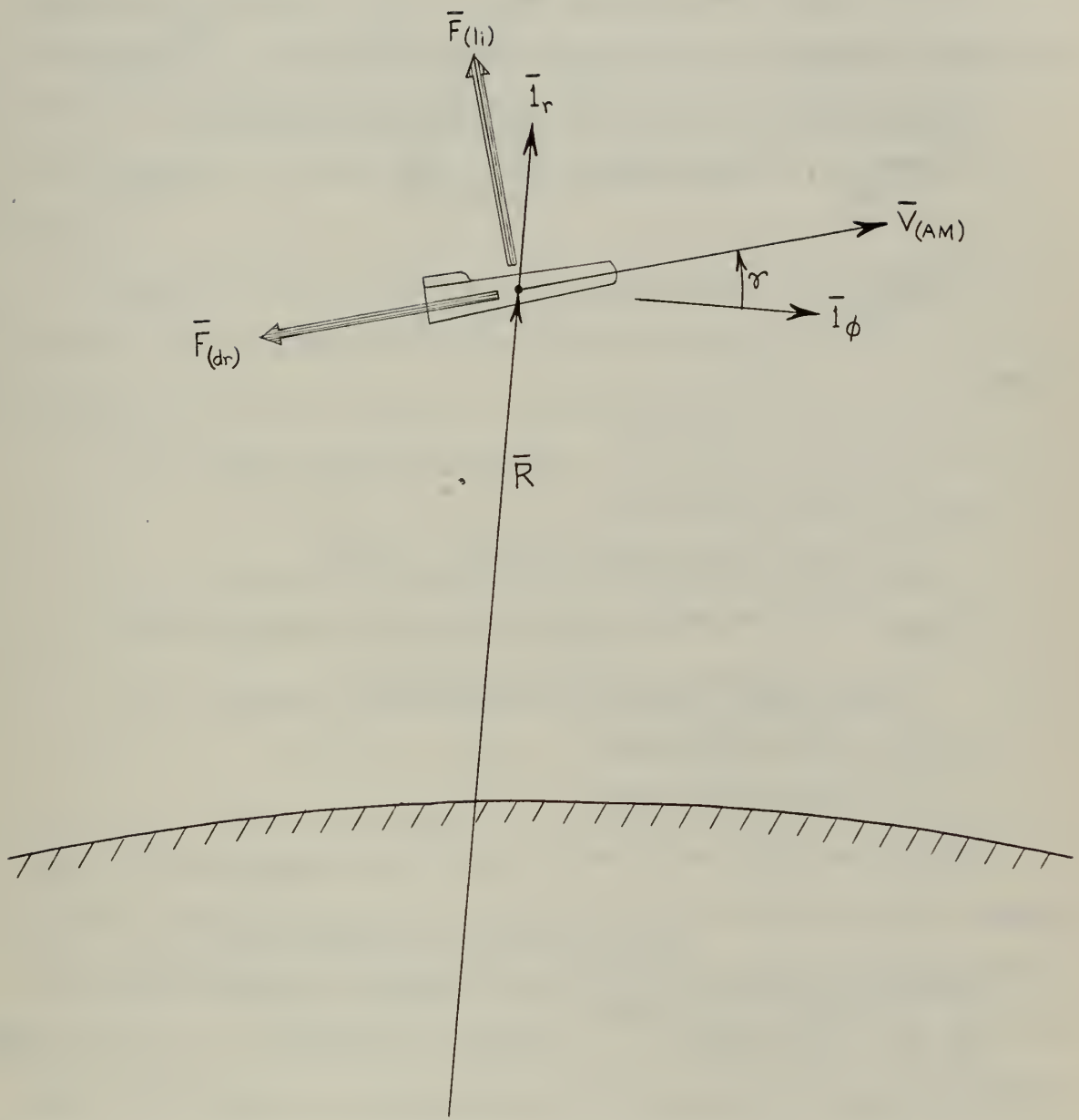

Fig. 5.1: Lift and Drag Specific Force Vectors.

planet (when wind* is zero). The analysis is generalized to include the effects of wind. The vectors $\overline{F_{(dr)}}$, $\overline{F_{(li)}}$, and $\overline{V_{(AM)}}$ are always coplanar, the vector $\bar{l}_r$ does not, in general, lie in this plane.

The magnitude of the lift and drag specific forces are:

$$\left|\overline{F_{(dr)}}\right| = D/M = (1/2)\,\rho\, V^2_{(AM)}\, \frac{C_D S}{M} \qquad (5\text{-}11)$$

$$\left|\overline{F_{(li)}}\right| = L/M = (1/2)\,\rho\, V^2_{(AM)}\, \frac{C_L S}{M} \qquad (5\text{-}12)$$

where:

D is the drag force

L is the lift force

ρ is the free stream atmospheric density

$V_{(AM)}$ is the vehicular velocity relative to the atmosphere

S is a reference area for the vehicle

C_L is lift coefficient

C_D is drag coefficient

The lift and drag coefficients vary with the angle of attack, Mach number, and configuration of the vehicle. Atmospheric density, viscous, elastic, and turbulence properties are significant in determination of lift and drag coefficients.[28] Analytical determination of lift and drag coefficients for other than the most simple shapes is difficult. Wind tunnel tests and other experimental methods for measuring lift and drag cannot be performed at this time for Mach numbers in excess of 10 to 15. Thus the specification of C_L and C_D for a particular entry vehicle may be subject to errors.

- - - - - - - - - - - - - - - - -

* Wind is defined as relative movement of the atmosphere with respect to coordinates fixed in the planet, $\overline{V}_{O(AM)}$.

In most of the analytical work of this thesis, $(C_D S)$ is assumed constant irrespective of the flow regimes traversed by the vehicle. In some missions, transition between flow regimes may occur in the Intermediate Phase. Should this situation occur, the altitude span of the Intermediate Phase may be slightly greater than that given in Chapter 8*.

The lift and drag characteristics of the entry vehicle depend strongly on its configuration. Many vehicle designs are under consideration for entry missions. Among these are[29]:

(1) High performance gliders

Vehicles with high lift-to-drag ratios that are similar in appearance to current high performance delta wing fighter aircraft.

(2) Gliders with wings having rounded leading edges

These are similar to (1) except sharp structural edges are avoided to prevent localized heating during entry.

(3) Lifting and non-lifting capsules

(4) Variable geometry vehicles with triangular planforms

Horizontal control surfaces are folded into the back of the vehicle until velocities are reduced below those values corresponding to maximum heating. The

- - - - - - - - - - - - - - - - -

* For example, if the drag coefficient and flight path angles are constant, the Intermediate Phase spans about 20 miles of altitude for entry into Earth's atmosphere. If the drag coefficient is reduced to one-half its free-molecular flow value during the time that the vehicle crosses the Intermediate Phase, the width of this phase increases to about 24 miles.

vehicles enter the atmosphere at near 90° angle of attack (high drag configuration); the nose is lowered to conventional angles of attack in low speed flight.

(5) Inflatable vehicles with large wing areas

These vehicles have exceptionally low wing loadings.

(6) Collapsible Wings

The wings for these vehicles resemble kites that are extended to increase lift capabilities.

The lift and drag coefficients are coupled in a different manner for different vehicle configurations. The general lift-drag polar may be approximated by[30]:

$$C_D = C_{Do} + K_{ind} C_L^2 \qquad (5\text{-}13)$$

C_{Do} is zero-lift drag coefficient

K_{ind} is induced drag factor

C_{Do} and K_{ind} are generally functions of Mach number.

Although this thesis was not concerned with a particular vehicle, it was necessary in many instances to select certain quantitative values of lift and drag coefficients either to illustrate the solutions derived or to compare the results with more exact numerical solutions. The following simplifying assumptions were made throughout this thesis:

(1) Lift and drag coefficients are independent of Mach number.

This is a reasonable assumption only for high Mach numbers*.

- - - - - - - - - - - - - - - -

* That is, at Mach numbers greater than approximately five.

(2) Lift and drag coefficients are independent of altitude.

As pointed out previously, the drag coefficient in the free molecular flow regime may be two or more times as great as that in the continuum flow regime. Since the Gas-Dynamic Phase is generally characterized by continuum flow throughout, and since lift and drag forces are of greatest significance in this particular phase, this assumption should not introduce limitations on the solutions. The altitude span of the Intermediate Phase discussed in Chapter 8 may be slightly conservative as a result of this assumption.

The lift and drag coefficients for bodies at small angles of attack in hypersonic flight may be expressed as[31] :

$$C_L = 2\alpha \tag{5-14}$$

$$C_D = C_{Do} + \alpha C_L = C_{Do} + C_L^2/2 \tag{5-15}$$

where α is angle of attack.

The zero-lift drag coefficient is approximately constant for a particular vehicle. From equations (5-15), (5-11) and (5-12):

$$\frac{L}{D} = \frac{C_L}{C_D} = \frac{C_L}{C_{Do} + C_L^2/2} \tag{5-16}$$

This equation has a maximum value when[31]:

$$C_{Do} = C_L^2/2 \tag{5-17}$$

Thus:

$$(L/D)_{max} = \frac{1}{2\alpha_{max}} = \frac{1}{C_{Lmax}} = \frac{1}{\sqrt{2C_{Do}}} = \frac{1}{\sqrt{C_{Dmax}}} \tag{5-18}$$

Table 5.1 summarizes lift and drag coefficients for three representative vehicle classes computed from Eq. (5-18).

Table 5.1: Lift and Drag Characteristics of Three Generalized Vehicle Classes.

$(L/D)_{max}$	C_{Do}	C_{Dmax}	C_{Lmax}
0.5	2.0	4.0	2.0
2.0	0.125	0.250	0.5
4.0	0.03125	0.0625	0.25

The vehicle classes summarized in Table 5.1, which have the lift-drag polar of equation (5-15), are used in the following sections of this thesis:

(1) Chapter 7: trajectory constraints imposed by human acceleration tolerances

Constraint bands are shown for each of the three vehicle classes in the velocity-altitude plane. The upper line of each band corresponds to flight at C_{Lmax}, the lower line corresponds to flight at $C_L = 0$.

(2) Chapter 8: phase boundaries between the Keplerian, Intermediate, and Gas-Dynamic Phases

It should be noted that for flight path angles less than about 10°, which includes most conceivable entry trajectories, the location of these boundaries is a strong function of the instantaneous drag characteristics of the vehicle and is essentially independent of

lift. The results presented graphically in Chapter 8, therefore, may be applied to a broad class of vehicles by entering the curves with the appropriate drag coefficient.

A particular specification of lift and drag coefficients were not required in the analytical solutions of Chapters 9 and 10. In order to determine quantitatively the accuracy of closed form solutions determined, however, comparison is frequently made to numerical solutions for vehicles with particular aerodynamic characteristics. The aerodynamic qualities of the vehicles chosen is clearly indicated in each case.

5.4 Vehicle Coordinate Triad and Engine Gimbal Triad:

The drag vector is directed anti-parallel to the velocity vector of the vehicle with respect to the atmosphere. The lift vector is perpendicular to this velocity vector and acts in the plane of symmetry of the vehicle. In the analysis performed herein, it is assumed that the entry vehicle has the capability of rotating the lift vector (i.e., banking) in order to produce curvature of the trajectory in a controlled manner to enable the vehicle to reach landing sites at some distance from the "no-bank" trajectory. For military vehicles, such as a reconnaissance platform, the banking capability may permit adequate military coverage of an entire hostile nation.

Two vehicle-centered coordinate triads are defined in Fig. 5.2; the Wings Level triad $\bar{l}_{x_{WL}}$, $\bar{l}_{y_{WL}}$, $\bar{l}_{z_{WL}}$ and the Vehicle triad $\bar{l}_x$, $\bar{l}_y$, $\bar{l}_z$. It is noted that both the Wings Level and the Vehicle triad are oriented along the velocity vector of the vehicle with respect

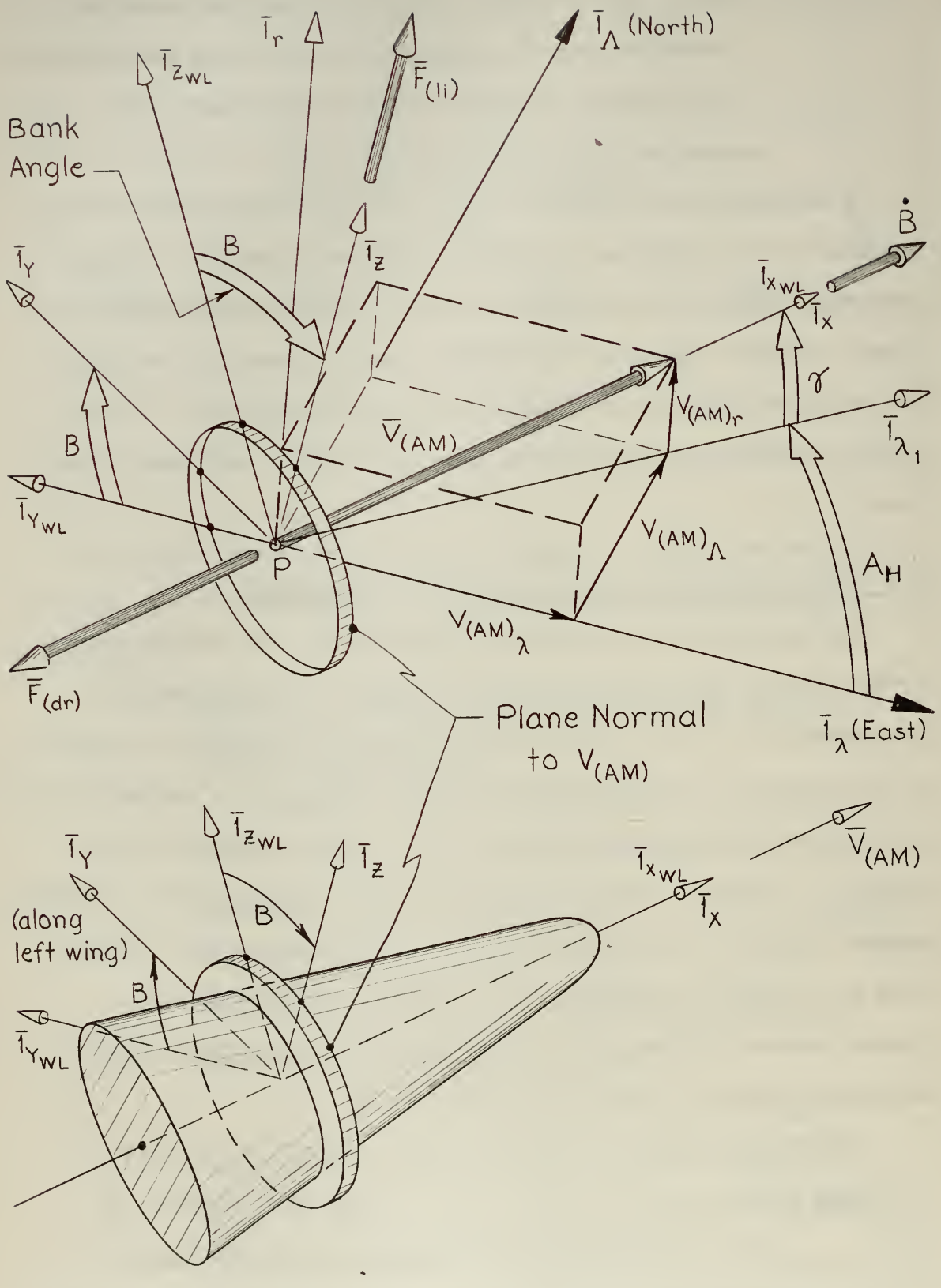

Fig. 5.2: "Wings Level" and "Vehicle" Coordinate Triads.

to the atmosphere. The left wing unit vector in the zero bank condition ($\bar{l}_{y_{WL}}$) always lies in the $\bar{l}_\lambda$ - $\bar{l}_\Lambda$ plane*. Rotation of the vehicle about $\bar{V}_{(AM)}$ (coincident with $\bar{l}_{x_{WL}}$, $\bar{l}_x$) causes the lift vector to move out of the vertical plane, hence causes a side force which tends to curve the trajectory. The amount of rotation of the vehicle from the wings level condition is defined as the bank angle, B.

Following is a brief description of the coordinate systems shown in Fig. 5.2:

$\bar{l}_{x_{WL}}$, $\bar{l}_{y_{WL}}$, $\bar{l}_{z_{WL}}$ Wings Level Triad: Orthogonal set of unit vectors centered at vehicle center of gravity. $\bar{l}_{x_{WL}}$ is along the velocity vector of the vehicle with respect to the atmosphere. $\bar{l}_{y_{WL}}$ is along the left wing of the vehicle in the zero bank condition. $\bar{l}_{z_{WL}}$ is along the lift vector in the zero bank condition.

$\bar{l}_x$, $\bar{l}_y$, $\bar{l}_z$ Vehicle Coordinate Frame: Orthogonal set of unit vectors centered at vehicle center of gravity. $\bar{l}_x$ is along the velocity vector of the vehicle with respect to the atmosphere. $\bar{l}_y$ is along the left wing of the vehicle; $\bar{l}_z$ is in the plane of symmetry of the vehicle and is a unit vector in the lift direction.

It is noted that $\bar{l}_x$ and $\bar{l}_{x_{WL}}$ are always coincident. $\bar{l}_y$ differs from $\bar{l}_{y_{WL}}$ and $\bar{l}_z$ differs from $\bar{l}_{z_{WL}}$ by the angle of bank B. In the zero bank condition, both triads are coincident.

- - - - - - - - - - - - - - - - -

* $\bar{l}_\lambda$ is positive in the geocentric East direction. $\bar{l}_\Lambda$ is positive in the North direction. The $\bar{l}_\lambda$ - $\bar{l}_\Lambda$ plane is the geocentric horizontal plane, or "level plane" - hence the term "Wings Level" coordinate system.

The following angles are defined in Fig. 5.2:

$A_H = A\left[\bar{l}_\lambda - \bar{l}_{\lambda_1}\right]$: angle between East ($\bar{l}_\lambda$) and horizontal component of vehicular velocity with respect to the atmosphere.

$\gamma = A\left[\bar{l}_{\lambda_1} - \bar{l}_\chi\right]$: angle between the horizontal component of vehicular velocity with respect to the atmosphere (i.e., the component in the $\bar{l}_\lambda - \bar{l}_\Lambda$ plane) and the total velocity vector of the vehicle with respect to the atmosphere.

$B = A\left[\bar{l}_{y_{WL}} - \bar{l}_y\right] = A\left[\bar{l}_{z_{WL}} - \bar{l}_z\right]$: bank angle of vehicle. Corresponds to rotations about the l_x axis from the wings level condition.

Following are definitions of A_H and γ in terms of velocity components:

$$A_H = \arctan \frac{V_{(AM)\Lambda}}{V_{(AM)\lambda}} = \arcsin \frac{V_{(AM)\Lambda}}{\left[V^2_{(AM)\lambda} + V^2_{(AM)\Lambda}\right]^{1/2}} = \arccos \frac{V_{(AM)\lambda}}{\left[V^2_{(AM)\lambda} + V^2_{(AM)\Lambda}\right]^{1/2}}$$

$$\gamma = \arctan \frac{V_{(AM)r}}{\left[V^2_{(AM)\lambda} + V^2_{(AM)\Lambda}\right]^{1/2}} = \arcsin \frac{V_{(AM)r}}{V_{(AM)}} = \arccos \frac{\left[V^2_{(AM)\lambda} + V^2_{(AM)\Lambda}\right]^{1/2}}{V_{(AM)}} \quad (5\text{-}19)$$

(5-20)

Rotations from the $\bar{l}_r$, $\bar{l}_\lambda$, $\bar{l}_\Lambda$ triad to the $\bar{l}_z$, $\bar{l}_x$, $\bar{l}_y$ triad are performed in the following order:

(1) Rotate ($\bar{l}_r$, $\bar{l}_\lambda$, $\bar{l}_\Lambda$) to ($\bar{l}_r$, $\bar{l}_{\lambda_1}$, $\bar{l}_{y_{WL}}$) by angle A_H about $\bar{l}_r$ axis.

(2) Rotate ($\bar{l}_r$, $\bar{l}_{\lambda_1}$, $\bar{l}_{yWL}$) to ($\bar{l}_{zWL}$, $\bar{l}_{xWL}$, $\bar{l}_{yWL}$) by angle γ about - $\bar{l}_{yWL}$ axis.

(3) Rotate ($\bar{l}_{zWL}$, $\bar{l}_{xWL}$, $\bar{l}_{yWL}$) to ($\bar{l}_z$, $\bar{l}_x$, $\bar{l}_y$) by angle B about $\bar{l}_{xWL}$ axis.

Direction cosines between $\bar{l}_r$, $\bar{l}_\lambda$, $\bar{l}_\Lambda$ triad and the $\bar{l}_x$, $\bar{l}_y$, $\bar{l}_z$ triad are given in Table 5.2.

Table 5.2: Direction Cosines between $\bar{l}_r$, $\bar{l}_\lambda$, $\bar{l}_\Lambda$ Triad and $\bar{l}_x$, $\bar{l}_y$, $\bar{l}_z$ Triad.

	l_r	$\bar{l}_\lambda$	$\bar{l}_\Lambda$
$\bar{l}_x$	$\sin\gamma$	$\cos\gamma \cos A_H$	$\cos\gamma \sin A_H$
$\bar{l}_y$	$\cos\gamma \sin B$	$-\sin A_H \cos B$ $-\sin\gamma \cos A_H \sin B$	$\cos A_H \cos B$ $-\sin\gamma \sin A_H \sin B$
$\bar{l}_z$	$\cos\gamma \cos B$	$\sin A_H \sin B$ $-\sin\gamma \cos A_H \cos B$	$-\cos A_H \sin B$ $-\sin\gamma \sin A_H \cos B$

The coordinate systems defined above are not those used in conventional aircraft analysis where it is common to define a set of axes fixed to the airframe. It is necessary to define a set of vehicle-fixed axes if the stability and control characteristics are to be studied - a subject beyond the scope of this thesis.

Thrust forces generated by the propulsion system of the entry vehicle will, in general, be applied in such a direction as to slow the vehicle down* (retro-thrust). It is assumed that the thrust vector passes at all times through the vehicle center of gravity in order to avoid excessive moments. The engine gimbal angles shown in Fig. 5.3 were selected to describe the thrust direction.

Rotation from the $\bar{l}_x$, $\bar{l}_y$, $\bar{l}_z$ to the thrust triad ($\bar{l}_{x2}$, $\bar{l}_{y2}$, $\bar{l}_{z2}$) is performed in the following order:

(1) Rotate ($\bar{l}_x$, $\bar{l}_y$, $\bar{l}_z$) to ($\bar{l}_{x1}$, $\bar{l}_{y1}$, $\bar{l}_{z1}$) by angle A_e about $-\bar{l}_y$ axis.

(2) Rotate ($\bar{l}_{x1}$, $\bar{l}_{y1}$, $\bar{l}_{z1}$) to ($\bar{l}_{x2}$, $\bar{l}_{y2}$, $\bar{l}_{z2}$) by angle A_d about $\bar{l}_{z1}$ axis.

Direction cosines between $\bar{l}_{x2}$, $\bar{l}_{y2}$, $\bar{l}_{z2}$ triad and $\bar{l}_x$, $\bar{l}_y$, $\bar{l}_z$ triad are given in Table 5.3.

Table 5.3: Direction Cosines between $\bar{l}_{x2}$, $\bar{l}_{y2}$, $\bar{l}_{z2}$ Triad and $\bar{l}_x$, $\bar{l}_y$, $\bar{l}_z$ Triad

	$\bar{l}_x$	$\bar{l}_y$	$\bar{l}_z$
$\bar{l}_{x2}$	$\cos A_e \cos A_d$	$\sin A_d$	$\sin A_e \cos A_d$
$\bar{l}_{y2}$	$-\cos A_e \sin A_d$	$\cos A_d$	$-\sin A_e \sin A_d$
$\bar{l}_{z2}$	$-\sin A_e$	0	$\cos A_e$

- - - - - - - - - - - - - - - - -

* Except possibly in the landing phase.

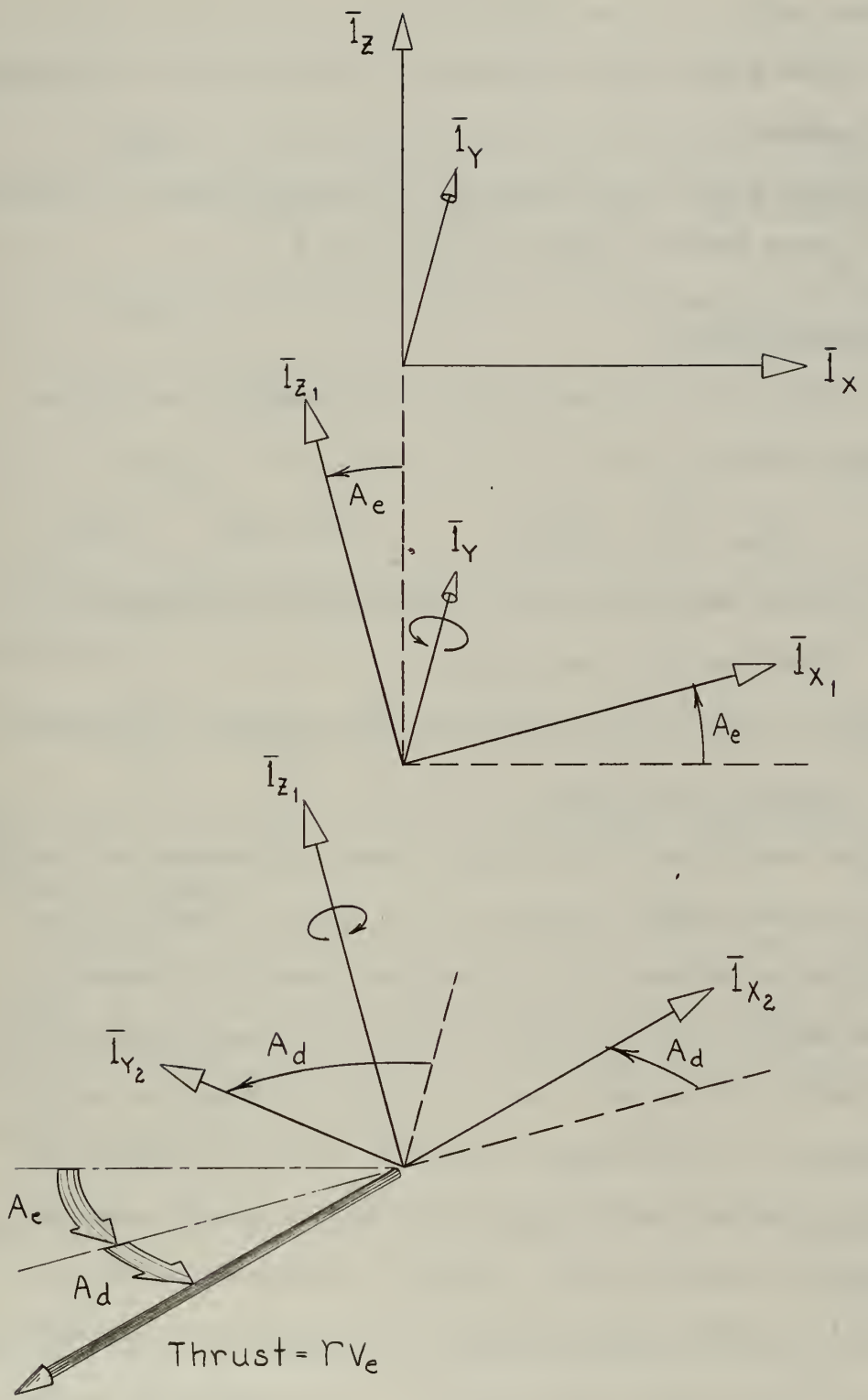

Fig. 5.3: Engine Gimbal Angles

The following angles are shown in Fig. 5.3:

A_e: Engine gimbal angle generated by rotations about the negative $\bar{l}_y$ axis.

A_d: Engine gimbal angle generated by rotations about the displaced $\bar{l}_z$ axis (after rotating through angle A_e).

5.5 Components of Drag.

The velocity vector of the vehicle with respect to the atmosphere, $\bar{V}_{(AM)}$, is:

$$\bar{V}_{(AM)} = \bar{V}_I - \bar{V}_{I(AM)} \qquad (5\text{-}21)$$

where: $\bar{V}_I$ is the velocity vector of the vehicle with respect to fixed inertial coordinates.

$\bar{V}_{I(AM)}$ is the velocity vector of the atmosphere with respect to inertial coordinates.

Under no-wind conditions, the air mass rotates with respect to inertial space with the same angular velocity as the planet. Winds are the result of relative movement of the atmospheric mass with respect to coordinates rotating with the planet. In terms of geographic coordinates, wind may be considered to have a vertical component, a north-south component, and an east-west component. Winds encountered are generally not constant, particularly for a vehicle whose geographic position may be changing rapidly. Updrafts and downdrafts (vertical winds) may, to a first order, be considered as essentially cancelling each other over the long ranges traversed by the entry vehicle; they are generally localized effects[32]. Neglecting vertical components of atmospheric winds, the wind vector is:

$$\bar{V}_{o(AM)} = V_{o(AM)_\lambda}\ \bar{1}_\lambda + V_{o(AM)_\Lambda}\bar{1}_\Lambda \qquad (5\text{-}22)$$

where:

$\bar{V}_{o(AM)}$ is the velocity vector of the moving atmosphere with respect to coordinates fixed in the planet (wind).

$V_{o(AM)_\lambda}$ is the east component of wind (may be positive or negative).

$V_{o(AM)_\Lambda}$ is the north component of wind (may be positive or negative).

The velocity vector of the atmosphere with respect to inertially fixed coordinates is:

$$\bar{V}_{I(AM)} = \bar{V}_{o(AM)} + W_{IO}R\cos\Lambda\bar{1}_\lambda \qquad (5\text{-}23)$$

where W_{IO} is the angular velocity of the planet with respect to inertial coordinates.

Substituting equations (5-22) and (5-23) into equation (5-21), and using $\bar{V}_I$ (in latitude-longitude coordinates) derived in Chapter 3 gives the following equation for the velocity of the vehicle with respect to the moving atmosphere:

$$\bar{V}_{(AM)} = \dot{R}\bar{1}_r + \left[R(\dot{\lambda}_{IP} - W_{IO})\cos\Lambda - V_{o(AM)\lambda}\right]\bar{1}_\lambda + \left[R\dot{\Lambda} - V_{o(AM)\Lambda}\right]\bar{1}_\Lambda \qquad (5\text{-}24)$$

Equation (5-24) is transformed to the instantaneous great circle triad with the aid of Table 3.1:

$$\bar{V}_{(AM)} = \dot{R}\bar{1}_r + \left[V_{I\phi} - (W_{IO}R\cos\psi + V_{o(AM)\phi})\right]\bar{1}_\phi + \left[W_{IO}R\sin\psi\cos\phi - V_{o(AM)\psi}\right]\bar{1}_\psi \qquad (5\text{-}25)$$

The drag specific force vector is:

$$\bar{F}_{(dr)} = - \rho \frac{C_D S}{2M} V^2_{(AM)} \bar{l}_x \tag{5-26}$$

By definition:

$$\bar{l}_x = \frac{\bar{V}_{(AM)}}{\bar{V}_{(AM)}} \tag{5-27}$$

Therefore:

$$\bar{F}_{(dr)} = - \rho \frac{C_D S}{2M} V_{(AM)} \bar{V}_{(AM)} \tag{5-28}$$

The drag components are readily written from equations (5-24), (5-25), and (5-28):

I. Geocentric Latitude-Longitude Coordinates:

A. No wind conditions ($\bar{V}_{o(AM)} = 0$):

$$F_{(dr)_r} = - \rho \frac{C_D S}{2M} V_{(AM)} \dot{R} \tag{5-29}$$

$$F_{(dr)_\lambda} = - \rho \frac{C_D S}{2M} V_{(AM)} R\cos\Lambda (\dot{\lambda}_{IP} - W_{IO}) \tag{5-30}$$

$$F_{(dr)_\Lambda} = - \rho \frac{C_D S}{2M} V_{(AM)} R\dot{\Lambda} \tag{5-31}$$

where:

$$V^2_{(AM)} = \dot{R}^2 + \left[R\cos\Lambda (\dot{\lambda}_{IP} - W_{IO})\right]^2 + (R\dot{\Lambda})^2 \tag{5-32}$$

B. With atmospheric winds ($V_{o(AM)} \neq 0$):

$$F_{(dr)_r} = - \rho \frac{C_D S}{2M} V_{(AM)} \dot{R} \tag{5-33}$$

$$F_{(dr)_\lambda} = -\rho \frac{C_D S}{2M} V_{(AM)} \left[R\cos\Lambda(\dot{\lambda}_{IP} - W_{IO}) - V_{o(AM)\lambda} \right] \quad (5\text{-}34)$$

$$F_{(dr)_\Lambda} = -\rho \frac{C_D S}{2M} V_{(AM)} \left[R\dot{\Lambda} - V_{o(AM)\Lambda} \right] \quad (5\text{-}35)$$

where:

$$V^2_{(AM)} = \dot{R}^2 + \left[R\cos\Lambda(\dot{\lambda}_{IP} - W_{IO}) - V_{o(AM)\lambda} \right]^2 + \left[R\dot{\Lambda} - V_{o(AM)\Lambda} \right]^2 \quad (5\text{-}36)$$

II. Instantaneous Great-Circle Coordinates:

A. No wind conditions ($\bar{V}_{o(AM)} = 0$):

$$F_{(dr)r} = -\rho \frac{C_D S}{2M} V_{(AM)} \dot{R} \quad (5\text{-}37)$$

$$F_{(dr)\phi} = -\rho \frac{C_D S}{2M} V_{(AM)} \left[V_{I\phi} - W_{IO} R\cos\psi \right] \quad (5\text{-}38)$$

$$F_{(dr)\psi} = -\rho \frac{C_D S}{2M} V_{(AM)} \left[W_{IO} R\sin\psi\cos\phi \right] \quad (5\text{-}39)$$

where:

$$V^2_{(AM)} = \dot{R}^2 + (V_{I\phi} - W_{IO} R\cos\psi)^2 + (W_{IO} R\sin\psi\cos\phi)^2 \quad (5\text{-}40)$$

B. With atmospheric winds ($V_{o(AM)} \neq 0$):

$$F_{(dr)r} = -\rho \frac{C_D S}{2M} V_{(AM)} \dot{R} \quad (5\text{-}41)$$

$$F_{(dr)\phi} = -\rho \frac{C_D S}{2M} V_{(AM)} \left[V_{I\phi} - W_{IO} R\cos\psi - V_{o(AM)\phi} \right] \quad (5\text{-}42)$$

$$F_{(dr)\psi} = -\rho \frac{C_D S}{2M} V_{(AM)} \left[W_{IO} R\sin\psi\cos\phi - V_{o(AM)\psi} \right] \quad (5\text{-}43)$$

where:

$$V^2_{(AM)} = \dot{R}^2 + \left[V_{I\phi} - W_{IO} R \cos\psi - V_{o(AM)\phi} \right]^2 + \left[W_{IO} R \sin\psi \cos\phi - V_{o(AM)\psi} \right]^2 \tag{5-44}$$

5.6 Components of Lift

The lift force is directed along the vehicle's $\bar{l}_z$ axis shown in Fig. 5.2:

$$\overline{F_{(li)}} = \rho \frac{C_L S}{2M} V^2_{(AM)} \bar{l}_z \tag{5-45}$$

By using the angular relations of Tables 3.1 and 5.2, the components of lift may be written as follows:

I. Latitude-Longitude Coordinates

$$F_{(li)r} = \rho \frac{C_L S}{2M} \left[V^2_{(AM)\lambda} + V^2_{(AM)\Lambda} \right]^{1/2} V_{(AM)} \cos B \tag{5-46}$$

$$F_{(li)\lambda} = \rho \frac{C_L S}{2M} V_{(AM)} \frac{\left[V_{(AM)} V_{(AM)\Lambda} \sin B - \dot{R} V_{(AM)\lambda} \cos B \right]}{\left[V^2_{(AM)\lambda} + V^2_{(AM)\Lambda} \right]^{1/2}} \tag{5-47}$$

$$F_{(li)_\Lambda} = -\rho \frac{C_L S}{2M} V_{(AM)} \frac{\left[V_{(AM)} V_{(AM)\lambda} \sin B + \dot{R} V_{(AM)\Lambda} \cos B \right]}{\left[V^2_{(AM)\lambda} + V^2_{(AM)\Lambda} \right]^{1/2}} \tag{5-48}$$

In these equations

$$\bar{V}_{(AM)} = \dot{R} \bar{l}_r + \left[R \left(\dot{\lambda}_{IP} - W_{IO} \right) \cos\Lambda - V_{o(AM)\lambda} \right] \bar{l}_\lambda + \left[R \dot{\Lambda} - V_{o(AM)\Lambda} \right] \bar{l}_\Lambda \tag{5-49}$$

II. Great-Circle Coordinates:

$$F_{(li)r} = \rho \frac{C_L S}{2M} \left[V^2_{(AM)\phi} + V^2_{(AM)\psi} \right]^{1/2} V_{(AM)} \cos B \qquad (5\text{-}50)$$

$$F_{(li)\phi} = \rho \frac{C_L S}{2M} V_{(AM)} \frac{\left[V_{(AM)} V_{(AM)\psi} \sin B - \dot{R} V_{(AM)\phi} \cos B \right]}{\left[V^2_{(AM)\phi} + V^2_{(AM)\psi} \right]^{1/2}} \qquad (5\text{-}51)$$

$$F_{(li)\psi} = \rho \frac{C_L S}{2M} V_{(AM)} \frac{\left[V_{(AM)} V_{(AM)\phi} \sin B + \dot{R} V_{(AM)\psi} \cos B \right]}{\left[V^2_{(AM)\phi} + V^2_{(AM)\psi} \right]^{1/2}} \qquad (5\text{-}52)$$

In these equations:

$$\bar{V}_{(AM)} = \dot{R} \bar{1}_r + \left[V_{I\phi} - W_{IO} R \cos \psi - V_{o(AM)\phi} \right] \bar{1}_\phi + \left[W_{IO} R \sin \psi \cos \phi - V_{o(AM)\psi} \right] \bar{1}_\psi \qquad (5\text{-}53)$$

In the special case that atmospheric winds are zero, $\bar{V}_{o(AM)} = 0$ in the foregoing equations.

5.7 Thrust Forces

Thrust or its equivalent must be generated in many phases of astronautical missions in order to perturb the trajectory of the vehicle. For example, in the mid-course phase of an interplanetary ellipse, engines or solar pressure techniques must be used if adjustments of the path of the vehicle are required. In the particular case of the entry mission, thrust forces must be generated for substantial perturbation of the stable reconnaissance orbit since atmospheric perturbations of

this orbit are negligible.

Optimum use of thrust depends very much on the requirements established for the mission. If the vehicle is in a stable reconnaissance orbit initially, and if maximum payload weight is an over-riding requirement for the mission, then the minimum energy trajectory is desired; i.e., it is desired that entry be effected with minimum expenditure of propellant mass. Minimum propellant mass is expended by generating retro-thrust tangentially at apogee in the stable reconnaissance orbit. As a result of this reduction in velocity at apogee, the perigee next following will be at a lower altitude. By generating just enough thrust for the perigee to drop within the sensible atmosphere, the degenerate reconnaissance orbit is established. Controlled entry is possible from the degenerate reconnaissance orbit, particularly if the vehicle has variable drag capabilities[9] .

If payload requirements are not as critical as the requirement for a relatively short time of flight, or if the vehicle has only modest capabilities for changing its aerodynamic characteristics due to structural design limitations, then the minimum energy profile as mentioned above is not necessarily the most efficient method for satisfying mission objectives. Under these conditions, a second retro-thrust application at perigee is a more suitable mission concept than the minimum energy profile of the previous paragraph[33]. This scheme for the entry mission induces the direct entry profile. Considerable landing point control is available if the vehicle is capable of generating lift.

If payload capabilities of the entry vehicle are secondary to stringent requirements on landing point accuracy, the initial retro-

thrust application at apogee in the reconnaissance orbit may be increased a sufficient amount to cause the following perigee to drop beneath the surface of the planet. If the propellant mass expended at apogee in the stable reconnaissance orbit is approximately twice that required for the minimum energy profile, then the transfer ellipse will intersect the atmosphere after the vehicle travels roughly one-fourth of the distance around the planet rather than one-half. The flight path angle at atmospheric penetration is considerably greater under these conditions than when lesser amounts of fuel are expended, hence variations in atmospheric density from standard will result in much lower range errors. This mission concept has advantages from the guidance standpoint, but these advantages are paid for in terms of payload capabilities.

The foregoing qualitative discussion is presented for the purpose of emphasizing that the optimum use of the vehicle's engines is a strong function of mission objectives. There is no single optimum engine program applicable to all entry missions.

The type or configuration of the propulsion system is not considered in detail in this thesis. Among propulsion systems suitable for astronautical vehicles are[34]:

(1) Chemical propellants:
    (a) Liquid propellants
        1. Bi-propellants
        2. Mono-propellants
    (b) Solid propellants
(2) Nuclear propulsion systems:
    (a) Fission

(b) Fusion

(c) Radioactive decay isotopes

(3) Electrical propulsion systems:

(a) Arc heating

(b) Ion propulsion

(c) Magneto plasma systems

(4) Solar heating rocket.

(5) Light wave propulsion:

(a) Solar sail

(b) Photon rocket

It is generally planned at this time to use chemical propellants for entry missions. In the atmospheric portions of the flight, air breathing engines may be used in addition to those listed above.

The mass of chemical propellants required to perturb the trajectory a given amount depends on the specific impulse of the propellant. The higher the specific impulse, the better the propellant*. Specific impulse is determined experimentally by measuring the thrust generated and dividing it by the fuel flow rate:

$$I_{sp} = \frac{\text{Thrust}}{\Gamma G} = \frac{V_e}{G} \text{ seconds} \qquad (5\text{-}54)$$

where I_{sp} is specific impulse,

Γ is mass flow rate of fuel

V_e is the effective exhaust velocity of the gases.

- - - - - - - - - - - - - - - -

* This statement must be qualified because other characteristics must be considered besides the specific impulse. For example, if the density of the propellant is low, then a larger volume of space may be required to achieve a given total impulse than is required by a more dense competitive fuel of lower specific impulse.

The following relation must be satisfied between vehicle mass, time, and propellant mass flow:

$$\dot{M} + \Gamma(t) = 0 \qquad (5\text{-}55)$$

Exhaust velocity is usually computed from measurements of I_{sp}, not vice-versa. Specific impulse may be predicted fairly accurately by applying the laws of thermodynamics to the chemicals involved.

It is shown in reference (34) that values of specific impulse presently attainable or expected in the foreseeable future for chemical rockets range from 200 to 420 seconds.

The total impulse, I_t, is the integral of the thrust over the burning time of the engine:

$$I_t = \int_o^{t_b} (\text{Thrust})\, dt = \int_o^{t_b} \Gamma V_e dt \qquad (5\text{-}56)$$

where t_b is propellant burning time. For constant exhaust velocity:

$$I_t = V_e (M_i - M_f) \qquad (5\text{-}57)$$

where M_i and M_f denote initial and final mass of the vehicle.

Requirements for astronautical missions are often stated in terms of the change of velocity required:

$$\delta V = V_e \ln \frac{M_i}{M_f} \qquad (5\text{-}58)$$

where δV is the magnitude of the velocity change of the vehicle resulting from the thrust impulse. The velocity impulse must be added <u>vectorially</u> to the vehicular velocity prior to "turning on" thrust in order to determine final velocity of the craft after thrust perturbation.

In this thesis the power plant is assumed to be an ideal rocket engine with a constant equivalent exit velocity. It is assumed that both the magnitude and direction of the applied thrust may be controlled; that is, the engine may be rotated by means of a gimbal system and the engine is capable of being throttled. The magnitude of the applied thrust is $V_e \Gamma(t)$, where $\Gamma(t)$ is a controllable propellant mass flow rate. $\Gamma(t)$ may vary between zero (coasting flight) and Γ_{max} (maximum engine output). Miele[30] represents the propellant mass flow rate in parametric form as shown in Fig. 5.4.

The following three operation regimes are possible:

(1) $-\infty \leq u \leq u_1$; $\Gamma = 0$; $\frac{d\Gamma}{dt} = 0$; coasting flight.

(2) $u_2 \leq u \leq +\infty$; $\Gamma = \Gamma_{max}$; $\frac{d\Gamma}{dt} = 0$; maximum engine output.

(3) $u_1 \leq u \leq u_2$; $\frac{d\Gamma}{du} \neq 0$; variable thrust

Referring to the engine gimbal triad in Fig. 5.3, the following may be written for the thrust vector:

$$\overline{F_{(th)}} = -\frac{\Gamma V_e}{M} \bar{l}_{x_2} \tag{5-59}$$

Using the angular relations of Table 5.3, this may be written:

$$\overline{F_{(th)}} = -\frac{\Gamma V_e}{M} \left[\cos A_e \cos A_d \, \bar{l}_x + \sin A_d \, \bar{l}_y + \sin A_e \cos A_d \, \bar{l}_z \right] \tag{5-60}$$

Thrust components may be written in component form in the $\bar{l}_r$, $\bar{l}_\lambda$, $\bar{l}_\Lambda$ triad by using the direction cosines given in Table 5.2.

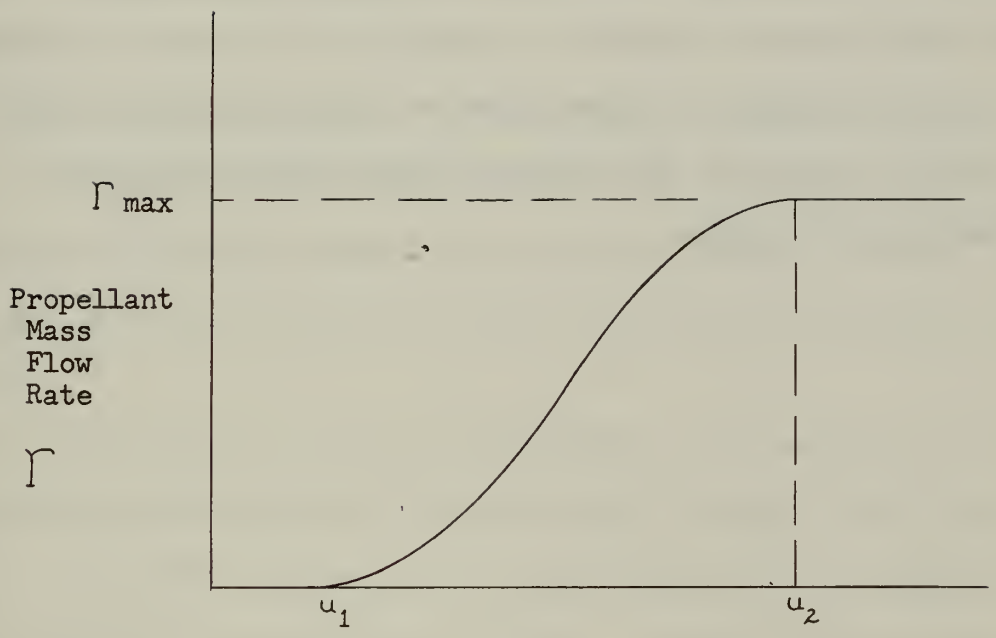

u : A parameter having no physical meaning: $-\infty < u < +\infty$

$\Gamma_{(u)}$: Variable propellant mass flow rate. A controllable quantity that is a function of u.

Fig. 5.4: Parametric Representation of Propellant Mass Flow.[30]

These components may, in turn, be transformed to the $\bar{1}_r$, $\bar{1}_\phi$, $\bar{1}_\psi$ triad by the table of cosines and angular conversions of Table 3.1.

Once the velocity requirements of the entry vehicle are established, the propulsion system must be designed in such a way that thrust may be applied in the proper direction with the proper magnitude and for the proper length of time; i.e., thrust vector control. Thrust vector control is also important for generation of orientation torques for attitude stability; problems connected with thrust vector control for attitude orientation and rotational moment stability are not considered in this thesis.

Chapter 6

THE THEORY OF PLANAR MOTION

A two-dimensional model of the trajectory is generally assumed in most dynamical studies of astronautical missions before the additional complexity of the third dimension is introduced into the problem. In this way, the problem statement is made successively more complete and complex.

An investigation of the three-dimensional characteristics of the trajectory was undertaken first in this thesis, however, before simplifying the problem statement to two dimensions in order to emphasize the limitations on assuming planar motion. In some situations, the trajectory of the vehicle may remain in a plane essentially fixed with respect to inertial coordinates. In other situations, the orientation of the plane of the trajectory is rapidly changing. Section 6.1 discusses conditions under which the trajectory may be accurately described by a two-dimensional model.

6.1 Limitations of the Theory if Planar Motion

Determination of three-dimensional dynamical equations of motion of the entry vehicle in two separate guidance grids was discussed in chapters 3 through 5. These equations were generalized to describe entry of lifting or non-lifting vehicles in banking or wings-level

flight with variable thrust capabilities into the atmosphere of oblate, rotating planets with or without atmospheric winds. The resulting vector equation was:

$$\overline{F}_{(li)} + \overline{F}_{(dr)} + \overline{F}_{(th)} = \overline{A} - \overline{G} \qquad (6\text{-}1)$$

Even if the left-hand side of equation (6-1) vanishes, which corresponds to powerless flight in a vacuum, it was shown in Chapter 4 that the resulting motion of the vehicle is <u>not</u> confined to a single plane in space because of non-spherical components of gravitational mass attraction. Gravitational perturbations lead to periodic oscillation of the angle of inclination and to secular effects such as regression of the line of nodes and advance of perigee. During the powered portions of the trajectory ($\overline{F}_{(th)} \neq 0$) and during the atmospheric phase of flight ($\overline{F}_{(li)}$ and $\overline{F}_{(dr)} \neq 0$), the left-hand side of equation (6-1) is of great importance in specifying the ultimate path of the vehicle.

Variables which define the orientation of the orbital plane are ψ, the inclination of the trajectory plane with respect to the equatorial plane, and λ_{IT}, the longitude of the line of nodes measured as an angle with respect to fixed inertial coordinates. The plane of the entry vehicle's trajectory remains fixed in inertial space under the following conditions:

(1) In the special case of an equatorial trajectory ($\psi = 0$), the requirement for planar motion is simply:

$$\dot{\psi} = 0 \qquad (6\text{-}2)$$

(2) If the trajectory has a finite inclination to the equatorial plane ($\psi \neq 0$), both the longitude of the

line of nodes, λ_{IT}, and the inclination of the orbital plane, ψ, must remain constant in order that the trajectory be confined to a single plane in space. Therefore, if $\psi \neq 0$, then

$$\dot{\lambda}_{IT} = 0$$
$$\dot{\psi} = 0 \qquad (6\text{-}3)$$

must simultaneously be satisfied in order to apply the theory of planar motion.

The line of nodes cannot be visualized in the special case of an equatorial trajectory since it is defined as the line of intersection of the equatorial plane with the trajectory plane. Movement of any line in the equatorial plane does not contribute to a change in orientation of the trajectory plane with respect to inertial coordinates as long as the trajectory plane is coincident with the equatorial plane; therefore, there is no restriction on $\dot{\lambda}_{IT}$ in case (1) above.

Equation (3-14) showed that:

$$\dot{\lambda}_{IT} \cos\phi \sin\psi = \dot{\psi} \sin\phi \qquad (3\text{-}14)$$

From equations (4-23) and (6-1), the time rate of change of longitude of the line of nodes is:

$$\dot{\lambda}_{IT} = \frac{\sin\phi}{V_{I\phi} \sin\psi}(F_\psi + G_\psi) \qquad (6\text{-}4)$$

Using equations (3-14) and (6-4), the time rate of change of the inclination of the trajectory plane is as follows:

$$\dot{\psi} = \frac{\cos \phi}{V_{I\phi}} (F_{\psi} + G_{\psi}) \qquad (6\text{-}5)$$

In powerless flight, thrust terms in F_{ψ} are equal to zero. Substituting lift*, drag*, and gravitational terms as written in Chapter 5 into equations (6-4) and (6-5) gives, under zero bank conditions (i.e., B = 0):

$$\dot{\lambda}_{IT} = -\frac{\sin\phi}{V_{I\phi}} \left\{ 12\nu G_{sp} \left(\frac{R_{(eq)o}}{R}\right)^2 \sin\phi \cos\psi + \frac{\rho C_D S}{2M} VRW_{IO} \cos\phi \left(1 - \frac{L}{D} \frac{\dot{R}}{\left[(V_{I\phi} - RW_{IO}\cos\psi)^2 + (RW_{IO}\sin\psi\cos\phi)^2\right]^{1/2}}\right)\right\} \qquad (6\text{-}6)$$

$$\dot{\psi} = -\frac{\cos\phi \sin\psi}{V_{I\phi}} \left\{\begin{array}{l}\text{Same as curly bracket} \\ \text{term in Eq. (6-6)}\end{array}\right\} \qquad (6\text{-}7)$$

The theory of planar motion therefore requires the right-hand side of both equations (6-6) and (6-7) to be equal to zero in the case of a finite angle of inclination ($\psi \neq 0$). In the special case of an equatorial trajectory ($\psi = 0$), it is sufficient that the right-hand side of equation (6-7) alone vanish. Because of the $\sin\psi$ term in the numerator of equation (6-7), it is seen that planar motion results for powerless (no thrust), wings-level flight in the equatorial plane in the special case that wind components normal to the trajectory plane do not exist.

The theory of planar motion is therefore valid under the following

- - - - - - - - - - - - - - - - -

* Atmospheric winds were assumed zero in this substitution, i.e., $\bar{V}_{o(AM)} = 0$. When wind is zero, the velocity vector of the vehicle with respect to the atmosphere $\bar{V}_{(AM)}$ is the same as the velocity vector of the vehicle with respect to coordinates rotating with the planet, $\bar{V}$. Thus, under no-wind conditions, $\bar{V} = \bar{V}_{(AM)}$.

limiting circumstances:

(1) Equatorial trajectory ($\psi = 0$)

(a) Components of atmospheric winds normal to the trajectory plane are zero ($V_{o(AM)} = 0$).

(b) The angle of bank of the vehicle is zero ($B = 0$).

(c) There are no components of thrust generated normal to the trajectory plane ($A_d = 0$).

(d) Gravity anomalies do not exist.

(2) Trajectory that is not in the equatorial plane ($\psi \neq 0$)

Lift, drag, and thrust must be programmed such that

(a) $\dot{\psi} = 0$

(b) $\dot{\lambda}_{IT} = 0$

In much of the analytical work described in subsequent chapters of this thesis, planar motion is assumed. For purposes of generality, the angle of inclination ψ is retained in these equations and is assumed constant. The following factors contribute to changing the orientation of the trajectory plane if $\psi \neq 0$:

(1) Non-spherical components of the planet's gravitational field.

(2) Gravity anomalies.

(3) Lift and drag components normal to the $\bar{l}_r - \bar{l}_\phi$ plane resulting from:

(a) The rotating atmosphere

(b) Atmospheric winds

(c) Banking the vehicle.

(4) Thrust components normal to the $\bar{l}_r - \bar{l}_\phi$ plane.

6.2 The Two-Dimensional Equations of Motion

Fig. 6.1 shows the forces acting at the center of mass of the entry vehicle and defines the positive direction of the various angles, velocities and forces. From the kinematic equations of Chapter 3:

$$A_r = \ddot{R} - V_{I\phi}^2/R \tag{6-8}$$

$$A_\phi = \dot{V}_{I\phi} + (\dot{R}/R)\ V_{I\phi} \tag{6-9}$$

The acceleration components are written in terms of components in the tangential ($\bar{I}_x$) direction and the normal ($\bar{I}_z$) direction by noting that:

$$A_x = A_r \sin\gamma + A_\phi \cos\gamma \tag{6-10}$$

$$A_z = A_r \cos\gamma - A_\phi \sin\gamma \tag{6-11}$$

The horizontal component of the velocity of the vehicle with respect to the rotating atmosphere, V_ϕ , is related to the horizontal component of velocity with respect to fixed Newtonian coordinates, $V_{I\phi}$, by:

$$V_{I\phi} = V_\phi + W_{IO}R\cos\psi = V\cos\gamma + W_{IO}R\cos\psi \tag{6-12}$$

The rate of change of radius is related to velocity and flight path angle by:

$$\dot{R} = V \sin\gamma \tag{6-13}$$

Equation (6-12) is used to eliminate $V_{I\phi}$ and equation (6-13) is used to eliminate $\dot{R}$ and $\ddot{R}$ from equations (6-8) and (6-9). The resulting acceleration components are written in the tangential and normal directions by using equations (6-10) and (6-11):

$$A_x = \dot{V} - W_{IO}^2\, R\cos^2\psi\ \sin\gamma \tag{6-14}$$

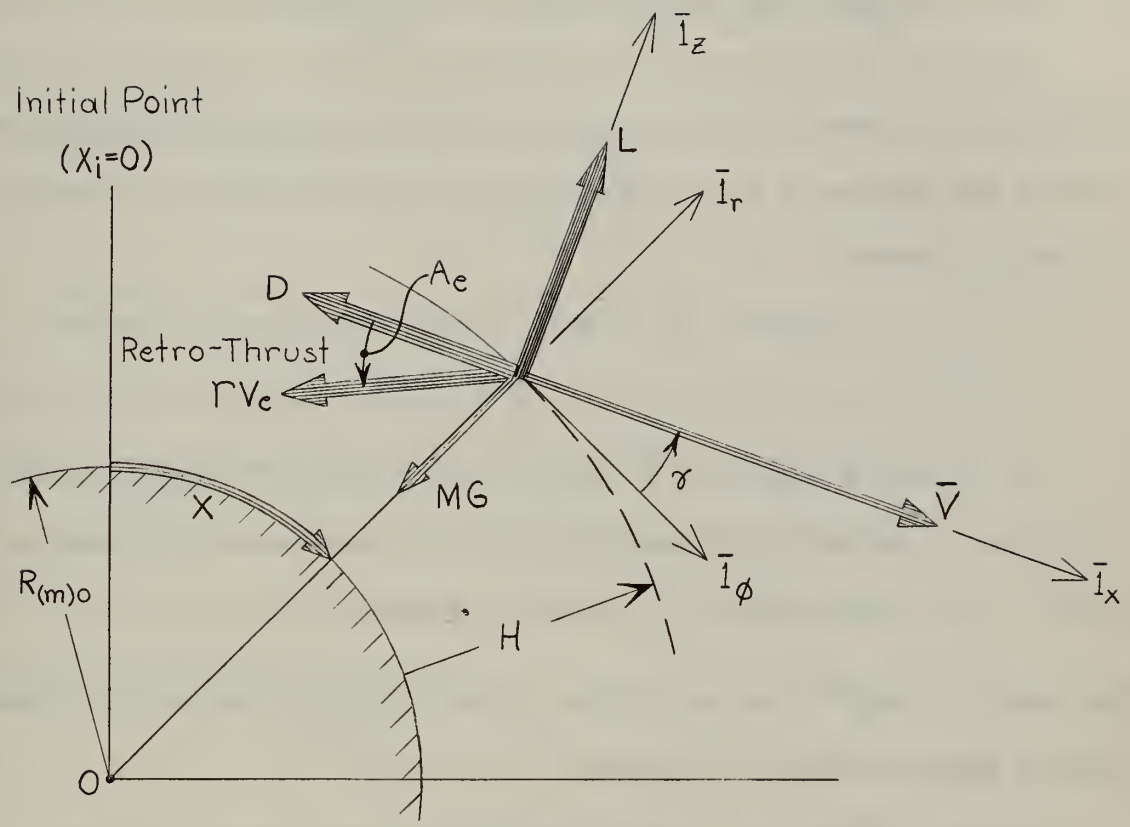

Definitions:

X = distance flown

$\bar{V}$ = velocity of vehicle with respect to coordinates rotating with the planet (same as velocity of vehicle with respect to the planetary atmosphere, $\bar{V}_{(AM)}$, for no-wind condition)

H = altitude of vehicle above planet

γ = flight path angle with respect to local geocentric horizon - positive as shown.

Γ = mass flow rate of propellant

V_e = equivalent exit velocity of rocket propellant (assumed constant)

M = instantaneous mass of vehicle

D = drag

L = lift

A_e = engine gimbal angle of retro-rocket; angle the thrust vector makes with negative $\bar{I}_x$ axis.

Fig. 6.1: The Two-Dimensional Trajectory

$$A_z = V\dot{\gamma} - \frac{V^2 \cos\gamma}{R} - W_{IO}^2 R\cos^2\psi \cos\gamma - 2 W_{IO} V\cos\psi \qquad (6\text{-}15)$$

The following terms in these kinematic equations are the consequence of stating the problem in a reference space which is rotating with respect to inertial space:

(1) $2 W_{IO} V\cos\psi$ is Coreolis acceleration due to coupling of vehicular velocity with angular velocity of the planet.

(2) The $W_{IO}^2 R\cos^2\psi$ terms in both equations are centrifugal components associated with the rotation of the planet with respect to inertial coordinates.

The quantity $\frac{V^2 \cos\gamma}{R}$ is centrifugal force resulting from motion of the vehicle with respect to the planet.

Assuming a spherical planet, the gravitational specific force vector reduces to:

$$\bar{G} = - G_{sp} \bar{l}_r = - G_{sp} \left(\sin\gamma \bar{l}_x + \cos\gamma \bar{l}_z \right) \qquad (6\text{-}16)$$

The vector sum of external specific forces are readily written from Fig. 6.1:

$$\bar{F} = - \left(\frac{D}{M} + \frac{\Gamma V_e \cos A_e}{M} \right) \bar{l}_x + \left(\frac{L}{M} - \frac{\Gamma V_e \sin A_e}{M} \right) \bar{l}_z \qquad (6\text{-}17)$$

Substituting equations (6-14) through (6-17) into equation (6-1) and rearranging gives:

$$\dot{V} + (G_{sp} - W_{IO}^2 R\cos^2\psi) \sin\gamma + \frac{D}{M} + \frac{\Gamma}{M} V_e \cos A_e = 0 \qquad (6\text{-}18)$$

$$V\dot{\gamma} - \frac{V^2 \cos\gamma}{R} + (G_{sp} - W_{IO}^2 R\cos^2\psi)\cos\gamma - \frac{L}{M} + \frac{\Gamma V_e}{M} \sin A_e - 2 V W_{IO}\cos\psi = 0 \qquad (6\text{-}19)$$

The following kinematic equations are required in addition to the two dynamical equations in order to complete the theory of planar motion. From equation (5-55):

$$\dot{M} + \Gamma = 0 \tag{6-20}$$

From equation (6-13):

$$\dot{R} - V \sin\gamma = 0 \tag{6-21}$$

In establishing guidance requirements for the entry system, the range capability under given flight conditions is a fundamental quantity that must be predicted. Defining X on Fig. 6.1 as distance flown, range rate may be readily written as follows:

$$\dot{X} - \frac{R_{(m)o}}{R} V \cos\gamma = 0 \tag{6-22}$$

6.3 Dimensionless Planar Equations of Motion

Numerical solutions to guidance parameters and constraints may be applied to a broad class of entry missions if the solutions are presented in dimensionless form. Subsequent chapters of this thesis are devoted exclusively to examination of the entry problem in dimensionless form.

The convention generally followed in this thesis is to represent dimensional quantities by capital letters and the same quantity in dimensionless form by lower case letters. It will be noted that there are certain exceptions to this rule because, at times, conflicts in notation arise; however, in most cases this convention is obeyed.

The following parameters were chosen for purposes of converting the various dimensional quantities into non-dimensional form:

(1) The reference length chosen was the mean radius of the planet, $R_{(m)o}$.

(2) The reference velocity chosen was the satellite velocity at the surface of the planet:

$$V_S = \sqrt{G_{(m)o} R_{(m)o}} \qquad (6\text{-}23)$$

(3) The reference acceleration chosen was the mean gravitational acceleration at the surface of the planet, $G_{(m)o}$.

$$G_{(m)o} = \frac{\gamma_g M_o}{R_{(m)o}^2} \qquad (6\text{-}24)$$

(4) The reference mass chosen was the initial mass of the entry vehicle prior to the expenditure of rocket fuel during the particular segment of the trajectory being examined.

(5) Reference time was chosen from items (1) and (2) above as follows:

$\tau \equiv$ dimensionless time

$$\tau = \frac{V_S}{R_{(m)o}} t = \sqrt{\frac{G_{(m)o}}{R_{(m)o}}}\, t \qquad (6\text{-}25)$$

With these reference quantities, the following dimensionless terms were defined:

(1) $v \equiv$ dimensionless velocity of the vehicle with respect to coordinates rotating with the planet.

$$v = \frac{V}{V_S} \qquad (6\text{-}26)$$

(2) $v_I \equiv$ dimensionless velocity of the vehicle with respect to planet centered inertial coordinates.

$$v_I = \frac{V_I}{V_S} \tag{6-27}$$

(3) $\frac{d(\ )}{d\tau} \equiv$ dimensionless time rate of change of the quantity in paranthesis.

$$\frac{d(\ )}{d\tau} \equiv (\ )' = \sqrt{\frac{R_{(m)o}}{G_{(m)o}}}\ \frac{d(\ )}{dt} = \sqrt{\frac{R_{(m)o}}{G_{(m)o}}}\ (\dot{\ }) \tag{6-28}$$

(4) $m \equiv$ dimensionless mass of the vehicle.

$$m = \frac{M}{M_i} \tag{6-29}$$

(5) $r \equiv$ dimensionless radius from the center of the planet to the vehicle.

$$r = \frac{R}{R_{(m)o}} \tag{6-30}$$

(6) $h \equiv$ dimensionless altitude

$$h = \frac{H}{R_{(m)o}} \tag{6-31}$$

(7) $X_N \equiv$ dimensionless distance flown.

$$X_N = \frac{X}{R_{(m)o}} \tag{6-32}$$

(8) Γ_N dimensionless propellant mass flow rate.

$$\Gamma_N = \frac{\Gamma}{M_i}\sqrt{\frac{R_{(m)o}}{G_{(m)o}}} \tag{6-33}$$

(9) $v_e \equiv$ dimensionless equivalent exit velocity of exhaust gases.

$$v_e = \frac{V_e}{V_S} \tag{6-34}$$

(10) $\Omega \equiv$ dimensionless angular velocity of the planet about

its polar axis.

$$\Omega = W_{IO} \sqrt{\frac{R_{(m)o}}{G_{(m)o}}} \tag{6-35}$$

(11) $n_D \equiv$ drag load factor

$$n_D = \frac{F_{(dr)}}{G_{(m)o}} = \frac{D}{M\, G_{(m)o}} \tag{6-36}$$

(12) $n_L \equiv$ lift load factor.

$$n_L = \frac{F_{(li)}}{G_{(m)o}} = \frac{L}{M\, G_{(m)o}} \tag{6-37}$$

Gravitational mass attraction appears in the following form in the dimensionless equations of motion.

$$\text{Dimensionless } G_{sp} = \frac{G_{sp}}{G_{(m)o}} = \left(\frac{R_{(m)o}}{R}\right)^2 = \frac{1}{r^2} \tag{6-38}$$

Dimensionless radius and altitude are related as follows:

$$r = 1 + h \tag{6-39}$$

With the foregoing dimensionless quantities, the equations of motion given in section 6.2 are written as follows:

$$v' + \left(\frac{1}{r^2} - r\Omega^2\cos^2\psi\right)\sin\gamma + n_D + \frac{\Gamma_N}{m} v_e \cos A_e = 0 \tag{6-40}$$

$$v\gamma' - \frac{v^2}{r}\cos\gamma + \left(\frac{1}{r^2} - r\Omega^2\cos^2\psi\right)\cos\gamma - n_L + \frac{\Gamma_N}{m} v_e \sin A_e - 2v\Omega\cos\psi = 0 \tag{6-41}$$

$$m' + \Gamma_N = 0 \tag{6-42}$$

$$r' - v \sin\gamma = h' - v \sin\gamma = 0 \tag{6-43}$$

$$X_N' - (v/r)\cos\gamma = 0 \tag{6-44}$$

6.4 An Alternate Set of Planar Equations:

Equations (6-40) and (6-41) describe the dynamics of entry in the $\bar{l}_x$ and $\bar{l}_z$ directions. In some of the investigations described in subsequent chapters of this thesis, it was found more convenient to work with the tangential and radial components of velocity instead of velocity and flight path angle as primary dependent variables. For this statement of the entry problem the following quantities were defined:

$$v_r \equiv v \sin\gamma \tag{6-45}$$

$$v_\phi \equiv v \cos\gamma \tag{6-46}$$

Differentiating these equations and substituting for v' from equation (6-40) and γ' from equation (6-41) gives:

$$v_r' - \frac{v_\phi^2}{r} + n_D \sin\gamma\left(1 - \frac{L}{D}\cot\gamma\right) + \left(\frac{1}{r^2} - r\Omega^2\cos^2\psi\right)$$

$$+ \frac{v_e}{m}\Gamma_N \sin(\gamma + A_e) - 2v_\phi\Omega\cos\psi = 0 \tag{6-47}$$

$$v_\phi' + \frac{v_r v_\phi}{r} + n_D\cos\gamma\left(1 + \frac{L}{D}\tan\gamma\right) + \frac{v_e}{m}\Gamma_N\cos(\gamma + A_e)$$

$$+ 2v_r\Omega\cos\psi = 0 \tag{6-48}$$

Equations (6-47) and (6-48) are the equations of motion in the $\bar{l}_r$ and $\bar{l}_\phi$ directions respectively. The following additional equations complete this planar set of equations:

$$m' + \Gamma_N = 0 \tag{6-49}$$

$$r' - v_r = h' - v_r = 0 \tag{6-50}$$

$$X_N' - \frac{v_\phi}{r} = 0 \tag{6-51}$$

6.5 Energy and Angular Momentum

The dimensionless equations of motion which describe planar entry were specified in the $\bar{1}_x$ and $\bar{1}_z$ directions in section 6.3. These equations in turn were written in the $\bar{1}_r$ and $\bar{1}_\phi$ directions in section 6.4. An equivalent set of dimensionless equations is described in the following paragraphs; total energy and angular momentum are used as prime dependent variables in this particular description of the entry problem.

Total energy and angular momentum are conserved in Keplerian trajectories. In a system characterized by the presence of external torques and non-conservative forces*, energy and angular momentum are not conserved.

The total energy of the vehicle was written in equation (4-10) as:

$$\frac{\mathcal{E}_{(tot)}}{M} = - G_{sp}R + \frac{V_I^2}{2} \tag{6-52}$$

The zero level of potential energy in this equation is at infinity, hence the system is characterized by a negative total energy.

- - - - - - - - - - - - - - - - -

* Conservative forces are forces which depend on position only. Gravitational mass attraction, for example, is a conservative force. All other classes of forces, such as velocity-dependent forces, are non-conservative forces.

Dimensionless total energy per unit mass is defined as follows:

$$E_{(tot)} \equiv \frac{\mathcal{E}_{(tot)}}{M\ V_s^2} \qquad (6\text{-}53)$$

Equation (6-52) therefore reduces to:

$$E_{(tot)} = \frac{v_I^2}{2} - \frac{1}{r} \qquad (6\text{-}54)$$

The time rate of change of total energy is the dot product of the non-conservative force vector and the velocity vector of the vehicle. In dimensionless form, this is equivalent to:

$$E'_{(tot)} = \bar{f} \cdot \overline{v_I} \qquad (6\text{-}55)$$

where $\bar{f}$ is the vector sum of all external specific forces in mean surface g's of the planet.

$$f \equiv \frac{\bar{F}}{G_{(m)o}} = \frac{1}{G_{(m)o}} \left(\bar{F}_{(dr)} + \bar{F}_{(li)} + \bar{F}_{(th)}\right) \qquad (6\text{-}56)$$

The dot product of force and velocity in equation (6-55) is the rate of working of the force, or the <u>power</u>. The rate at which the vehicle is transferring energy, given by equation (6-55), may be measured by the instrumentation system as follows:

$$E'_{(tot)} = v_{I_r} \text{ (Accelerometer output in } \bar{l}_r \text{ direction)} + v_{I_\phi} \text{ (Accelerometer output in } l_\phi \text{ direction)} \qquad (6\text{-}57)$$

or

$$E'_{(tot)} = v_{I_x} \text{ (Accelerometer output in } \bar{l}_x \text{ direction)}$$

$$+ v_{I_z} \quad \text{(Accelerometer output in } \bar{I}_z \text{ direction).} \tag{6-58}$$

Equation (6-55) may be written as follows:

$$\frac{d}{d\tau}\left(\frac{v_I^2}{2} - \frac{1}{r}\right) = -\left[\left(n_D + \frac{v_e}{m}\Gamma_N \cos A_e\right)\left(v + r\cos\gamma\,\Omega\cos\psi\right) + \left(n_L - \frac{v_e}{m}\Gamma_N \sin A_e\right)\left(r\sin\gamma\,\Omega\cos\psi\right)\right] \tag{6-59}$$

Equation (6-55) can be written in integral form as follows:

$$E_{(tot)} - E_{(tot)_i} = \int_0^\tau \left(\bar{f} \cdot \bar{v}_I\right) d\tau \tag{6-60}$$

Equation (6-60) is equivalent to:

$$\left(\frac{v_I^2}{2} - \frac{1}{r}\right)\Bigg|_{\tau=0}^{\tau} = \int_0^\tau d\tau \left[\left(n_D + \frac{v_e}{m}\Gamma_N \cos A_e\right)\left(v + r\Omega\cos\gamma\cos\psi\right) + \left(n_L - \frac{v_e}{m}\Gamma_N \sin A_e\right)\left(r\Omega\sin\gamma\cos\psi\right)\right] \tag{6-61}$$

Angular momentum was defined in equation (4-1) as:

$$P = R\,V_{I_\phi} \tag{4-1}$$

The dimensionless angular momentum is defined as follows:

$$p \equiv \frac{P}{R_{(m)_0}\,V_S} \tag{6-62}$$

Therefore, dimensionless angular momentum may be written:

$$p = r\left(v_\phi + r\Omega\cos\psi\right) \tag{6-63}$$

The time rate of change of angular momentum is equal to the external torque applied, therefore:

$$\bar{p}' = \bar{r} \times \bar{f} \tag{6-64}$$

The rate at which the vehicle is transferring angular momentum because of applied external forces may be measured by the instrumentation system as follows:

$$p' = r \text{ (Accelerometer output in } \bar{l}_\phi \text{ direction)} \tag{6-65}$$

Equation (6-65) is equivalent to:

$$(r v_{I\phi})' = -r\left[n_D \cos\gamma\left(1 + \frac{L}{D}\tan\gamma\right) + \frac{\Gamma_N}{m} v_e \cos(\gamma + A_e)\right] \tag{6-66}$$

Equation (6-65) can be written in integral form as:

$$p - p_i = \int_0^\gamma r\, f_\phi \, d\gamma \tag{6-67}$$

Equation (6-67) is equivalent to:

$$r(v_\phi + r\Omega\cos\psi)\Big|_{\gamma=0}^{\gamma} = -\int_0^\gamma d\gamma\left\{r\left[n_D\cos\gamma\left(1 + \frac{L}{D}\tan\gamma\right) + \frac{\Gamma_N}{m} v_e \cos(\gamma + A_e)\right]\right\} \tag{6-68}$$

The dynamical equations of motion were written as dimensionless equations in the $\bar{l}_x$ and $\bar{l}_z$ directions as equations (6-40) and (6-41) and in the $\bar{l}_r$ and $\bar{l}_\phi$ directions as equations (6-47) and (6-48). These sets are equivalent to the energy and angular momentum equations derived in differnetial form as equations (6-59) and (6-66) and in integral form as equations (6-61) and (6-68).

6.6 Instrumentation of Planar Entry

Section 6.5 showed that the energy and angular momentum levels of the entry vehicle can be determined from velocity, altitude, and specific force measurements as follows:

$$E_{(tot)} = E_{(tot)_i} + \int_0^\tau d\tau \left(f_r v_{I_r} + f_\phi v_{I\phi} \right) \tag{6-69}$$

$$p = p_i + \int_0^\tau d\tau \left(r f_\phi \right) \tag{6-70}$$

where: $r = 1 + h$: radius to the vehicle, non-dimensionalized with respect to mean radius of the planet.

f_r, f_ϕ are specific force measurements in the geocentric vertical and horizontal directions respectively (non-dimensionalized with respect to mean surface g's of the planet).

v_{Ir}, $v_{I\phi}$ are vertical and horizontal components of velocity with respect to planet-centered inertial coordinates (non-dimensionalized with respect to circular satellite velocity at the surface of the planet).

If r is measured by some external means, such as with radar, and if initial values of energy and angular momentum are known, then it is possible to design a system to compute position and velocity based on equations (6-69) and (6-70) and the definitions of energy and angular momentum:

$$p = r\, v_{I\phi} \tag{6-71}$$

$$E_{(tot)} = \frac{v_I^2}{2} - \frac{1}{r} \tag{6-72}$$

The operation of this system depends, of course, on the ability

of the system to measure specific force components in the vertical and horizontal directions; this is equivalent to saying that some means must be available for indicating the vertical. Angular momentum may be continuously computed in accordance with equation (6-70) from externally derived altitude data and from measurements of the horizontal component of specific force. With the computed value of angular momentum and the observed altitude, the horizontal component of the velocity is determined directly by equation (6-71). Equations (6-69) and (6-72) may be written:

$$\frac{p^2}{2r^2} + \frac{v_{Ir}^2}{2} - \frac{1}{r} = E_{(tot)_i} + \int_0^{\gamma} d\gamma \left(f_r v_{I_r} + f_\phi \frac{\rho}{r} \right) \tag{6-73}$$

Assuming that the system is capable of measuring f_r and f_ϕ, and with the computed value of p and the measured value of r, the radial component of velocity is determined from (6-73). The system has therefore determined all quantities important for navigating the vehicle: v_{Ir}, $v_{I\phi}$ and r. From these quantities the flight path angle γ, distance flown X, position, etc., may be computed. The instantaneous energy level is useful in predicting the number of orbits (range) capable of being traveled by the vehicle. Range prediction from energy levels is discussed further in Chapter 10.

Chapter 7

TRAJECTORY CONSTRAINTS: VEHICULAR HEATING AND HUMAN ACCELERATION TOLERANCES

7.1 Energy Transfer During Entry

A vehicle approaching a planetary atmosphere possesses a large amount of energy; for example, the kinetic energy of a vehicle in a circular orbit around the Earth is of the order of 13,500 BTU per pound. All of the mechanical energy possessed by the vehicle need not be converted to heat within the body itself during its passage through the atmosphere; there is sufficient energy to vaporize the entire vehicle unless a large percentage of this energy is transferred to the atmosphere. The energy must be transferred in a manner that will not prove disastrous either to the vehicle or its human occupants. The original energy of the vehicle is transformed, through the mechanism of gas-dynamic drag, into thermal energy of the gas surrounding the craft; the fraction of the original energy that ultimately appears as thermal energy of the vehicle itself depends on the characteristics of the gaseous flow.

The build-up of appreciable heating and deceleration loads are two of the most important effects encountered during entry of a vehicle into a planetary atmosphere. Both the deceleration loads and the heating rates are most severe when there is a combination of high atmospheric density and high vehicular velocity; it is therefore

necessary that the guidance system operate in such a way as to prohibit high velocities from persisting down to low altitudes. This undesirable condition most likely will occur if the flight path angle γ is large and if the approach velocity is very great.

The velocity of the vehicle at atmospheric penetration depends on the mission concept. If atmospheric penetration is permitted at the termination of an interplanetary transfer ellipse, then the velocity at penetration is of the order of escape velocity. If entry is initiated from a reconnaissance orbit around the planet, then the velocity at atmospheric penetration is near circular orbital velocity. The velocity at initial atmospheric penetration can be changed a significant amount only by large scale thrust perturbations; this leads to severe penalties in terms of payload capabilities. The flight path angle, on the other hand, may generally be selected at a lesser cost in terms of weight, provided thrust perturbations are applied at the proper time and in the proper direction. For example, a small thrust perturbation during the interplanetary transfer ellipse (when the vehicle is far from its destination planet) can change the flight path angle at initial atmospheric penetration a very large amount. It must be emphasized that a small error in thrust perturbation at this point, however, can lead to gross errors in penetration angle; thus guidance accuracy requirements go up with an increase in the sensitivity of the system to control actions.

A shallow flight path angle (tangential approach) tends to limit the region of high velocities to high altitudes. Consequently, choosing a shallow trajectory tends to minimize heating rates and deceleration loads encountered. Inaccurate knowledge of the density characteristics

of the planetary atmosphere, however, may lead to considerably greater range errors for entry at shallow flight path angles than for steep flight path angles. Therefore, it may be seen that the flight path angle at atmospheric penetration must be selected as a compromise between two conflicting mission requirements:

(1) Heating rates and deceleration loads are appreciably reduced at shallow flight path angles.

(2) Range accuracy is generally greater for steep flight path angles.

The coupling of payload requirements, sensitivity to control actions, vehicular heating rates, acceleration loads, and guidance accuracy in determination of the best entry profile are not the only conflicting considerations that must be resolved by the design engineer of the entry mission system. The mechanism of energy transfer to the planetary atmosphere is also a function of the configuration of the vehicle. High drag (blunt) vehicles cause deceleration to take place at higher altitudes than is the case for low drag shapes. Lifting vehicles allow more gradual descents; hence the high velocity portion of the flight can be restricted to higher altitudes with lift in order to reduce deceleration loads and heating rates. Table 7.1, taken from reference (7), shows the wide range of deceleration loads which may be encountered during entry. The deceleration loads are a sensitive function of the initial conditions of the problem and of the gas-dynamic characteristics of the vehicle.

In subsequent sections of this chapter, the manifestation of energy transfer from the vehicle to the planetary atmosphere in the form of heating and deceleration are discussed. The general approach taken in

Table 7.1: Maximum Decelerations Encountered During Atmospheric Entry (Values given in Earth g's)

Direct Entry at Escape Velocity (Zero-Lift Vehicle)	Venus	Earth	Mars
$\gamma_i = -5°$	28.6	28.3	1.6
$\gamma_i = -20°$	112	111	6.3
$\gamma_i = -90°$	326	324	18.3
Direct Entry at Orbital Velocity:			
A. Zero-Lift Vehicle			
$\gamma_i = 0$	8.9	9.5	1.4
$\gamma_i = -5°$	14.3	14.2	0.8
$\gamma_i = -20°$	56	55.5	3.2
$\gamma_i = -90°$	163	162	9.2
B. Lifting Vehicles at $\gamma_i = 0°$			
L/D = 1	0.88	1.0	0.38
L/D = 2	0.44	0.5	0.2
L/D = 5	0.18	0.2	0.07

this thesis is that the choice of a reference or nominal trajectory should not necessarily be that trajectory for which heating and decelerations are minimized. Instead, these materializations of energy transfer between vehicle and atmosphere should be viewed as establishing constraints on allowable profiles for any given mission. Trade-offs may be made among other mission factors in arriving at an optimum entry profile for any particular entry system as long as these constraints are not violated. These are one-sided constraints on the entry guidance problem since maximum allowable values alone are of concern to the designer. Maximum allowable accelerations for the human crew, of course, are a function of the direction in which they are applied.

In this chapter, heating and acceleration constraints are presented in analytical and in graphical form as a series of velocity-altitude plots for entry into the atmosphere of Venus, Earth, and Mars. In order to determine quantitative values for graphical representation of these one-sided constraints, it is necessary that the density characteristics of the atmosphere and the lift and drag characteristics of the vehicle be specified. The exponential model of the planetary atmosphere* and the lift-drag characteristics of the three classes of vehicles summarized in Table 5.1 were chosen as sufficiently general to be representative of many possible entry situations.

In addition to trajectory constraints resulting from energy transfer considerations, viz. heating and acceleration loads encountered during the atmospheric phase of flight, radiation bands surrounding the planet may offer enough of a hazard to manned entry to influence the selection

- - - - - - - - - - - - - - - -

* Atmospheric models of the various planets are discussed in Appendix E.

of a suitable mission profile. Possible constraints on the entry trajectory as a result of radiation belts around the planet are discussed briefly in section 7.2.

7.2 Radiation Constraints on Entry

The discovery in December, 1958, of belts of energetic particles trapped in the Earth's magnetic field has suggested re-evaluation of certain entry mission concepts. These radiation belts, named after Dr. James A. Van Allen who first disclosed their discovery, were detected by the Army's Pioneer III lunar probe. Pioneer III showed two distinct belts; the inner belt is centered approximately 2400 miles and the outer belt centered at approximately 10,000 miles above the surface of the Earth. Maximum radiation rate was estimated to be of the order of 10 Roentgens per hour. A comparatively free area exists between the two belts; for example, the measured radiation rate at 6000 miles was approximately 0.3 Roentgens per hour. Pioneer IV (March 1959) reported particle densities in the outer belt to be many times greater than those measured by Pioneer III. It is believed that the particles in these belts are of solar origin.

It is reasonable to assume that Van Allen radiation belts may exist around any planet possessing a magnetic field. Drake[15] suggests that radio waves from Jupiter originate from the Jovian version of the Van Allen belts. He estimates radiation intensities to be 100 times as strong in the Jovian belts as in the Earth belts. Experimental verification of Venusian, Martian, and other planetary belts should be one of the important functions of unmanned planetary probes, the first of which has not yet been launched.

The effects of radiation on human beings depend not only on the total amount absorbed, but also on the area of the body exposed and on the rate of absorption. The biological effect of a given dose of radiation decreases as the rate of exposure decreases; for example, 600 Roentgens would almost certainly be fatal if absorbed by the whole body in one day, but would probably have no noticeable consequences if spread over 20 years. If the radiation rate is small, the damaged tissues have a chance to recover.

Because large doses have been accepted by human beings only as a result of accidents of one kind or another, it is not possible to state definitely that a particular amount of radiation will have certain consequences. The following table[35] gives an approximate indication of the early effects on humans of occasional large doses of radiation absorbed in a short period of time over the whole body. Somewhat larger doses may be accepted if the exposure is protracted over several days or weeks.

Table 7.2: Approximate Effects of Radiation Doses to Human Beings

Dose	Probable Effect
0-25 Roentgens	No obvious injury
25-50 R.	Possible blood changes. No severe injury.
50-100 R.	Blood-cell changes, some injury, no disability.
100-200 R.	Injury, possible disability
200-400 R.	Injury and disability certain, death possible.
400 R.	Fatal to 50%.
600 R. or more	Fatal.

Quantitative constraints on the entry trajectory resulting from planetary radiation belts cannot be accurately determined until more data on these belts is accumulated. The most severe consequence of these belts should be restrictions on the allowable altitudes of the planetary reconnaissance orbits. The path of the reconnaissance orbit must be such that the crew does not accumulate total radiation dosages beyond prescribed human radiation maximums. The allowable maximum, of course, must be well below lethal levels; the successful completion of the mission is jeopardized if the pilot or crew incur mild radiation sickness to the extent of experiencing feelings of discomfort or uneasiness (malaise), depression, or bodily fatigue.

For reconnaissance orbits with perigees below the inner radiation belt, the eccentricity of the orbit must be low enough that radiations incurred by penetration of this belt in the vicinity of apogee are mild. Since entry is effected in the degenerate orbital profile by atmospheric perturbations in the vicinity of perigee (which is well below the inner radiation belt), the energy possessed by the vehicle in excess of the energy level corresponding to circular orbital energy at perigeal altitude must be constrained. Chapter 10 discusses methods for predicting apogeal altitudes from prescribed perigeal flight conditions for the degenerate orbit.

The major advantage of the degenerate orbital profile as a concept for the entry phase of interplanetary probes is the high payload weights possible (since a thrust generating mechanism is not required). The presence of planetary radiation belts may make it mandatory, however, that severe restrictions be established on allowable eccentricities of the first few braking passes. It is for this reason that the direct

first-pass entry profile is worthy of serious consideration, even though it presents a more severe guidance problem in combatting heating and acceleration hazards.

Data accumulated on the radiation belts around Earth show the belts to resemble distorted donuts with comparatively free areas along the polar axis. Trajectories from outer space which are oriented in polar directions will encounter considerably less radiations than trajectories oriented in equatorial directions. Radiation considerations may be important in prescribing the most favorable direction for approaching the planet.

The radiation belts may be viewed in the context of this thesis as presenting constraints on the initial conditions of the entry problem. The direction of approach to the planet prescribes the initial orientation of the trajectory plane. If a reconnaissance orbit is part of the mission concept, the radiation belts constrain the initial values of the parameters of the reconnaissance ellipse to certain maximums. Once the initial conditions of the entry phase of the mission are prescribed, the primary trajectory constraints which must be considered are heating and acceleration loads resulting from the passage of the vehicle through the planetary atmosphere. These are considered in subsequent sections of this chapter.

7.3 Heating of the Entry Vehicle

The reduction of the total energy of a vehicle during its passage through a planetary atmosphere is accompanied by an increase in thermal energy of the surrounding gas. Most of the critical problems associated with this heat transfer occur in the continuum flow regime[36]. Some

of this thermal energy is transferred to the surface of the vehicle; the fraction of thermal energy which reaches the vehicle's surface is of primary concern to the designer. This fraction depends on the mechanism of heat transfer between the hot gas and the vehicle surface and on vehicle shape, velocity, and altitude. At extremely high altitudes, the heat energy is developed directly at the vehicle's surface. At lower altitudes, thermal energy appears in the gas between the shock wave and the vehicle. Heat is transferred from this hot gas to the body by conduction and convection through the viscous boundary layer. Radiation from the hot gas may also contribute appreciably to the surface heating.

The net rate of heat input to an element of the surface of the vehicle is:

(1) the rate of heat entering by convection ($\dot{Q}_c$)

plus (2) the rate of heat entering by gaseous radiation ($\dot{Q}_r$)

minus (3) the rate of heat re-radiated from the surface ($\dot{Q}_{rad}$)

minus (4) the rate of heat conducted to adjacent elements of the surface

minus (5) the rate of heat conducted to the interior of the vehicle

minus (6) the rate of heat radiated to the interior of the vehicle.

The net rate of heat input to this surface element causes its temperature to change. The temperature change may be sufficient for the material either to melt or to sublimate. The heating of the vehicle determines the type of surface protection required. Methods for protecting a payload from high external heating include[7]:

(1) Thickening of skin: to absorb heat in a greater mass of material (in the case of transient heating) and to

compensate for decreased material strength at elevated temperatures (in the case of equilibrium conditions).

(2) Insulation of the outer surface: to reduce transmission of external heat into the interior of the vehicle.

(3) Cooling of the inner skin surface: absorbing transmitted heat by heating a coolant fluid.

(4) Transpiration cooling: pumping of gas or vapor through a porous skin to carry heat away from and to insulate the vehicle.

(5) Ablation cooling: carrying away heat and insulating by vaporizing the surface material of the vehicle.

(6) Combination of methods (1) through (5).

The basic mechanism of gas-dynamic heating is influenced by the geometry of the vehicle. Fig. 7.1 shows the flow pattern around a blunt vehicle and around a slender vehicle[37].

(1) Blunt vehicle: The shock wave is detached and ahead of the vehicle is nearly normal to the velocity vector. The gas between the body and the shock wave is hot and moves slowly with respect to the vehicle. The velocities of the gas in the boundary layer are small enough that little viscous dissipation occurs. The temperature in the boundary layer rises smoothly from a relatively low value at the surface to the high value characteristic of the gas between the vehicle and shock wave. Heat is convected from this gas to the surface of the vehicle.

(2) Slender vehicle: The shock wave is oblique to the stream,

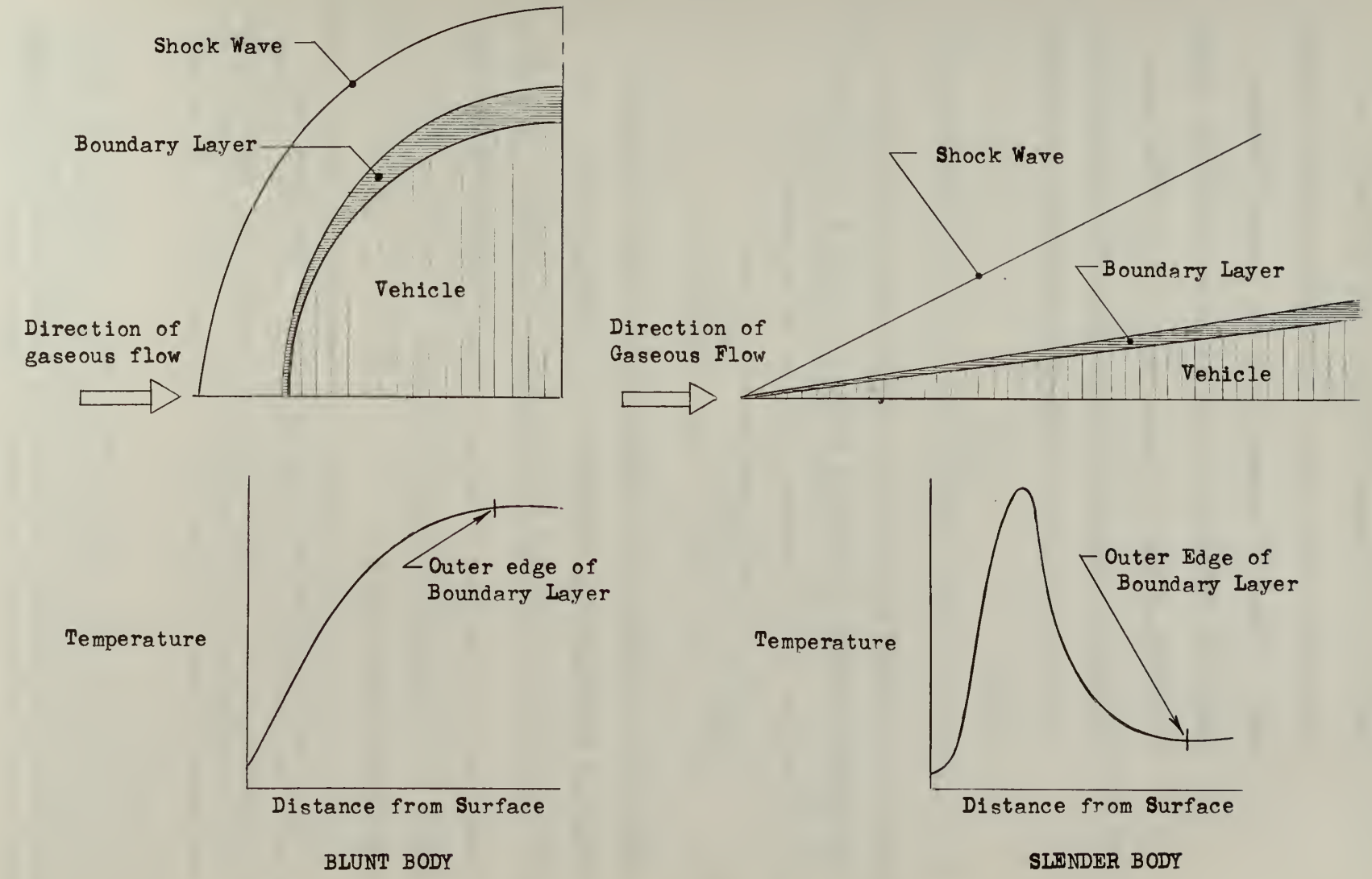

Fig. 7.1: Effect of Body Shape on the Mechanism of Gas-dynamic Heating[37].

hence the gas between the shock wave and vehicle is moving fast with respect to the vehicle and is relatively cool. Since the boundary layer has a steep velocity shear, the viscosity of the gas causes mechanical energy to be transformed to thermal energy within this layer. The maximum temperature occurs within the boundary layer and is convected both toward and away from the vehicle's surface.

It is apparent from these examples that the rate of heat transfer by convection is different for vehicles of different configurations.

The convective heating rate at a stagnation point $(\dot{Q}_c)_s$, with radius of curvature R, in hypersonic flow can be expressed as:

$$(\dot{Q}_c)_s = \frac{C_{(atm)}}{\sqrt{R}} \left(\frac{\rho}{\rho_{(SL)}}\right)^n \left(\frac{V_{(AM)}}{\sqrt{GR}}\right)^m Y \qquad \frac{BTU}{ft^2\text{-}sec} \qquad (7\text{-}1)$$

The dimensionless constants m and n depend on the type of boundary layer flow and the dimensional constant $C_{(atm)}$ (dimensions: BTU-ft.$^{-3/2}$ sec^{-1}) is a function of the planetary atmosphere. Y is unity for a sphere and is a function of angle of attack, angle of sweep, and Mach number if the vehicle has lifting surfaces.

For laminar flow*: $n = \frac{1}{2}$

If the viscosity of the gas is proportional to the square root of the temperature: $m = 3$. Other values of m determined theoretically and experimentally are: 3.1 (ref. 38); 3.15 (ref. 39); 3.22 (references 40 and 41).

- - - - - - - - - - - - - - - - -

* During entry, the Reynolds numbers in the regions important for heat transfer are almost always low enough to insure laminar flow[15][36].

$C_{(atm)}$ for the Earth's atmosphere is variously given as follows:

16,800	BTU/ft.$^{3/2}$ - sec.	(ref. 38)
17,000		(ref. 15)
17,600		(refs. 37 and 39)
19,800		(refs. 40 and 41).

Radiation heating rates from the hot gas to the surface of the vehicle may be expressed as follows:

$$\dot{Q}_r = \left(\frac{K_g}{l_g}\right) K_{boltz}\, T_t\, l_g \qquad \frac{BTU}{ft^2\ sec.} \qquad (7\text{-}2)$$

where K_g/l_g = radiation emissivity of the gas per unit path length

K_{boltz} = Stefan-Boltzman constant (4.81×10^{-13} $\frac{BTU}{sec.\ ft.^2\ {}^\circ R^4}$)

T_t = stagnation temperature of the gas (°R).

l_g = path length of gas.

Blunt bodies experience more heating by gaseous radiation than do slender bodies. Rubensin[37] shows that the magnitudes of K_g and T_t in equation (7-2) must be determined for the real gas rather than using ideal gas relations*.

The total heat input to a surface element of the vehicle is the sum of equations (7-1) and (7-2). In the analysis performed in this thesis, thermal contributions from gaseous radiation to the surface of the vehicle are ignored. Gaseous radiation contributes a small percentage of the total heat for small vehicles, hence the neglect of this

- - - - - - - - - - - - - - - - -

* Ideal gas stagnation temperatures for entry into the Earth's atmosphere at satellite speeds are approximately four times as great as real gas temperatures. Emissivity, K_g, results directly from real gas effects.[37]

quantity is not serious in this case. For example, Rubensin shows that gaseous radiation contributes less than 1% of the total heat input for the following specific vehicles:

(1) Non-lifting hemisphere with diameter of one foot, weight 82 lbs., and W/C_DS = 26 lbs./ft.^{2}

(2) Non-lifting hemisphere with diameter of one foot, weight 45.5 lbs., and W/C_DS = 14.5 lbs./ft.^{2}

(3) Lifting vehicle with triangular wings of blunt leading edges and thickness equal to 10% of total length. Other characteristics of vehicle:

(a) Angle of sweep = 60°

(b) C_L = 0.59

(c) L/D = 0.7

(d) α = 42°

(e) W = 57 lbs.

(f) Length of wing: 3.6 ft.

(g) Area of wing: 7.4 ft.^{2}

Vehicles five times as large as the foregoing, with the same M/S, are more representative of small manned entry vehicles. Gaseous radiation for these larger vehicles contributes approximately 10% of the total heat input[37]. For winged vehicles at very large angles of attack (near 90°), gaseous radiation should contribute more than the percentage estimated above. Neglect of thermal inputs due to gaseous radiation should lead to inaccuracies of less than 20% in the computations described subsequently in this thesis. Simplified methods for computing this radiation are not available at present. Determination of accurate analytical methods for including gaseous radiation warrants further study.

Four aspects of gas-dynamic heating of the entry vehicle may be important to the design engineer:

(1) The total heat input:

Total coolant weight* required depends on the total heat input.

(2) The maximum time rate of average heat input per unit area:

Peak average rates of fluid coolants and the required structural strength (where thermal stresses predominate) depend on the maximum time rate of average heat input per unit area.

(3) The maximum time rate of local heat input per unit area.

(4) The maximum local skin temperature.

Local heating is a serious problem with hypervelocity vehicles. "Hot spots" occur at the stagnation region of the nose and leading edges of planar surfaces used for developing lift and obtaining stable and controlled flight.

For entry missions of short duration, such as non-lifting entry at a steep flight path angle, the maximum heating rates are high but the total heat input is low. Re-radiation from the surface of the vehicle plays a minor role in cooling the craft. Vehicles designed for this type of entry generally must rely on a structure that:

(1) Absorbs heat by raising the temperature of a mass of material**;

- - - - - - - - - - - - - - - - -

* The coolant may be solid (e.g., the structure), liquid, gas, or combination thereof.

** Beryllium is a favorable structural material in this case.

(2) Absorbs heat with a heat shield that decomposes and changes phase in a self-controlled process (ablation)*.

For entry missions of long duration, the total heat input is large but the heating rates are generally small enough that re-radiation may be adequate for cooling the vehicle. Internal cooling systems may be desired for special areas of large vehicles. Strong structural materials can generally withstand the maximum temperatures encountered; weak refractory materials may be used at leading edges and tips of planar surfaces where hot spots develop and where the capability of withstanding heavy structural loads is not required.

Re-radiation from the surface of the vehicle may be written as follows:

$$\dot{Q}_{rad} = K_{rad} K_{boltz} T_{surf}^4 \qquad \frac{BTU}{ft^2\ sec} \qquad (7\text{-}3)$$

where $\dot{Q}_{rad}$ = rate of heat re-radiated from the surface.

K_{rad} = surface radiation emissivity.

K_{boltz} = Stefan-Boltzman constant.

T_{surf} = temperature of the surface in degrees Rankine.

K_{rad} is of the order of 0.8 at high surface temperatures for representative metals of vehicles with thin shell structure.

For missions of short duration, which generally involve heat-sink type vehicles, the total heat input must not exceed design maximums. The total heat absorbed during entry is the sum of convective heating

- - - - - - - - - - - - - - - - -

* Teflon (polyletrofluorethylene) is commonly referenced in the unclassified literature as a suitable material for this purpose.

and gaseous radiation thermal inputs:

$$Q_{tot} = \int_{S_w} \int_{0}^{t_f} \dot{Q} \, dt \, dS_w \qquad (7\text{-}4)$$

where: S_w is the wetted area

$$\dot{Q} = \dot{Q}_c + \dot{Q}_r$$

and t_f is total time of flight.

The heating rate at any point on the entry vehicle is a certain fraction, k_1, of the stagnation point heating rate. The magnitude of k_1 varies with the location of the unit area and the geometry of the vehicle.

$$k_1 = \frac{\dot{Q}}{\dot{Q}_s} \qquad (7\text{-}5)$$

$\dot{Q}_s$ is heating rate per unit area at the stagnation point and is independent of the wetted area.

Thus equation (7-4) may be written with the aid of equation (7-5):

$$Q_{tot} = \left[\frac{1}{S_w} \int k_1 \, dS_w \right] S_w \int_0^{t_f} \dot{Q}_s \, dt \qquad (7\text{-}6)$$

The quantity in square brackets is a function of the geometry of the vehicle. For hemispheres, it is approximately equal to 0.5[15][37].

For missions of long duration, which generally involve vehicles which are cooled by re-radiation, the heating rates must not exceed design maximums. In this case, the mission is usually conceived as one for which the vehicle operates at radiation equilibrium temperatures throughout the trajectory. The stagnation surface temperature experienced during entry of a vehicle designed to operate at radiation

equilibrium temperatures is calculated by equating the input heating rate to the re-radiation heating rate:

$$\dot{Q}_c + \dot{Q}_r = \dot{Q}_{rad} \qquad (7\text{-}7)$$

Neglecting the input heating due to gaseous radiation since it generally contributes a small percentage of the total heat, Eq. (7-7) is written as follows from equations (7-1) and (7-3):

$$\frac{C_{(atm)}}{\sqrt{R}}\left(\frac{\rho}{\rho_{(SL)}}\right)^{\frac{1}{2}}\left(\frac{V_{(4M)}}{\sqrt{GR}}\right)^{3} = K_{rad}K_{boltz}T_s^{4} \qquad (7\text{-}8)$$

In equation (7-8), T_s is stagnation point temperature; laminar flow is assumed ($n = \frac{1}{2}$); m is assumed equal to 3 from the ideal gas relation; and Y is assumed equal to 1.0.

7.4 Analytical Representation of Trajectory Constraints Resulting from Convective Heating of Vehicles Designed to Operate at Radiation Equilibrium Temperatures

Equation (7-8) is the fundamental equation used in this thesis for expressing constraints on the trajectory resulting from gas-dynamic heating. Temperatures in the vicinity of the stagnation point or stagnation line may be useful from the guidance standpoint because:

(1) Temperatures conceivably can be measured either directly or indirectly in flight.

(2) The temperature history for a given nominal profile of a particular vehicle entering the atmosphere of a particular planet may be predicted as shown in subsequent chapters of this thesis. Guidance information can be deduced by comparing measured and predicted values.

(3) Temperatures change rapidly early in the mission while changes in specific force level are more abrupt later in the mission.* Temperature readings may be useful in early determination of atmospheric conditions actually being encountered in flight.

In order to write an analytical expression for stagnation point temperature from equation (7-8) for entry into the atmosphere of an arbitrary planet, it is necessary to investigate the atmospheric model of the planet. Lees[40] shows that:

$$C_{(atm)} \cong (\text{Constant})\left(\rho_{(SL)}\mu_{(SL)}\right)^{\frac{1}{2}}(GR)^{\frac{3}{2}}Pr^{-\frac{2}{3}}\left(\frac{\gamma_o - 1}{\gamma_o}\right)^{\frac{1}{4}} \qquad (7\text{-}9)$$

The following symbols are used in equation (7-9):

P_r = Prandtl number

γ_o = C_p/C_v = ratio of atmospheric heat capacity

C_p = heat capacity at constant pressure

C_v = heat capacity at constant volume

$\mu_{(sl)}$ = sea level coefficient of viscosity of the planetary atmosphere (slug/ft.-sec.).

Assuming no atmospheric winds ($V_{o(AM)} = 0$), then:

$$V_{(AM)} = V \qquad (7\text{-}10)$$

Non-dimensionalizing velocity in accordance with the procedure of Chapter 6:

$$v = \frac{V}{V_s} = \frac{V}{\sqrt{G(m)_o\, R(m)_o}} \qquad (7\text{-}11)$$

---

* Maximum temperature levels are encountered when the vehicle velocity has slowed to about 0.8 circular satellite velocity, while maximum accelerations occur at much slower velocities (see Chapt. 9).

Substituting equations (7-9) through (7-11) into equation (7-8) gives:

$$K_{rad} K_{boltz} T_s^4 = (\text{Constant}) \left(\frac{\rho \mu_{(SL)}}{R} \right)^{\frac{1}{2}} V_s^3 r^3 P_r^{-\frac{2}{3}} \left(\frac{\gamma_o - 1}{\gamma_o} \right)^{\frac{1}{4}} \qquad (7\text{-}12)$$

Various models of planetary atmospheres are discussed in appendix E. Assuming the exponential model:

$$\rho = \rho_{(\overline{SL})} e^{-KH} \qquad (7\text{-}13)$$

where $\rho_{(\overline{SL})}$ is the "assumed" mean sea level atmospheric density. This is not necessarily equal to the true sea level density $\rho_{(SL)}$. The "assumed" quantity is the intercept of the straight line which best fits the curve log ρ vs. altitude.

K is the atmospheric density decay parameter, ft.$^{-1}$.

H is the altitude of the vehicle above the surface of the planet, ft.

The following constants were assumed for the planetary radius and for the parameters of the exponential atmospheric model (see Appendix E):

	Venus	Earth	Mars
$R_{(m)o}$, ft.	20.27×10^6	20.89×10^6	11.08×10^6
$\rho_{(\overline{SL})}$, slugs/ft.^{3}	0.0326	0.0027	0.000193
K, ft.$^{-1}$	4.89×10^{-5}	4.25×10^{-5}	1.67×10^{-5}

Assuming for the Earth's atmosphere the following values:

$$C_{(atm)} = 17{,}000 \text{ BTU ft.}^{-3/2} \text{ sec}^{-1}$$

$$P_r = 1.0^*$$

$$\gamma_o = 1.4$$

---

* The assumption that $P_r = 1$ for hypersonic flow in the Earth's atmosphere is generally made[31].

then the (Constant) in equation (7-12) is written:

$$(\text{Constant}) = \frac{590}{\sqrt{2}} \mu_{(SL)E}^{-\frac{1}{2}} G_{(m)E}^{-\frac{3}{2}} R_{(m)E}^{-\frac{5}{4}} K_E^{-\frac{1}{4}} Pr_E^{\frac{2}{3}} \left(\frac{\gamma_E - 1}{\gamma_E}\right)^{-\frac{1}{4}} \tag{7-14}$$

The subscript E in equation (7-14) denotes values of the various quantities for the Earth and its atmosphere.

Substituting Eq. (7-13) and (7-14) into equation (7-12) gives:

$$K_{rad} K_{boltz} T_s^4 = \frac{590}{\sqrt{2}} \left(\frac{\rho_{(SL)}}{R}\right)^{\frac{1}{2}} (HR)_{EO} \left(\frac{R_{(m)O}}{K}\right)^{\frac{1}{4}} v^3 e^{-\frac{KH}{2}} \tag{7-15}$$

where $(HR)_{EO}$ represents the "heating ratio" of the atmosphere of planet O with respect to the Earth:

$$(HR)_{EO} = \left(\frac{\mu_{(SL)}}{\mu_{(SL)E}}\right)^{\frac{1}{2}} \left(\frac{G_{(m)O}}{G_{(m)E}}\right)^{\frac{3}{2}} \left(\frac{R_{(m)O}}{R_{(m)E}}\right)^{\frac{5}{4}} \left(\frac{K}{K_E}\right)^{\frac{1}{4}} \left(\frac{Pr}{Pr_E}\right)^{-\frac{2}{3}} \left(\frac{\frac{\gamma_O - 1}{\gamma_O}}{\frac{\gamma_E - 1}{\gamma_E}}\right)^{\frac{1}{4}} \tag{7-16}$$

Equation (7-15) may be further simplified to:

$$K_{rad} K_{boltz} T_s^4 = \frac{417}{\sqrt{R}} (HF)_O v^3 e^{-\frac{kh}{2}} \tag{7-17}$$

In equation (7-17):

$k \equiv KR_{(m)O}$: dimensionless atmospheric density decay parameter

$h \equiv H/R_{(m)O}$: dimensionless altitude

$(HF)_O$ is the "heating function" of the planetary atmosphere.

$$(HF)_O = (HR)_{EO} \rho_{(SL)}^{\frac{1}{2}} \left(\frac{R_{(m)O}}{K}\right)^{\frac{1}{4}} \quad \text{slugs}^{\frac{1}{2}}/\text{ft.} \tag{7-18}$$

Equation (7-17) is written in the following form:

$$K_{rad}\, K_{boltz}\, T_s^4 = 18{,}000\, \frac{(HF)_{EO}}{\sqrt{R}}\, v^3 e^{-\frac{\beta h}{2}} \qquad \frac{BTU}{ft.^2\text{-sec.}} \tag{7-19}$$

where $(HF)_{EO}$ is the ratio of the heating function of the planetary atmosphere with respect to the heating function of Earth's atmosphere:

$$(HF)_{EO} = \frac{(HF)_O}{(HF)_E} \tag{7-20}$$

Table 7.3 summarizes approximate values of the heating function for the terrestrial planets.

Table 7.3 Heating Function of the Terrestrial Planets

Planet	$(HF)_O$	$(HF)_{EO}$	$(HF)_{EO}^{\frac{1}{4}}$
Venus	105	2.41	1.25
Earth	43.5	1.0	1.0
Mars	1.1	.0253	0.4

It should be noted that the right-hand side of equation (7-19) expresses the convective heat flow rate as a function of vehicular velocity, radius of curvature at the stagnation point, and flight altitude for entry into an arbitrary planetary atmosphere.

Equation (7-19) is solved for stagnation point temperature as follows:

$$T_s = 1.392 \times 10^4\, (HF)_{EO}^{\frac{1}{4}}\, (VF)^{\frac{1}{4}}\, v^{\frac{3}{4}}\, e^{-kh/8} \tag{7-21}$$

where (VF) represents a "vehicle design function":

$$(VF) = \frac{1}{K_{rad} R^{\frac{1}{2}}} \tag{7-22}$$

K_{rad} is of the order of 0.8 at high surface temperatures for representative thin shell structures.

Within the approximations made in arriving at equation (7-21), the following stagnation temperatures are derived for a vehicle with (VF) = 1.0 flying at circular orbital velocity at the surface of the terrestrial planets:

$$(T_s)_{Earth} = 14{,}000° \text{ Rankine}$$

$$(T_s)_{Venus} = 17{,}300° \text{ Rankine}$$

$$(T_s)_{Mars} = 5{,}600° \text{ Rankine}$$

The same vehicle traveling at 0.8 circular orbital velocity at 50 nautical miles altitude above Earth has a stagnation temperature of 2310° R. and at 40 statute miles a temperature of 3830° R. Rubensin[37] computed the following approximate maximum temperatures for hemispheres entering the Earth's atmosphere: For circular orbital decay, $(T_s)_{max}$ is equal to 3700° R; for entry with initial flight path angle of minus 4°, $(T_s)_{max} = 4850°$ R.

Stagnation temperature is a useful guidance parameter for vehicles designed to operate at radiation equilibrium temperatures. From the guidance standpoint, the trajectory must be constrained such that maximum design heat flow rates are not exceeded.

$$0 < \dot{Q}_c < (\dot{Q}_c)_{max} \tag{7-23}$$

where

$$\dot{Q}_c \cong 18{,}000 \frac{(HF)_{EO}}{\sqrt{R}} v^3 e^{-\frac{\beta h}{2}} \qquad \frac{BTU}{ft^2\,sec} \tag{7-24}$$

If input convective heat flow rate and re-radiation heat flow rate are

in equilibrium, equation (7-23) may be written in terms of stagnation point temperature, which is a measurable manifestation of the heat transfer.

$$0 < T_s < (T_s)_{max} \tag{7-25}$$

T_s is given by equation (7-21) and $(T_s)_{max}$ is the maximum allowable stagnation temperature. The inequality (7-25) may be written as an equality which must be satisfied by all <u>acceptable</u>* trajectories. Since stagnation temperatures must not exceed a certain design maximum while no restriction is placed on minimum temperatures, this temperature limitation on trajectories is a "one-sided" constraint. One-sided constraints may be handled analytically as follows:

(1) Introducing two auxiliary real variables ξ_1 and β_1 [42]:

$$\begin{aligned} T_s - (T_s)_{max} + \xi_1^2 &= 0 \\ T_s - \beta_1^2 &= 0 \end{aligned} \tag{7-26}$$

(2) Introducing one auxiliary variable η_1 [43]:

$$(T_{s\,max} - T_s)T_s - \eta_1^2 = 0 \tag{7-27}$$

(3) Representing stagnation temperatures in parametric form such as given previously in Chapter 5 for propellant mass flow rate.

In the first method of representing the temperature constraint, ξ_1 is real for all negative values of T_s and for all positive values with a magnitude less than $(T_s)_{max}$. The expression involving β_1 would be

- - - - - - - - - - - - - - - - -

* Acceptable solutions in this case are guidance trajectories which do not compromise the structural integrity of the vehicle as a result of atmospheric heating.

required if minimum values of T_s were also to be constrained (such as to prevent negative temperatures). Since negative temperatures cannot enter if positive roots of equation (7-21) are the only solutions admitted, the first of equation (7-26) is the only one required. Representing this in dimensionless form by dividing through by $(T_s)_{max}$ and substituting for T_s from equation (7-21) gives:

$$(TC)v^{\frac{3}{4}}e^{-\frac{kh}{8}} - 1 + \zeta_1^2(\tau) = 0 \qquad (7\text{-}28)$$

where (TC) represents a "temperature constraint constant", a constant for a particular vehicle entering the atmosphere of a particular planet.

$$(TC) = \frac{1.392 \times 10^4 (HF)_{E0}^{\frac{1}{4}} (VF)^{\frac{1}{4}}}{(T_s)_{max}} \qquad (7\text{-}29)$$

For example, if (VF) = 1 and if $(T_s)_{max}$ = 3000° R, then (TC) equals 5.8 for Venus, 4.64 for Earth, and 1.86 for Mars. $\zeta_1(\tau)$ in equation (7-28) is some real function of dimensionless time which must satisfy this equation.

Equation (7-28) may be used as an analytic function for specifying temperature constraints in the application of the calculus of variations to determine extremals of guidance functions. Graphical representation of temperature constraints is described in Section 7.7.

7.5 Human Acceleration Tolerances

During the entry mission as well as during maneuvers in the free-fall phase of flight, the vehicle will encounter rolling, pitching, yawing and accelerations in the longitudinal and lateral directions. The effect of forces on the human occupants of the craft as a result of

these motions will depend on the position, posture, and adaptability of the individual crew members.

Human tolerances to specific forces encountered during the mission depend on the following factors:

(1) Absolute specific force level (accelerations)

(2) Duration of exposure

(3) Time rate of change of specific forces*.

During the manned entry mission, certain guidance and control functions may be required of the pilot. His performance generally deteriorates under high g-loads; even though these acceleration levels may be well below critical levels for survival or permanent physical damage. If the control functions are of the "off-on" type, the tolerable g-levels are greater than if the control functions require continuous precision corrections such as matching pointers. Auditory stimuli may be used to a limited extent to augment visual operations; however, auditory hallucinations are frequent at high acceleration levels.

The acceleration levels encountered by the entry vehicle must be constrained to values below that for which there is deterioration of the human control function. If the guidance system does not require any human actions, then the tolerable levels are limited only to the extent required to prevent physical damage to the human occupants. If the functions of the pilot involve movements of hands and arms and require that he make tactical decisions and operate complex equipment, then the accelerations that may be tolerated are small.

Studies have shown that humans can withstand considerably greater

- - - - - - - - - - - - - - - - -

* That is, the rise time to peak g-loads.

g-forces in the transverse direction (chest-to-back) than in the longitudinal direction (head-to-toe). The direction of g-forces are generally defined as follows:

(1) Transverse Prone: back to chest

(2) Transverse Supine: chest to back

(3) Longitudinal positive: head to toe

(4) Longitudinal negative: toe to head.

Table 7.4 summarizes the gross effects of acceleration forces on the human being[7].

Table 7.4: Gross Effects of Acceleration Forces. (taken from reference (7)).

Effects:	g's
Weightlessness	0
Earth normal	1
Hands and feet heavy; walking and climbing difficult	2
Walking and climbing impossible; crawling difficult	3
Movement only with great effort; crawling almost impossible	4
Only slight movements of arms and head possible	5
Positive longitudinal g's, short duration. (blood forced from head toward feet)	
Visual symptoms appear	2.5 - 7.0
Blackout	3.5 - 8.0
Confusion, loss of consciousness	4.0 - 8.5
Structural damage, especially to spine	(greater than 18-23)
Transverse g's, short duration. (Head and heart at same hydrostatic level)	
No visual symptoms or loss of consciousness	0 - 17
Tolerated	28 - 30
Structural damage may occur	(greater than 30-45)

It is seen from Table 7.4 that considerably greater forces may be tolerated in the transverse direction than in the longitudinal direction.

Fig. 7.2 shows human tolerances to steady-state positive longitudinal accelerations as a function of time-duration of exposure. Data for this graph was taken from references (7) and (44). From this figure it may be observed that 4 g's may be tolerated for only 10 seconds, 3 g's may be tolerated for about 2 minutes, and 2 g's may be tolerated indefinitely.

The reaction of man to transverse acceleration loads is summarized in Figs. 7.3 and 7.4. The first of these figures covers the time interval up to 9 seconds of exposure, the second covers exposure times from 9 to about 4000 seconds. Data for Fig. 7.3 was taken from reference (44) and data for Fig. 7.4 was taken primarily from reference (7). These figures show that man can safely withstand 10 g's transverse acceleration for 2 minutes and 5 g's for about 25-30 minutes.

A study of Figs. 7.2, 7.3, and 7.4 shows clearly that the tolerance of the crew of the entry vehicle to accelerations is a strong function of the direction of the applied forces and the time interval over which the force level is maintained. An important factor not shown in these figures is the decrement of the human operator in carrying out control functions; this factor is strongly dependent on the complexity of the control functions required of the man. As mentioned earlier in this section, precision operations involving movements of the hands and arms restrict tolerable g-levels to much lower levels than indicated by Figs. 7.2 through 7.4.

Woodling and Clark[44] describe recent studies with the centrifuge which were performed in order to determine pilot physiological tolerances to accelerations. One phase of the study involved programmed accelerations which were unaffected by pilot control actions, the second phase involved a series of runs in which the pilot actually controlled

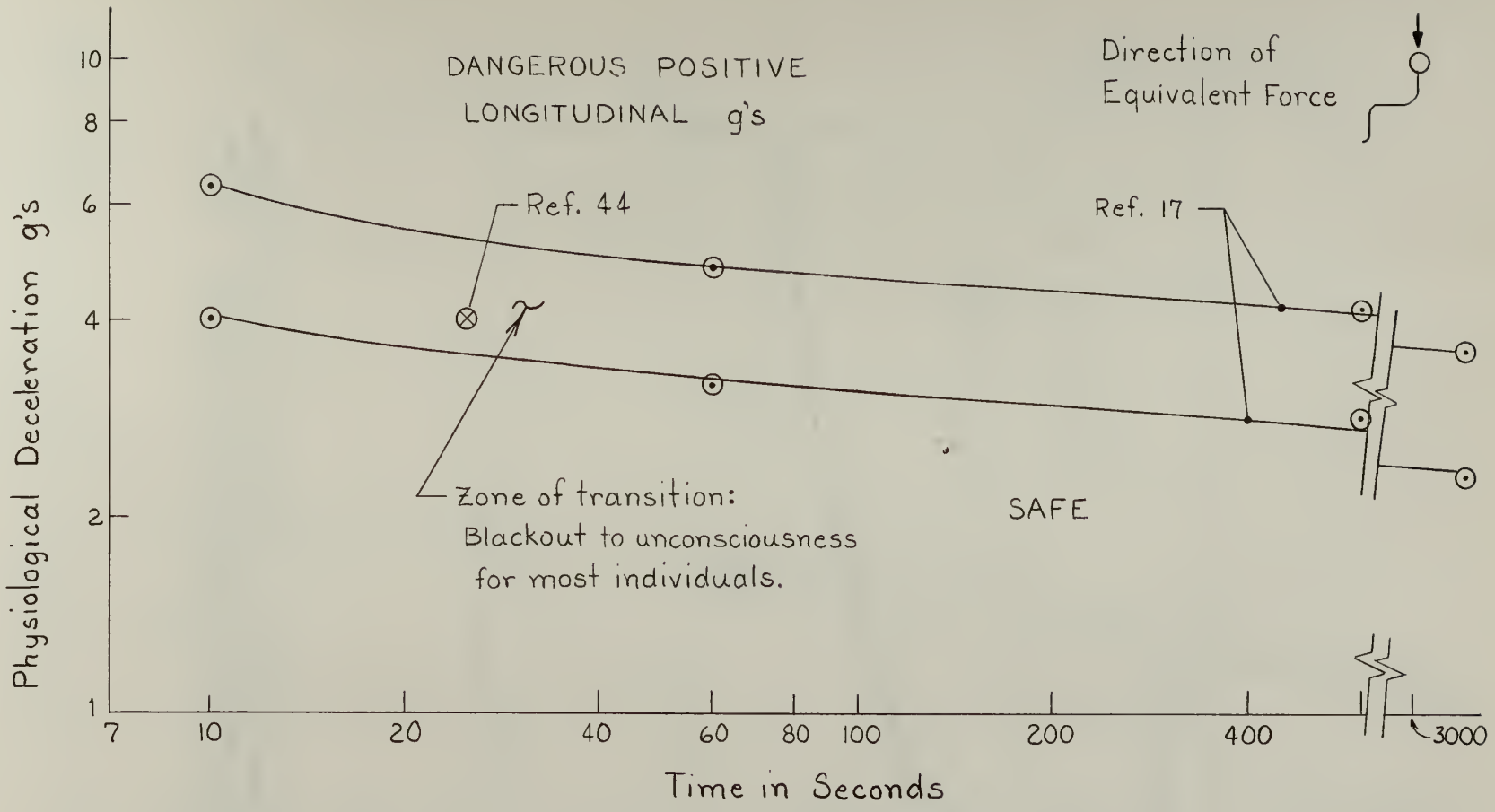

Fig. 7.2: Human Tolerances to Steady State Positive Longitudinal Accelerations.

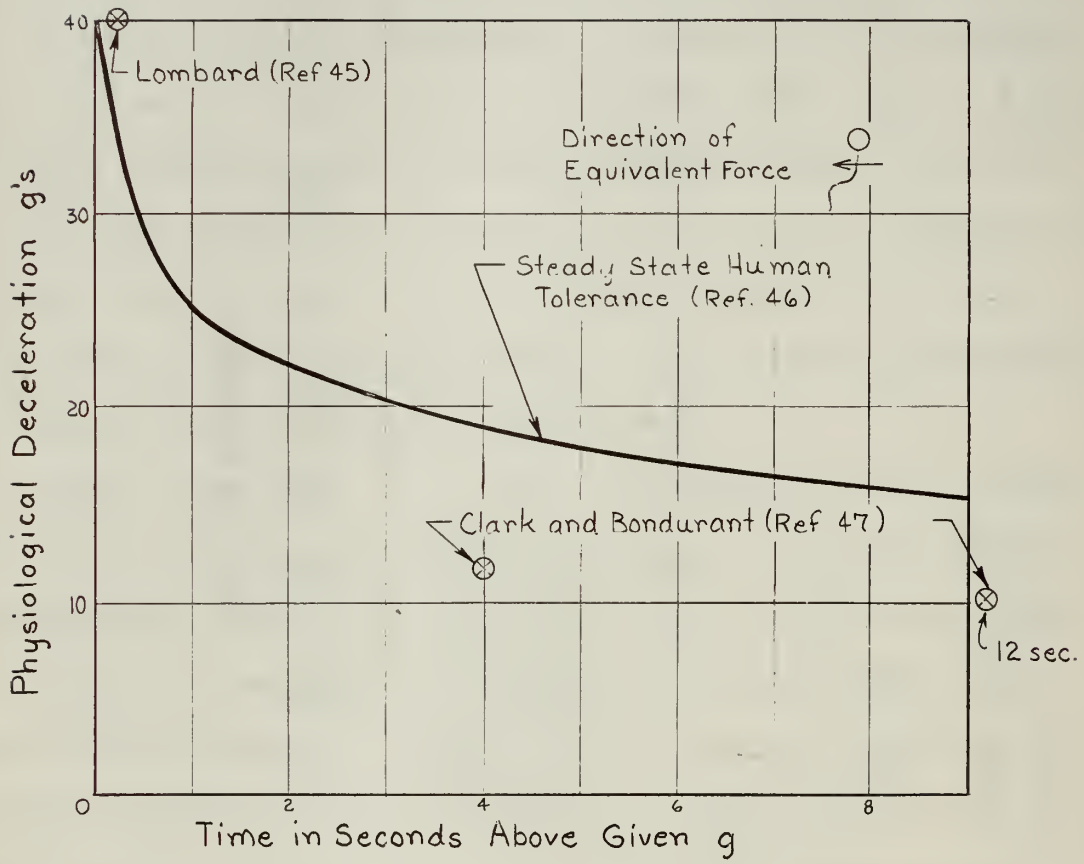

Fig. 7.3: Human Tolerances to Steady State Transverse Prone Accelerations Over Short Time Intervals. Equivalent Force Applied From Back to Chest.

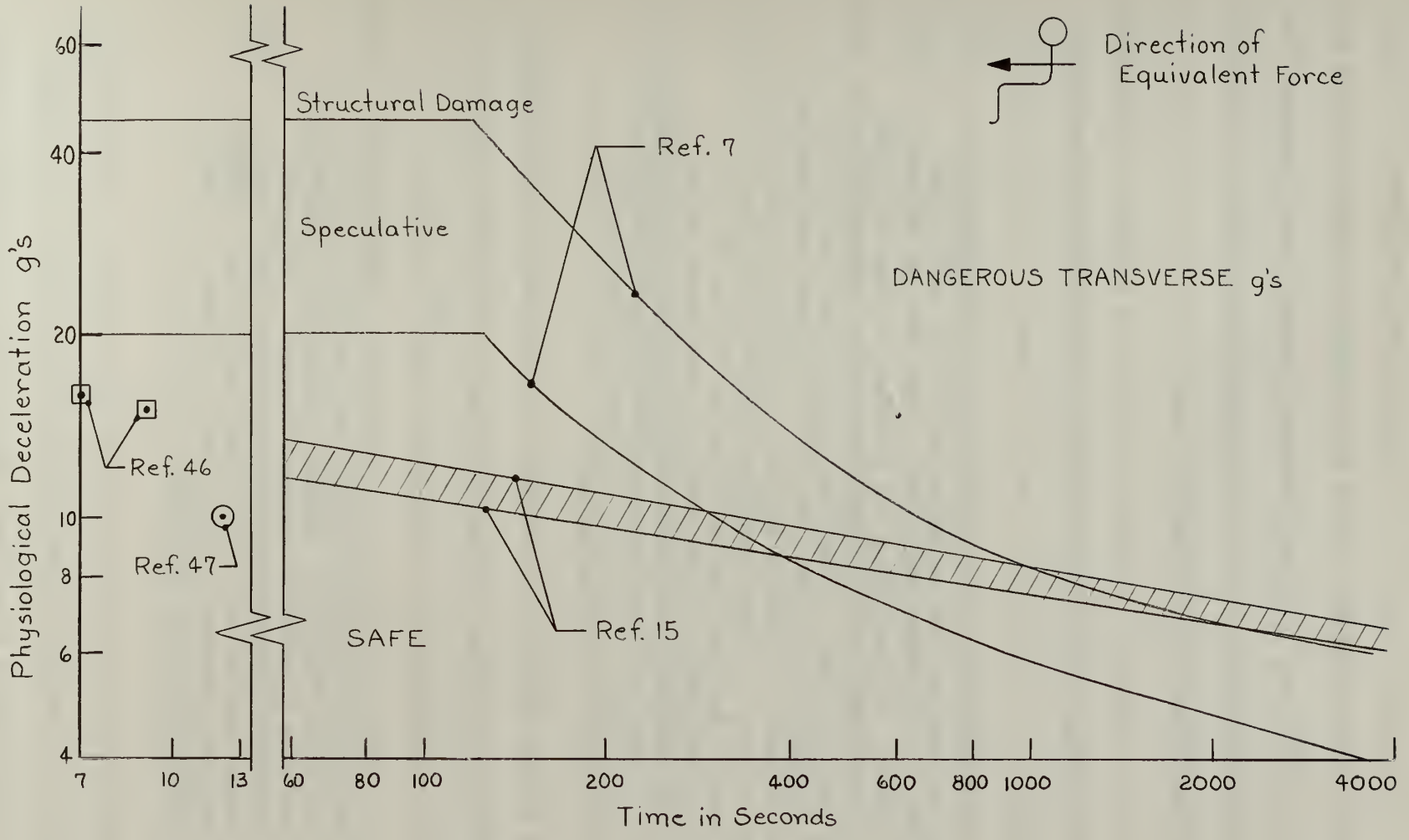

Fig. 7.4: Human Tolerances to Steady State Transverse Accelerations. Duration of Exposure = 7 to 4,000 seconds.

the motion of the centrifuge and the resulting accelerations to which he was subjected. In this study, pilots wore standard Navy Z-2-G-suits and were seated in contoured couches in order to minimize body pressure points and jostling effects due to oscillatory accelerations. Direction of g-forces were primarily from chest to back.

In the first phase of this study, pilots were assigned an arbitrary visual tracking task. Among the interesting results of this study were the following:

> An important factor in increasing the tolerance level during the runs was the technique with which the subject strained, as if he were trying to support someone standing on his chest. No chest pain was reported as long as proper straining was maintained, although breathing became difficult around the 12-g level. Blurring of vision was reported by some subjects at levels of g near 16. Subjects were able to operate a small, right-hand control stick under accelerations as high as 25-g. A thumb-operated stick was also used effectively. Although conclusive objective data was not obtained, performance of the tracking task showed deterioration with increasing accelerations but improved with experience. It was felt that the contoured type couch offered satisfactory means of support for entry accelerations as high as 25-g for a trained subject.

In the second phase of the studies in which the pilot controlled the centrifuge, a computer provided aerodynamic simulation of the vehicle under consideration. Woodling and Clark[44] reported:

> One extreme re-entry condition involved normal accelerations of 7 g's and longitudinal deceleration of 4 g's which lasted as long as 25 seconds, during which time the pilot was able to maintain adequate control. The blood pressure in the limbs increased and petechia (small skin hemorrhages) were noted in the forearm and ankles. Tingling and subsequent numbness of limbs were noted and in a few cases definite pain was reported.

In addition to the absolute specific force level and the duration of exposure, the rise time to peak levels is significant. Col. John Stapp, Air Force Missile Development Center, has investigated loadings

up to 45 g's sustained over a period of about 1/3 second. He concluded that for brief high g-loadings, the rate of change of g is a more important consideration than the peak magnitude[7]. Studies of the ability of a human to withstand a rapid rate of change of loading indicates the rate of onset of g-loadings should not exceed 200-250 g's per second.

During the Keplerian Phase of the entry mission, the crew will experience zero g's. There is limited information to date about the effects of weightlessness on the human being. Man has been exposed to weightlessness for periods of the order of only seconds or minutes to date; some individuals find it unpleasant while others seem to enjoy it. It is believed that some individuals will be able to adapt to a weightless condition for long periods of time.

7.6 Analytical Representation of Trajectory Constraints Imposed by Human Acceleration Tolerances

The vector sum of external specific forces measured by a set of orthogonal accelerometers in the vehicle is equivalent to the total accelerations experienced by the human crew. If it is required that the total specific force level be restricted to values below a certain maximum number of Earth g's, then:

$$(\text{Magnitude of total external specific force vector}) \leq c\, G_{(m)E} \qquad (7\text{-}30)$$

where $G_{(m)E}$ = mean surface gravitational acceleration of Earth

c = maximum allowable specific force level (number of $G_{(m)E}$).

Since it is likely that significant retro-thrust will be generated in bursts of short duration, the contribution to total specific force

due to thrust is not considered in this analysis.* Constraints in this thesis are imposed only on force levels resulting from lift and drag accelerations. Thus, equation (7-30) is written in dimensionless form as:

$$\left(n_D^2 + n_L^2\right)^{\frac{1}{2}} \leq c \frac{G_{(m)E}}{G_{(m)o}} \tag{7-31}$$

In accordance with the procedure previously discussed for temperature constraints in section 7.4, inequality (7-31) may be written as an equation which must be satisfied throughout the entry trajectory by introducing a new real variable ζ_2. Assuming the exponential model of the planetary atmosphere and no atmospheric winds, the following equation may be written:

$$(AC)\, \frac{v^2 S}{c\, M}\, e^{-\beta h}\left(C_D^2 + C_L^2\right)^{\frac{1}{2}} - 1 + \zeta_2^2(\tau) = 0 \tag{7-32}$$

where $\zeta_2(\tau)$ is some real function of dimensionless time which satisfies this equation.

(AC) represents an "acceleration constraint constant", a constant for entry into the atmosphere of a particular planet.

$$(AC) = \frac{\rho_{(\bar{S}L)}\, G_{(m)o}\, R_{(m)o}}{2\, G_{(m)E}} \qquad \frac{slugs}{ft^2} \tag{7-33}$$

The acceleration constraint constant is equal to the satellite dynamic pressure at the surface of the planet divided by the mean surface

- - - - - - - - - - - - - - - - -

* Figs. 7.2 and 7.3 show that high specific force levels may be tolerated for short periods of time provided the rate of change of specific force does not exceed 200-250 g/sec. Since high thrust levels will be generated over short periods of time only, the additional force level incurred during periods of engine operation can generally be tolerated.

gravitational force of the Earth. Table 7.5 gives approximate values of the acceleration constant for the terrestrial planets.

Table 7.5: Values of Acceleration Constraint Constant for Terrestrial Planets

	(AC)	$(AC)_{EO} = (AC)_O/(AC)_E$
Venus	2.86×10^5 slug/ft.^{2}	11.5
Earth	2.49×10^4	1.0
Mars	3.44×10^2	0.0138

Equation (7-32) is used as an analytic function for specifying trajectory constraints resulting from human acceleration tolerances. This equation may be used in the application of the calculus of variations to determining extremals of arbitrary guidance functions. Graphical representation of both heating and deceleration constraints are described in Section 7.7.

7.7 Graphical Representation of Heating and Acceleration Constraints

A velocity-altitude graph of the design maximum vehicular temperature and maximum permissible specific force level is instructive as an aid to visualizing trajectory restraints imposed by these manifestations of energy transfer from the vehicle to the planetary atmosphere. The guidance system must operate in such a way that the resulting trajectory does not violate these constraints; an "allowable operating region" is thereby established. Any guidance trajectory conceived for the mission can be plotted in the velocity-altitude plane and is an

acceptable trajectory with respect ot mission constraints as long as the path remains entirely within the allowable operating region. The optimum guidance trajectory may be selected from among all permissible trajectories based on evaluation of the other mission factors which are important in system design - factors such as payload requirements, range accuracy, flight time, system reliability, computational complexity, etc.

Either maximum allowable heat flow rates or stagnation point temperatures are readily represented in the velocity-altitude plane. To illustrate this method of representing constraints, stagnation point temperature was selected here; this presupposes a vehicle which is designed to operate at radiation equilibrium temperatures.

Assuming a certain maximum stagnation point temperature is prescribed, equation (7-21) is written:

$$h = \frac{18.44}{k}\left\{\frac{3}{4}\log v - \log\left[\frac{(T_s)_{max}}{1.392 \times 10^4 (HF)^{\frac{1}{4}} (VF)^{\frac{1}{4}}}\right]\right\} \qquad (7\text{-}34)$$

where log ( ) represents the logarithm to the base 10.

Using Equation (7-29), equation (7-34) is written:

$$h = \frac{18.44}{k}\left[\frac{3}{4}\log v + \log(TC)\right] \qquad (7\text{-}35)$$

Values of k are approximately as follows for the atmospheres of the terrestrial planets:

	k
Venus	1013
Earth	889
Mars	184.6

Equation (7-35) is plotted on Figs. 7.5, 7.6, and 7.7 for Earth, Venus,

and Mars, respectively. The following combinations of $\frac{(T_s)_{max}}{(VF)^{\frac{1}{4}}}$ are represented in these figures:

$$\frac{(T_s)_{max}}{(VF)^{\frac{1}{4}}} = 1000,\ 2000,\ 2500,\ \text{and}\ 3000\ \ ^{\circ}R\ \text{-ft.}^{\frac{1}{8}}$$

The similarity between entry into Earth and Venus from the atmospheric heating standpoint is clearly evident by comparing Figs. 7.6 and 7.5. Temperature constraints for entry into the atmosphere of Mars, on the other hand, are nearly constant velocity lines.

Representation of acceleration constraints require that the lift, drag, and mass characteristics of the vehicle be specified. For graphical representation in this thesis, the three families of vehicles described in Table 5.1 were selected. Maximum tolerable specific force level was chosen in this thesis to be at the level of six Earth g's. Judicious choice of the maximum specific force level is strongly dependent on the decrement of the human operator in performing guidance and control functions; choosing the 6-g level assumes that his control actions require little movement of hand and arms and are restricted primarily to "off-on" type operations.

Equation (7-31) is written:

$$h = \frac{1}{k \log e}\left\{2 \log v + \frac{1}{2}\log(C_L^2 + C_D^2) + \log\left[\frac{(AC)}{c\ M/S}\right]\right\} \qquad (7\text{-}36)$$

Equation (7-36) is plotted in Figs. 7.5, 7.6, and 7.7. for the terrestrial planets with $c = 6$ Earth g's. The acceleration constraints are represented as bands in these figures rather than lines. The bands result because:

(I) It was assumed that the lift-coefficient may vary between

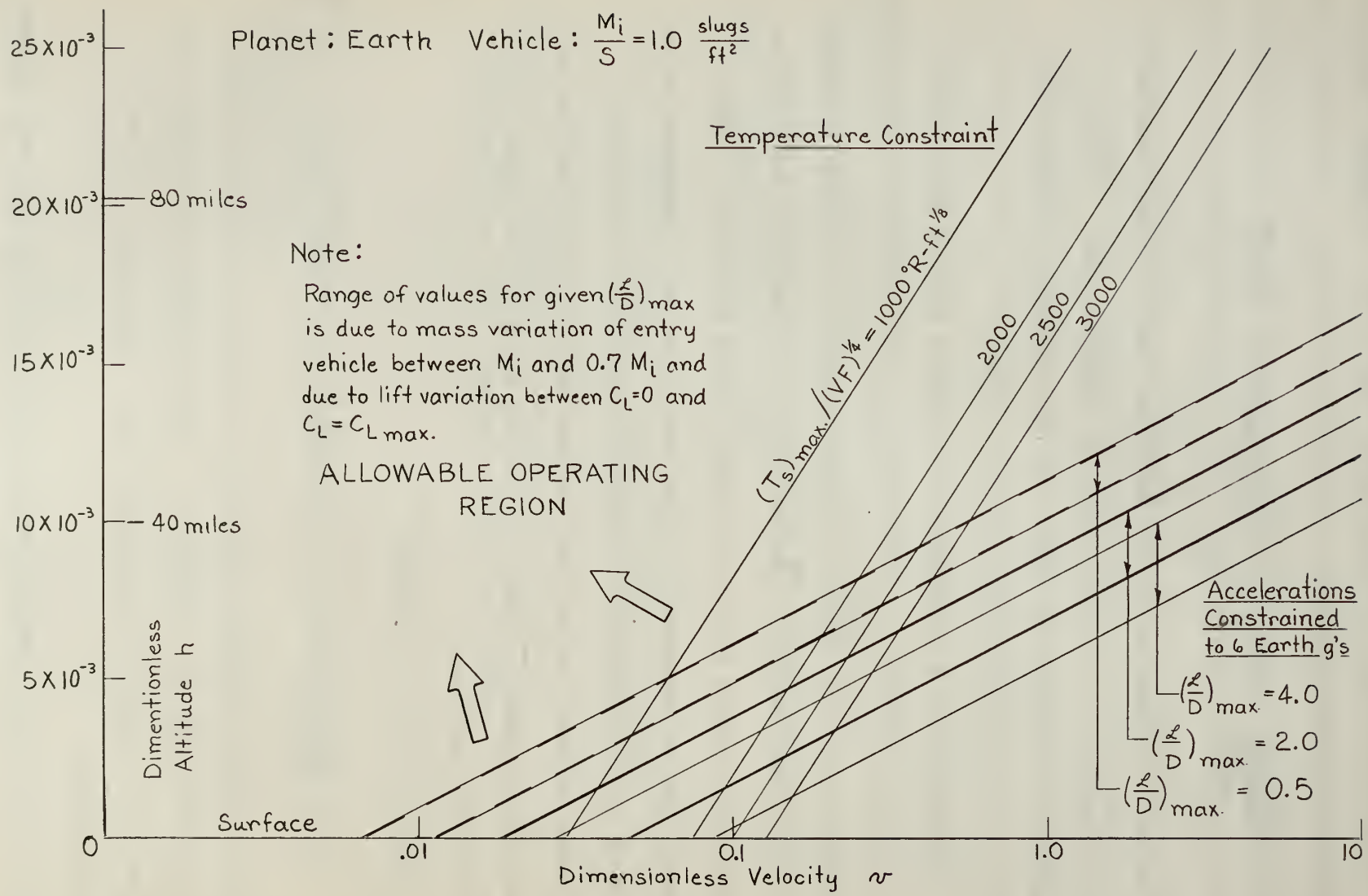

Fig. 7.5: Operating Regions Permitted by Constraints on Stagnation Temperatures and Human Accelerations for Entry into Earth's Atmosphere.

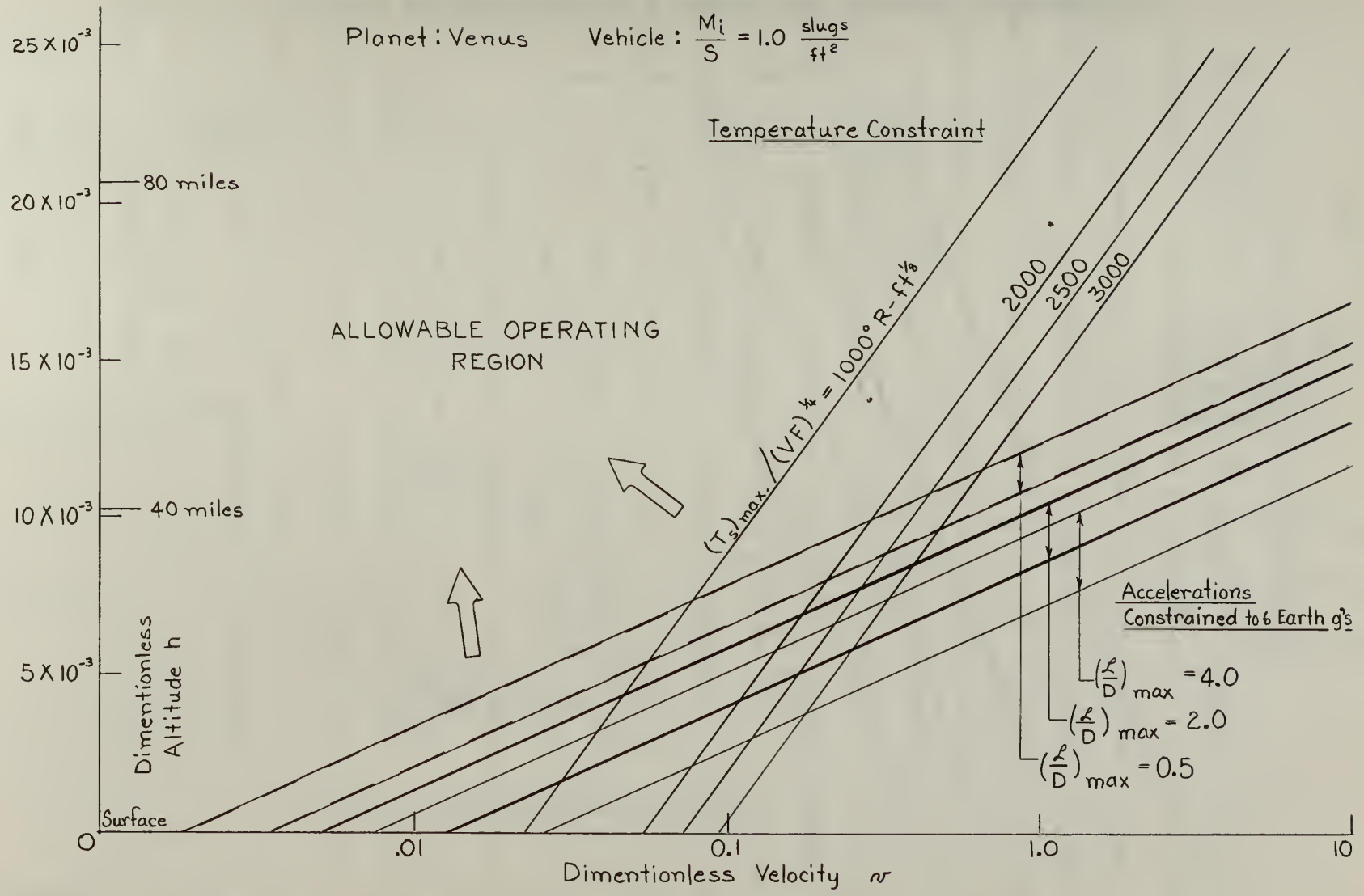

Fig . 7.6: Operating Regions Permitted by Constraints on Stagnation Temperature and Human Accelerations for Entry into Venusian Atmosphere .

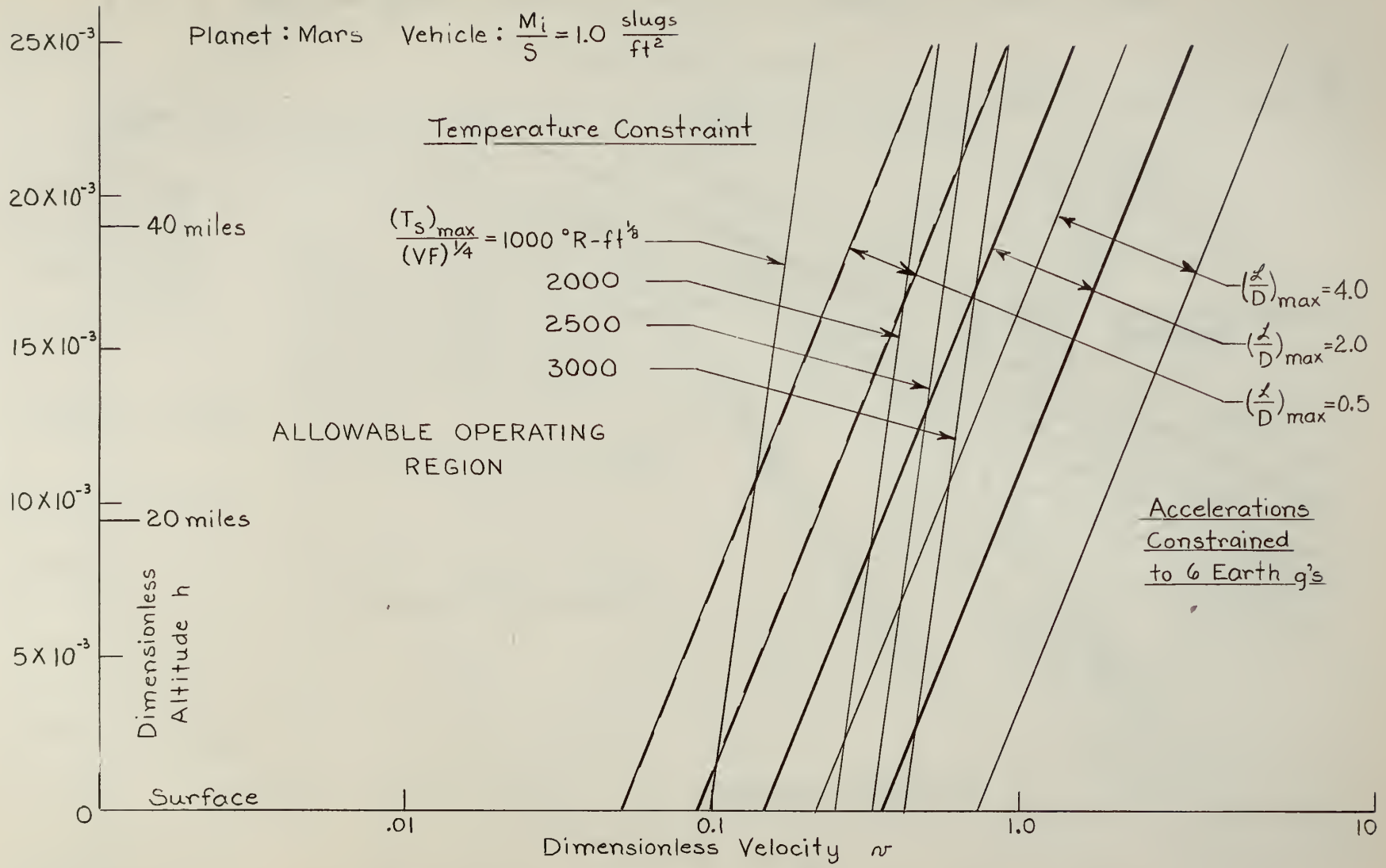

Fig. 7.7: Operating Regions Permitted by Constraints on Stagnation Temperature and Human Accelerations for Entry into Martian Atmosphere.

zero and $C_{L_{max}}$;

(2) A variable mass vehicle was assumed.

Mass variation was taken to be $M_{initial}$ to 0.7 $M_{initial}$ in Figures 7.5 through 7.7. This corresponds to an expenditure of propellant mass equivalent to seven separate 500 ft./sec. velocity impulses* if the specific impulse of the propellant is approximately 300 seconds. If the vehicle mass, lift, and drag coefficients were constant during entry, the acceleration bands of these figures would reduce to lines.

Acceleration constraints place a more severe restriction on allowable velocity-altitude loci than shown in Figs. 7.5 through 7.7 if the magnitude of c is reduced. If the vehicle flies in a high drag condition, such as near 90° angle of attack, the drag accelerations are more severe than indicated by these figures. It should be emphasized that the lift-drag polar of the vehicles plotted in Figs. 7.5 through 7.7 are valid only in the small angle of attack regions; that is, α may vary from zero to a value corresponding to $(L/D)_{max}$. The allowable operating region is reduced if the vehicle is operated on the other side of the lift curve due to the higher drag characteristics of this configuration.

For most vehicle-planet combinations, both heating and acceleration constraints must be examined in arriving at a suitable entry profile. Specific force levels are generally more restrictive on the mission at lower altitudes while heating considerations are predominant at high altitudes. The lower the maximum g-tolerance, the more severe are the effects of acceleration constraints on restricting the family of allowable

- - - - - - - - - - - - - - - - -

* See equation (5-58).

guidance trajectories. The higher the drag characteristics of the vehicle, the higher the altitude at which a given g-level is observed. If M/S is increased while drag coefficient is fixed, a particular specific force level is encountered at lower altitudes.

7.8 Locus, in Velocity-Altitude Plane, of Points where External Specific Forces Equal or Exceed Minimum Detectable Levels of Specific Force Measuring Subsystem.

Lift and drag forces may be utilized in a controlled manner to modify the trajectory of the entry vehicle when these forces are of such magnitudes as to be significant. These external forces become significant, from the guidance standpoint, when they are of such magnitudes as to be detectable by accelerometers carried in the vehicle. Until the vehicle has penetrated a sufficient distance into the planetary atmosphere for accelerations to exceed the threshold value detectable by the specific force measuring subsystem, the entry trajectory is basically that of the Keplerian transfer ellipse.

Defining:

$C_{th} \equiv$ threshold value of accelerations detectable by specific force measuring subsystem in Earth g's.

Equation (7-36) can be written:

$$K_{EO} h + C_a = \frac{1}{k_E \log e} \left\{ 2 \log v + \frac{1}{2} \log (C_L^2 + C_D^2) + \log \left[\frac{(AC)_E}{C_{th} M/S} \right] \right\} \quad (7\text{-}37)$$

where k_E = dimensionless atmospheric exponential decay parameter for Earth $\cong$ 889.

K_{EO} = ratio of dimensionless planetary atmospheric exponential decay parameter with respect to the decay parameter of the

Earth; i.e.,

$$K_{EO} = k/k_E \tag{7-38}$$

The magnitude of K_{EO} for Venus is 1.14, for Earth 1.0, and for Mars 0.207.

C_a is a constant for each planet and is defined as follows:

$$C_a \equiv - \frac{\log (AC)_{EO}}{k_E \log e} \tag{7-39}$$

$(AC)_{EO}$ was tabulated in Table 7.5.

The left side of equation (7-37) is dimensionless altitude when entry is made into the Earth's atmosphere. It is readily converted to altitude for entry into the atmospheres of other planets by using the conversion quantities listed in Table 7.6.

Table 7.6: Conversion Quantities for Use in Equation (7-37)

	Venus	Earth	Mars
K_{EO}	1.14	1.0	0.207
C_a	-2.75×10^{-3}	0	4.82×10^{-3}

Equation (7-37) is plotted on Figures 7.8 through 7.10. For these graphs, the three classes of vehicles summarized in Table 5.1 were used and the mass characteristics of the vehicles were taken to be M_i/S equal to 1.0 slug/ft.^{2} Values of threshold accelerations measurable by the specific force measuring subsystem were arbitrarily assumed as follows:

Fig. 7.8 : $C_{th} = 10^{-4}$ Earth g's

Fig. 7.9 : $C_{th} = 10^{-5}$ Earth g's

Fig. 7.10: $C_{th} = 10^{-6}$ Earth g's

For convenience, the information plotted in Figs. 7.5 through 7.7 was also plotted in the same manner in Figs. 7.8 through 7.10. The acceleration constraint bands are easily plotted by replacing C_{th} with the value of 6.0 previously chosen as representative for missions during which the human operator plays a relatively minor role in controlling the vehicle.

The stagnation temperature lines are represented by writing equation (7-35) as:

$$K_{EO}h + C_t = \frac{18.44}{k_E}\left[\frac{3}{4}\log v + \log\left(\frac{1.392 \times 10^4 (VF)^{1/4}}{(T_s)_{max}}\right)\right] \qquad (7\text{-}40)$$

where

$$C_t = \frac{-18.44}{4k_E}\log (HF)_{EO} \qquad (7\text{-}41)$$

Equation (7-40) is plotted on Figs. 7.8 through 7.10 for

$$\frac{(T_s)_{max}}{(VF)^{\frac{1}{4}}} = 2000,\ 2500,\ \text{and}\ 3000 \quad {}^{\circ}R\ ft.^{1/8}$$

The left side of equation (7-40) is dimensionless altitude for entry into the atmosphere of the planet Earth. Dimensionless altitudes for entry into the atmosphere of other terrestrial planets is readily determined with the aid of conversion quantities listed in Table 7.7:

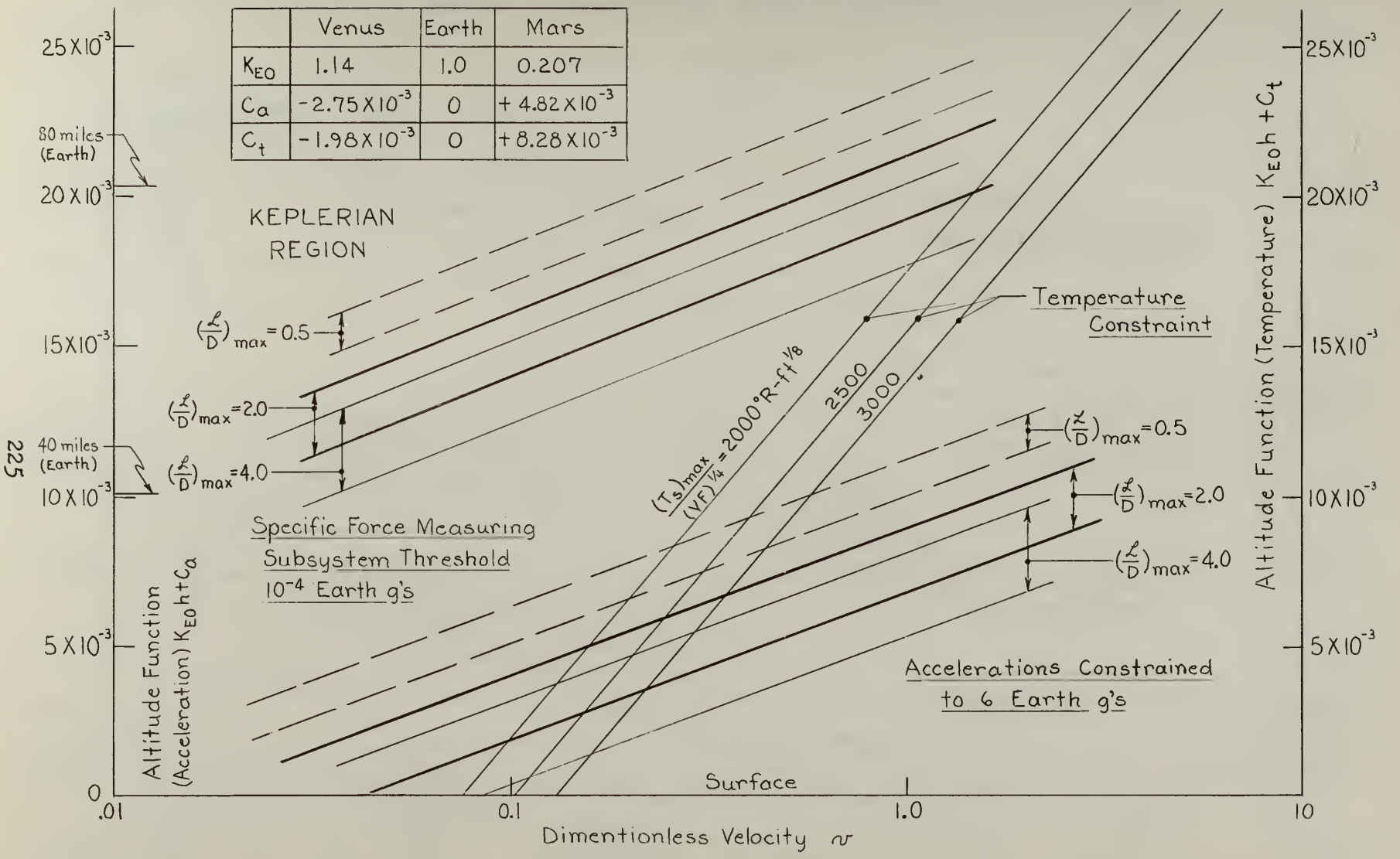

Fig. 7.8: Threshold of Specific Force Measuring Subsystem in Altitude-Velocity Plane. Specific Force Measuring Subsystem Threshold = 10^{-4} Earth g's.

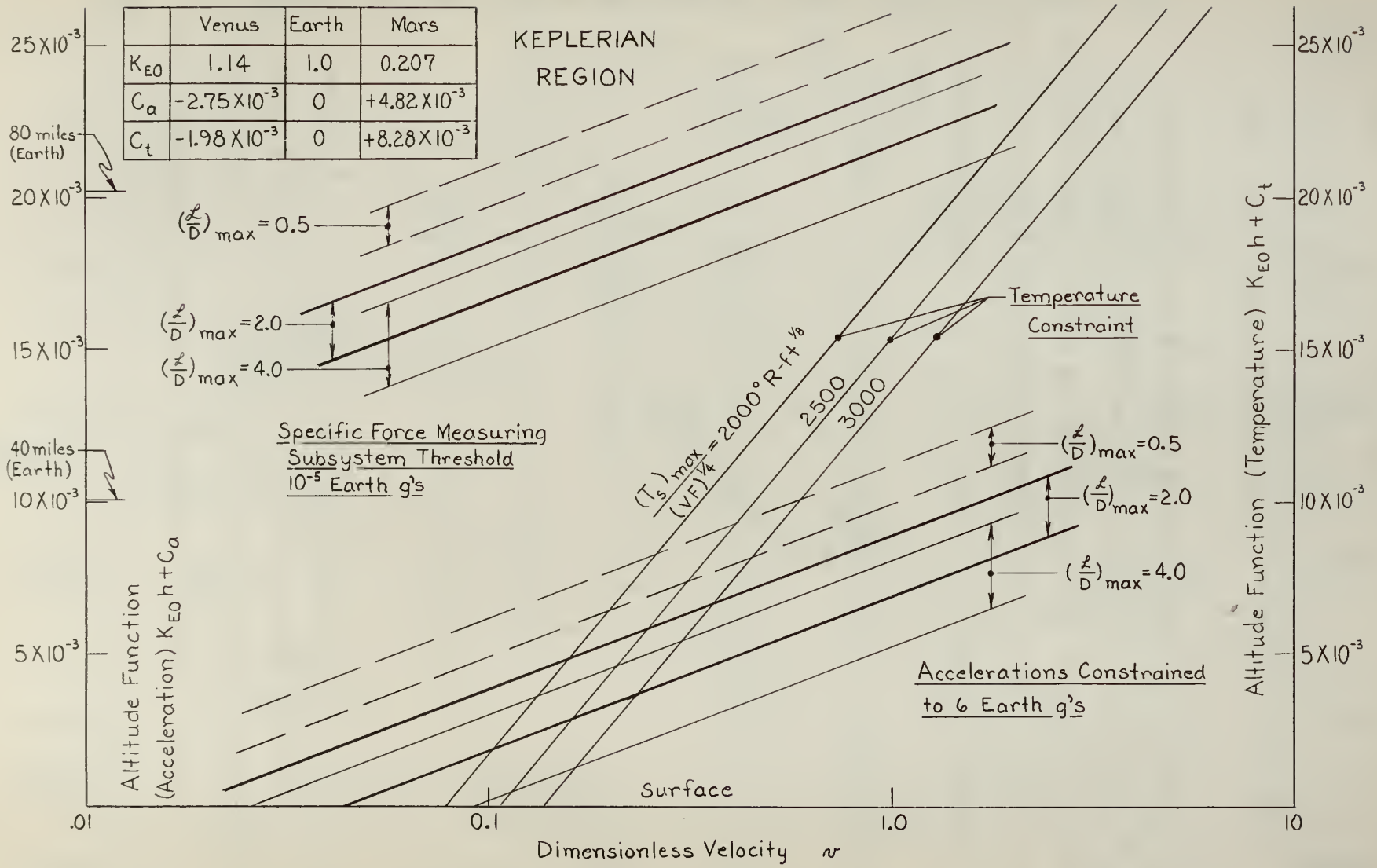

Fig. 7.9: Threshold of Specific Force Measuring Subsystem in Altitude-Velocity Plane. Specific Force Measuring Subsystem Threshold = 10^{-5} Earth g's.

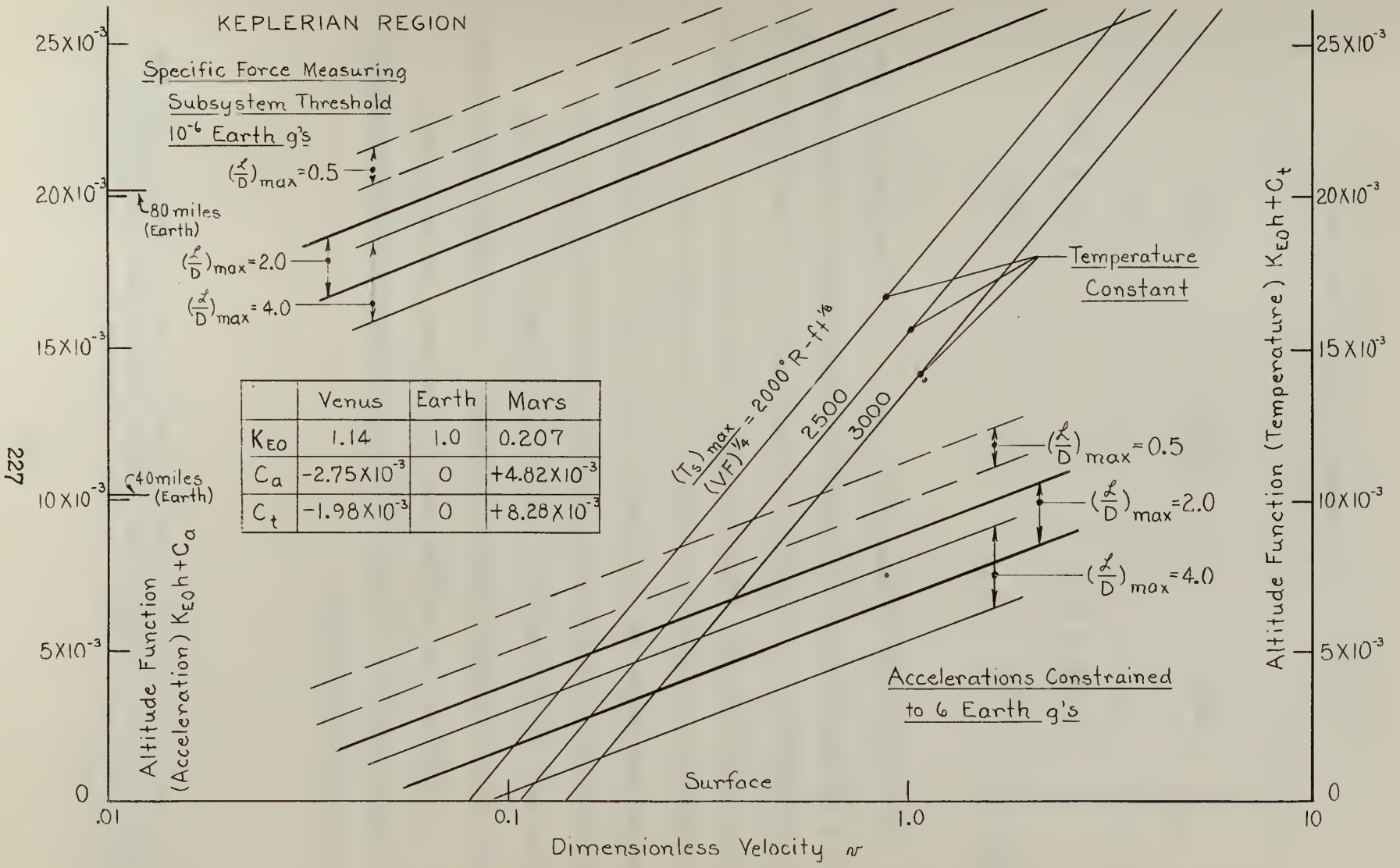

	Venus	Earth	Mars
K_{E0}	1.14	1.0	0.207
C_a	-2.75×10^{-3}	0	$+4.82\times10^{-3}$
C_t	-1.98×10^{-3}	0	$+8.28\times10^{-3}$

Fig. 7.10: Threshold of Specific Force Measuring Subsystem in Altitude-Velocity Plane. Specific Force Measuring Subsystem Threshold = 10^{-6} Earth g's.

Table 7.7: Conversion Quantities for Use in Equation (7-40)			
	Venus	Earth	Mars
K_{EO}	1.14	1.0	0.207
C_t	-1.981×10^{-3}	0	8.28×10^{-3}
$(HF)_{EO}$	2.41	1.0	0.0253

Plots exemplified by Figs. 7.8 through 7.10 are particularly useful as a background graph for comparing various guidance trajectories which are selected on the basis of optimizing other mission factors such as payload capabilities, range accuracy, flight time, etc. If a series of trajectory plots are made on Fig. 7.8, for example*, each having particular advantages for the mission under study, a straightforward comparison of the trajectories is readily made with respect to the altitude and velocity points at which the threshold value of the specific force measuring system is exceeded. The temperature and acceleration constraint loci on the same plot indicate the favorable or unfavorable character of each of the trajectories from the standpoint of energy transfer limitations.

- - - - - - - - - - - - - - - - -

* This plot would be used if the temperature and constraint lines are appropriate for the particular vehicle system under consideration and if the specific force measuring subsystem had a design threshold of 10^{-4} g's.